Spring 3-2025

Late Cretaceous ammonites and other non-rudist mollusks from Costa Rica and their paleoecology

Esteban David Lopez-Murillo
University of New Mexico

Recommended Citation

Lopez-Murillo, Esteban David. "Late Cretaceous ammonites and other non-rudist mollusks from Costa Rica and their paleoecology." (2025). https://digitalrepository.unm.edu/eps_etds/408

Esteban David Lopez-Murillo

Candidate

Earth and Planetary Sciences

Department

This thesis is approved, and it is acceptable in quality and form for publication:

Approved by the Thesis Committee:

PhD Corinne E. Myers , Chairperson

PhD Tyler Mackey

PhD Warren D. Allmon

LATE CRETACEOUS AMMONITES AND OTHER NON-RUDIST MOLLUSKS FROM COSTA RICA AND THEIR PALEOECOLOGY

by

ESTEBAN DAVID LOPEZ-MURILLO

B.S. IN GEOLOGY, UNIVERSIDAD DE COSTA RICA 2020

THESIS

Submitted in Partial Fulfillment of the
Requirements for the Degree of

Master of Science in
Earth and Planetary Sciences

The University of New Mexico
Albuquerque, New Mexico

May 2024

DEDICATION

I dedicate this thesis to my parents José Armando and Damaris, my grandma Eloina and my aunt María for their unconditional support in achieving my dreams.

Also to my Costa Rican friends for accompanying me during fieldwork.

ACKNOWLEDGMENTS

I want to acknodlege a lot of people for helping me reaching my dreams. I heartly thank my advisor Dr. Cori Myers for letting me propose my research project and giving me the opportunity to fulfill it. Also big thanks to Dr. Tyler Mackey and Dr. Warren Allmon for their observations regarding sedimentology and paleobiogography.

Furthermore, I am truly grateful to my undergraduate advisor and current chairperson of the Escuela Centroamericana de Geología (ECG) of the Universidad de Costa Rica (UCR) Dr. Guaria Cárdenes-Sandí, Dr. María Isabel Sandoval and Lic. Thais Ramírez for letting me use Costa Rican fossil collections for my research. Also for letting me store most of the collected fossil samples.

Thanks to Dr. Valentin Chesnel, Joan Valverde, Natalia Rodriguez, Andrea Vindas, David Rodriguez and Caleb Carvajal for their support during fieldwork in 2021-2023). Also to Dr. Kennet E. Flores for discussion of the stratigraphy and tuff dating. And experts in different groups fossil groups (Teresita Aguilar, Christina Ifrim, Neil H. Landman, Steffen Kiel, Hannes Löser, Ireneusz Walaszczyk). Lastly, big thanks to the American Museum of Natural History (AMNH) and Yale Peabody Museum (YPM) staff Bushra Hussaini, Anastasia Rashkova and Jessica Utrup for facilitating access to their fossil collections for comparison with my Costa Rican specimens.

LATE CRETACEOUS AMMONITES AND OTHER NON-RUDIST MOLLUSKS FROM COSTA RICA AND THEIR PALEOECOLOGY

by

ESTEBAN DAVID LOPEZ-MURILLO

B.S., Geology, Universidad de Costa Rica, 2020
M.S., Earth and Planetary Sciences, University of New Mexico, 2024

ABSTRACT

The Nicoya region in northwestern Costa Rica contains a rich record of Upper Cretaceous fossiliferous sediments. This area was the southernmost tip of North America, making it a unique crossroad between the western Tethys (Caribbean) and Pacific Oceans. After an early Late Campanian tectonic uplift (around 75 Ma), rudist reefs grew with a diverse community of other mollusks. During the following intervals through the latest Campanian and into the Early Maastrichtian (around 70 Ma), sea level oscillated along with changes in molluscan communities. Different groups show mixed paleobiogeographic affinity: Caribbean, Mediterranean Tethys, Californian, Gulf and Atlantic Coastal Plains and the Western Interior Seaway faunas. Also, belemnites and ammonite jaws are first reported from the Late Cretaceous of the Caribbean region. These results will help elucidate patterns of diversity and paleobiogeography in molluscan fauna of the tropical Caribbean Tethys, and effects of the Cretaceous-Paleogene extinction event in molluscan communities.

TABLE OF CONTENTS

APPENDICES

LIST OF FIGURES

LIST OF TABLES

INTRODUCTION

The Cretaceous evolution of Costa Rica shows important tectonic processes in the basement (i.e., Madrigal et al., 2015, 2016; Gazel et al., 2021). According to tectonic models, the northwestern part of Costa Rica, the Nicoya region, was positioned at the southernmost tip of North America during Campanian-Maastrichtian (~ 75 – 66 Ma; Johnson et al., 2002; Flores and Gazel, 2020). On top of the basement, there are Upper Cretaceous sediments which have been under-studied, and some of these stratigraphic units yield molluscan fossils. Northwestern Costa Rica's position during the Campanian-Maastrichtian is an important crossroad between the Caribbean Tethys region and the Pacific Coast of North America. Thus, by understanding these molluscan faunas we can better understand diversity and paleobiogeographic patterns of the tropical Caribbean Tethys close to the Cretaceous-Paleocene extinction event (K-Pg) near the impact zone of Chicxulub. To date, non-rudist molluscan fauna of these deposits has not been studied in detail to assess their paleoecological and paleobiogeographical patterns.

Mollusks (bivalve, gastropods, cephalopods) are common fossil organisms preserved in Campanian-Maastrichtian sediments of Costa Rica, and consequently they are often helpful for biostratigraphy (Blaszkiewicz, 1980) and/or for defining paleobiogeographic provinces (Kauffman, 1973). Sedimentary rocks of this age are particularly well-preserved in the Nicoya region of Costa Rica (Text-fig. 1). Here many stratigraphic units yield molluscan fossils, of which, only rudist bivalves have been studied in detail (e.g., Pons et al., 2016b). However, extensive fossil material is reposited in the Paleontology Collection of the Escuela Centroamericana de Geología (ECG) of the Universidad de Costa Rica (UCR) where most of this material is pending description and identification. The purpose of this study is to describe these molluscan fossils, and to place the assemblages into their paleoenvironmental and tectonic context using previous works (i.e., Flores and Gazel, 2020; Gazel et al., 2021) and new facies analysis.

This study is important because the Nicoya region, according to recent tectonic models (Flores and Gazel, 2020; Gazel et al., 2021), was located on the Pacific Coast of North America. This position is relevant because in previous molluscan paleobiogeographic discussions, there is a non-rudist mollusk information gap between California and Northern Peru (Kiel, 2002). Filling in this gap will better elucidate paleobiogeographic relationships between the Caribbean Tethys/Gulf of Mexico, Mediterranean Tethys, Pacific Ocean. There is an ongoing debate about whether a land bridge existed between North and South America at this time (Kiel, 2002), or if there was an oceanic passage between the Atlantic and the Pacific (Johnson et al., 2002). Using the molluscan fossil record of Costa Rica, I can contribute to this discussion, which has important implications for oceanic current flow throughout this region and, more broadly, for Atlantic-to-Pacific Ocean circulation and species' dispersal globally (Skelton and Wright, 1987; Johnson et al., 2002). The implications of these two proposals are important in term of thinking the warm surface ocean circulation of the Campanian-Maastrichtian, a landbridge could change the direction of these warm ocean circulation towards the temperate regions.

This is the first comprehensive description of Late Cretaceous non-rudist fauna, and their paleoenvironmental context, from Costa Rica – an area uniquely situated at the intersection of Tethyan migration through the Americas at this time. Using this new dataset, I explore two hypotheses: (1) different region-scale paleo-communities existed within the Late Cretaceous Costa Rican fauna that are associated with different paleoenvironments (e.g., shallow-water rudist reef vs. open shelf systems); (2) faunal migration is observable between the Tethyan and Pacific oceanic realms.

Upper Cretaceous sedimentary rocks cover more than 1,000 square kilometers in Costa Rica, but they and the fossils they contain have not received much scientific attention until relatively recently. The first mention of Late Cretaceous mollusks from Costa Rica in the scientific literature is a local report of “Guanacaste’s red marbles” of Santa Rosa, in northwestern Costa Rica (Segura, 1945a, 1945b), which are red rudist-bearing limestones, quarried for ornamental slabs (Loc. 26 in Text-fig. 1B) (Ulloa, 1977). The next record was a report of the gastropod *Nerinea epelys* Woodring, 1952 in rudist-bearing limestones with Late Cretaceous macroforaminifers at Cerro Cebollin of Bolson, in northwestern Costa Rica (Loc. 20 in Text-fig. 1B) (Malavassi, 1961).

During the 1970’s, geological mapping in northwestern Costa Rica resulted in publication of the first ammonite of southern Central America, *Pseudokossmaticeras?* sp. from the Campanian of San Buenaventura (Loc. 10 in Text-fig. 1B) (Schmidt-Effing, 1974). Rudist genera were reported by Galli-Olivier and Schmidt-Effing (1977); oil shales of Loma Chumico produced the ammonite *Neokentroceras* sp. from the early Late Albian (Loc. 15 in Text-fig. 1B) (Azema et al., 1979).

Seyfried and Sprechmann (1986) reported a neritic fauna from Los Almendros (Loc. 38 in Text-fig. 1B), which were determined by Fischer and Agular (1994). This fauna includes gastropods, bivalves and ammonites, which those authors interpreted as a mixture of age and environment preference in a deep-water conglomerate (Fischer and Aguilar, 1994). However, they noticed the strong affinity of the fauna with the Tethys Realm and the presence of a rocky shore (Fischer and Aguilar, 1994). Pons et al. (2016b) did the first taxonomic determination of Late Cretaceous mollusks by studying the rudists of El Viejo Formation; they also mentioned the presence of nerineid gastropods and other fauna in these deposits (Locs. 20, 23, 27, 38 in Text-fig. 1B). They determined the age of these localities as Middle Campanian on the basis of the rudist *Barrettia monilifera* Woodward, 1862 (Pons et al., 2016b). Little to no stratigraphic information was given.

Atlantic-Pacific migration has been hypothesized based on strong Caribbean affinity of the rudist faunas in the study area (Pons et al., 2016b) and the observation of Caribbean rudists and macroforaminifers on Pacific guyots (Camoin et al., 1995; Premoli Silva et al., 1995), even as far as Papua New Guinea (Glaessner, 1960) and Oman (Skelton and Wright, 1987). This dispersal potentially included cosmopolitan Tethyan taxa also found in Europe (such as the ammonite *Pseudokossmaticeras*), however, it could include some Californian (Squires and Saul, 2006) or Peruvian fauna (Philip and Jaillard, 2004; Dhont and Jaillard, 2005). Johnson et al. (2002) and Philip and Jaillard (2004) propose an SW-heading current along the northwestern coast of South America, traveling across the Caribbean island arcs, getting into northern Peru. This is based on the presence of Caribbean Province rudists in the Campanian-Maastrichtian of northern Peru. Johnson et al. (2002) propose ocean currents travelling south from California long the Pacific coast of North America to the Nicoya region. This route is more complicated due to the presence of Caribbean rudists in the Marshal Islands (Camoin et al., 1995).

Acronyms used in this paper are listed in Table 1.

Table 1. List of acronyms used in this paper.

Acronym	Meaning
ACP	Atlantic Coastal Plain
CF	Fossil collection (Spanish)
CLIP	Caribbean Large Igneous Province
ECG	Central American School of Geology (Spanish)
EMORB	Enriched mid-ocean ridge basalts
GCP	Gulf Coastal Plain
K-Pg	Cretaceous-Paleogene extinction event
LIP	Large igneous province
MCA	Multivariate correspondence analysis
MCOT	Mesquito Oceanic Composite Terrane
NMDS	Non-metric multidimensional scaling
SI	Similarity indexes
UCR	University of Costa Rica
WIS	Western Interior Seaway

GEOLOGICAL SETTING

The Late Cretaceous mollusk-bearing deposits of Costa Rica are located in the northwest of the country, in the Puntarenas and Guanacaste provinces, also known as the Nicoya region (Text-fig. 1). The sedimentary basins which contain Late Cretaceous mollusks are the Sandino and Tempisque Basins, which are separated by the Santa Elena Peninsula (Aguilar and Denyer, 2019) (Text-fig. 1B). The basement of northwestern Costa Rica consists of different fragments of oceanic crust that were docked against the Mesquito Composite Oceanic Terrain (MCOT) of Nicaragua and Honduras (Flores, 2009; Flores and Gazel, 2020; Gazel et al., 2021) (Text-fig. 1A).

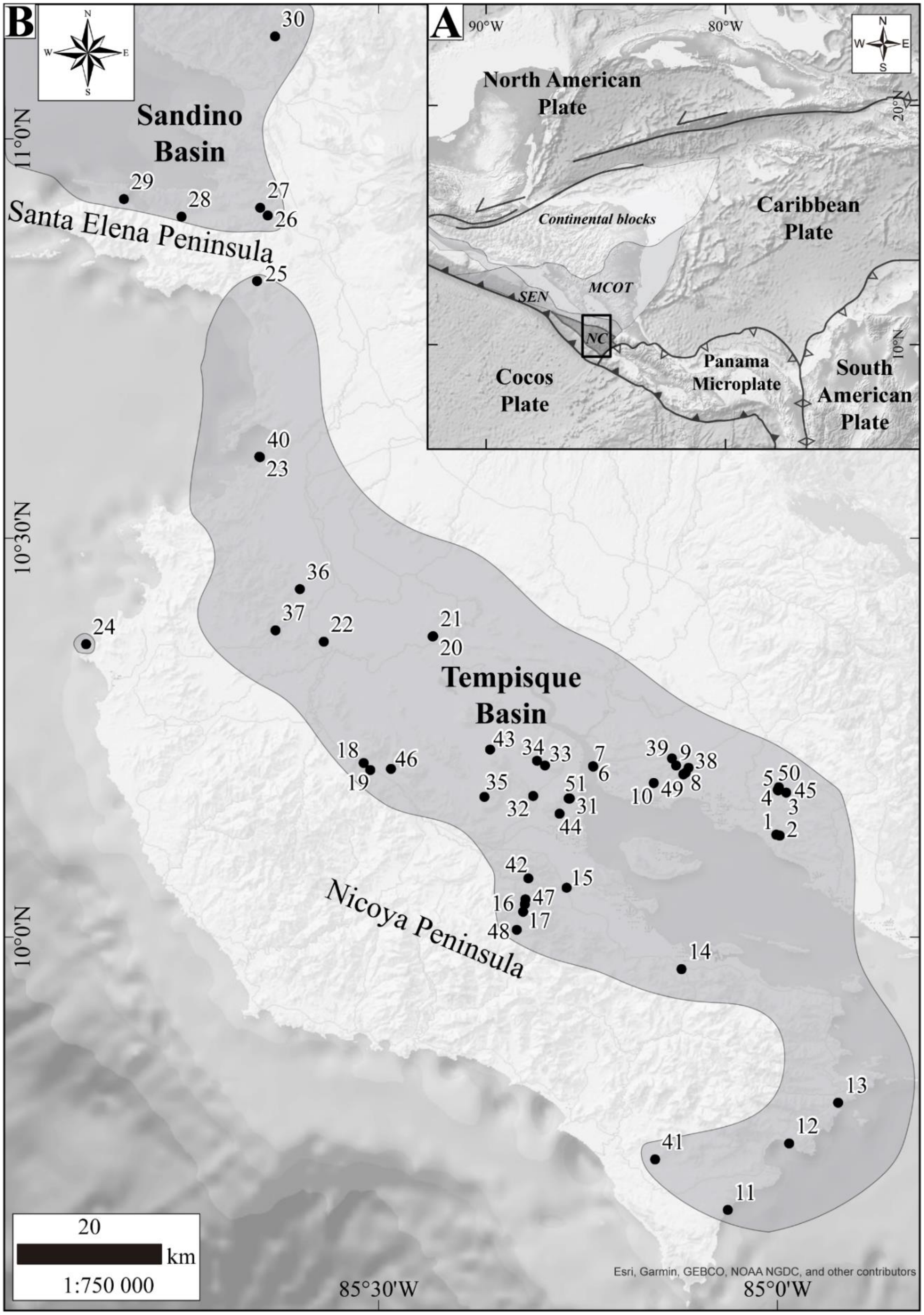
B
N
S
E
W
Sandino Basin
Santa Elena Peninsula
Tempisque Basin
Nicoya Peninsula
11°0'N
10°30'N
10°0'N
85°30'W
85°0'W
30
29
28
27
26
25
40
23
36
37
22
21
20
24
18
19
46
43
34
33
7
6
35
32
51
31
44
39
9
38
8
10
49
5
50
4
45
3
1
2
42
15
16
47
17
48
14
13
12
41
11
20
km
1:750 000
Esri, Garmin, GEBCO, NOAA NGDC, and other contributors
A
90°W
80°W
20°N
10°N
North American Plate
Caribbean Plate
Continental blocks
MCOT
SEN
NC
Cocos Plate
Panama Microplate
South American Plate

Text-fig. 1. Location map of the study area. A, Geotectonic context of the Nicoya region (modified from NOAA, 2009; Flores and Gazel, 2020; Gazel et al., 2021). MCOT = Mesquito Oceanic Composite Terrane, SEN = Santa Elena Nappe, NC = Nicoya Complex. B, Geographic distribution of the localities referenced in the present manuscript. For complete information about the localities see Appendix 2.

These areas have been well-mapped and characterized since the 1960's. Flores (2009) divides the Costa Rican territory into two different tectonic blocks with different basement and geologic history: (1) northwestern Costa Rica, closely associated with Nicaragua and Honduras, and (2) the rest of the country attached to the Panama Microplate (Figure 1B). Of these fragments, the Santa Elena Peninsula is formed by the Santa Rosa Accretionary Complex (Middle Jurassic seamount flank) overthrusted by the Santa Elena Nappe (serpentinized peridotites intruded by Barremian to Aptian pegmatitic gabbros and dolerites (Bandini et al., 2011; Buchs et a., 2013; Madrigal et al., 2015). Three kilometers south of the Santa Elena Peninsula, there are enriched mid-ocean ridge basalts (EMORB) forming the Nicoya Complex basaltic plateau (Dengo, 1962; Denyer et al., 2014; Madrigal et al., 2015, 2016); these basalts characterize the basement from south of the Santa Elena Peninsula to the southern tip of the Nicoya peninsula. The Nicoya Complex consists of mainly massive and pillow basalts, with associated gabbros, plagiogranites and komatiites (Denyer et al., 2014 and references therein). The basalts represent three different Pacific large igneous provinces (LIPs) dated as Valanginian (140 Ma), Aptian-Albian (120-110 Ma), and Cenomanian-Turonian (95-89 Ma) (Madrigal et al., 2016). The last pulse of basalt deposition is correlated to the Caribbean Large Igneous Province (CLIP), and has been aged with the gabbroic and komatiitic intrusion (89 Ma) (Denyer et al., 2014).

The diversity of oceanic basements in such a restricted area demonstrates a very complex geological history of accretions and docking that is well known throughout the Caribbean region. There is, however, ongoing debate surrounding the timing of emplacement of these complexes into the MCOT, but the maximum age of docking is constrained by the rudist-bearing deposits of El Viejo Formation. These deposits collectively form a major marker bed in the region and are referred to as “rudist bed” in this study (some localities yield rudist reefs, while other toppled solitary rudists); they lie on top of both basement complexes (Schmidt-Effing, 1974; Denyer et al., 2014; Pons et al., 2016b) (Text-figs. 2, 3).

Two sedimentary basins contain the units with the fossil molluscan record examined here (Text-fig. 3). In the Tempisque Basin, the oldest studied formation is the Loma Chumico Formation. It consists of basaltic and jasper breccias, and siliceous and oil shale deposits (Calvo, 1998; Flores, 2003; Andjic et al., 2019). The oil shale levels host the ammonite *Neokentroceras* sp. of early Late Albian age (Azema et al., 1979; Astorga, 1997). Up-section, the Nambi Formation consists of basaltic turbiditic sandstones, including inoceramid bivalves and a turritellid gastropod (Flores, 2003). The age of the lowest inoceramids was determined as Early Coniacian using strontium isotopes (Flores, 2003; Weber, 2013), and the top as Late Campanian based on planktonic foraminifera (Flores, 2003).

The El Viejo Formation consists of rudist limestones and rudist-bearing basaltic conglomerates (Schmidt-Effing, 1974; Denyer et al., 2014; Pons et al., 2016b). Besides rudists, it contains nerineid gastropods, ammonites, inoceramid bivalves, trigoniid bivalves, and other gastropods and bivalves (Rivier, 1983; Aguilar and Denyer, 2002; Pons et al., 2016b). Up-section, the Santa Ana Formation consists of calciturbidites with rudists, corals, algae, and nerineid and inoceramid fragments reported (Denyer et al., 2014). Transitionally overlying the El Viejo Fm., the San Buenaventura Formation (Flores, 2003) is composed of massive calcareous blue-grey sandstones in which *Pseudokossmaticeras?* sp. was reported (Schmidt-Effing, 1974). This unit has Late Campanian-Early Maastrichtian planktonic foraminifera (Calvo, 1998). The San Buenaventura Fm. is unconformably overlain by the Loma Danta Member. of the Santa Ana Formation (Rivier, 1983; Flores, 2003), which is composed of calciturbidites with limestone levels that have rudist and inoceramid fragments; the age of the Loma Danta Member is not well constrained, ranging from Late Maastrichtian to Late Paleocene (Rivier, 1983).

In both the west-central and southern Tempisque Basin, on top of both Loma Chumico and Nambi formations, are the red and white mudstones of the Piedras Blancas Formation (Flores, 2003). This unit includes inoceramid bivalves in the red basal mudstones at several localities, and has been dated as Latest Campanian (around 72 Ma) based on strontium isotopes in these areas (Weber, 2013). The top of this formation contains Late Campanian-Early Maastrichtian planktonic foraminifera (Flores, 2003). Conformably overlying the Piedras Blancas Formation are coarse grained turbidites known as the Curu Formation (Flores, 2003). In the west-central Tempisque Basin, ammonites and inoceramid bivalves have been recovered from the sandstones (Mora, 1978; Flores, 2003). At certain localities, the base of the Curu Formation are coarse conglomerates of the Quebrada Pavas Member (Flores, 2003), which contain inoceramid fragments dated as Latest Campanian using strontium isotopes (around 72 Ma), but they could be reworked from the Piedras Blanc Fm., since the base of the Quebrada Pavas Mb. is erosive (Flores, 2003; Weber, 2013). The age of the Curu Formation has been reported as Late Maastrichtian-late Paleocene (Astorga, 1987).

In the Sandino Basin (Text-fig. 3) the El Viejo Formation lies on top of the basement, north of the Santa Elena peninsula (Aguilar and Denyer, 2019). These rocks have been interpreted as shallow-water deposits, suitable for the growth of rudist reefs of Middle Campanian age (Pons et al., 2016b). Conformably overlying the El Viejo Formation, the red and white mudstones of the Piedras Blancas Formation lie (Aguilar and Denyer, 2019). However, no mollusks have been reported from this unit. Conformably above the Piedras Blancas Fm., there are coarse grained turbidites known as the Rivas Formation (Aguilar and Denyer, 2019). This unit contains inoceramid bivalves in life position north of the Santa Elena peninsula, close to the border with Nicaragua (Arroyo et al., 2016; Aguilar and Denyer, 2019).

El Viejo Formation was defined by Schmidt-Effing (1974) as the shallow marine deposits of Costa Rica which contained rudist bivalves forming reefs. This unit is a regional biomarker in both Tempisque and Sandino basins (Denyer et a., 2014). It is referred as the "rudist bed marker layer". Lateral correlation with El Viejo Formation are difficult to the lack of rudists, like Piedras Blancas Formation. El Viejo Formation shows heterogeneous lithologies with rudists bivalves in life position (Text-fig. 2). The rudist material was studied in detail by Pons et a. (2016b), they provided little information about the stratigraphy and distribution of the rudists. These rudists show strong affinity with the *Barrettia monilifera* limestone found in Jamaica, Cuba and Chiapas (Pons et al., 2016b).

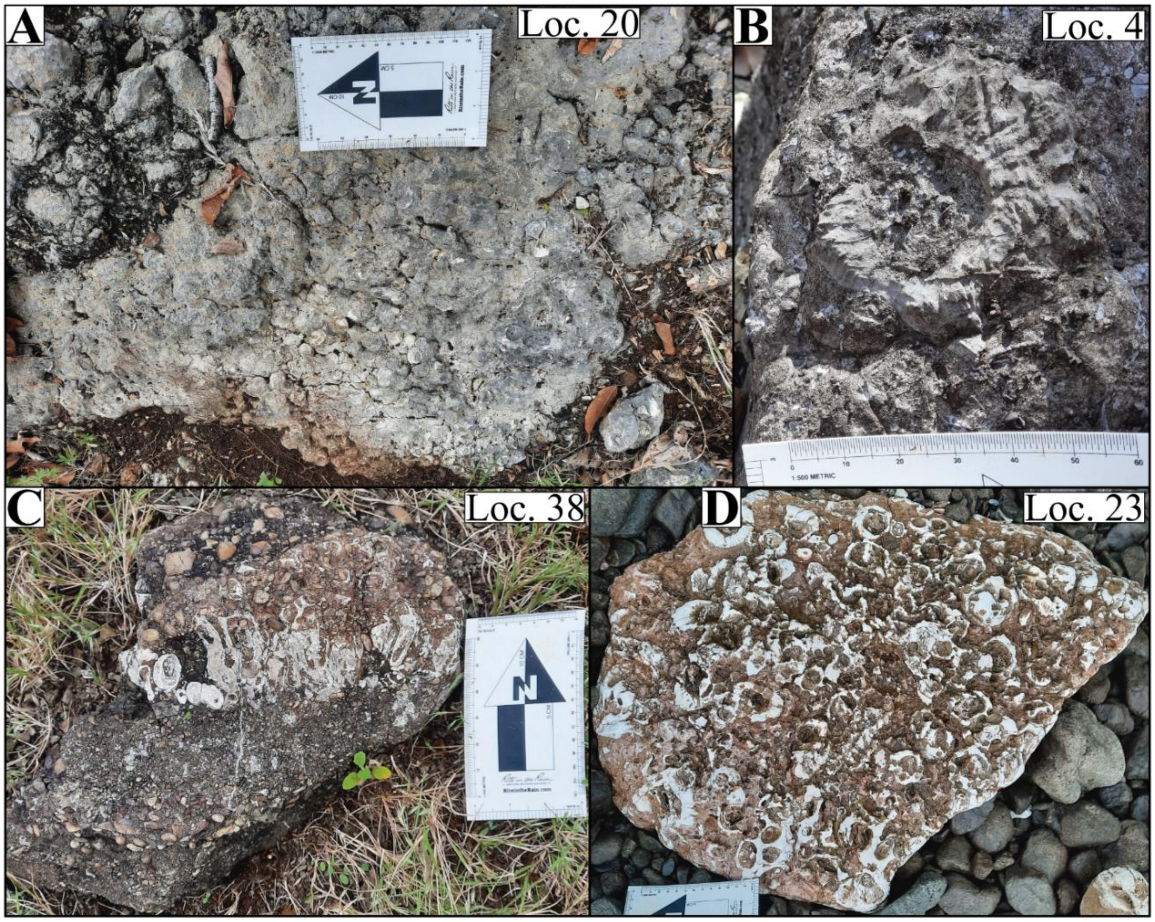

Text-fig. 2. Early late Campanian rudist bed marker layer. A, Raidolitid *Alencasterites mooretownensis* (Trechmann, 1924) framestone with rudstone matrix (Locality 20: Top of Cerro Cebollin). B, Toppled hippuritid *Barrettia monilifera* Woodward, 1862 in conglomeratic rudstone (Locality 4: Unnamed ridge). C, Radiolitid *Alencasterites mooretownensis* (Trechmann, 1924) reef level between medium conglomerates (Locality 38: Los Almendros Quarry). D, Block of hippuritid (*Barrettia?* sp.) reef level with medium conglomerate matrix (Locality 23: Playa Panama).

Given this excellent description of rudists, this research focuses the non-rudist molluscan assemblages from the relatively well-dated early Late Campanian to Early Maastrichtian of northwest Costa Rica. Fossiliferous deposits have been collected and characterized from 42 localities in the Sandino and Tempisque basins. Historical collections and those acquired through this project (reposited at the ECG paleontology collection of the UCR), are combined with 30 high-resolution stratigraphic logs characterizing the geology and facies context of fossil-bearing locations. This work updates and/or expands 51 fossil localities which were defined by looking at the labels of the ECG collection or reported in the literature.

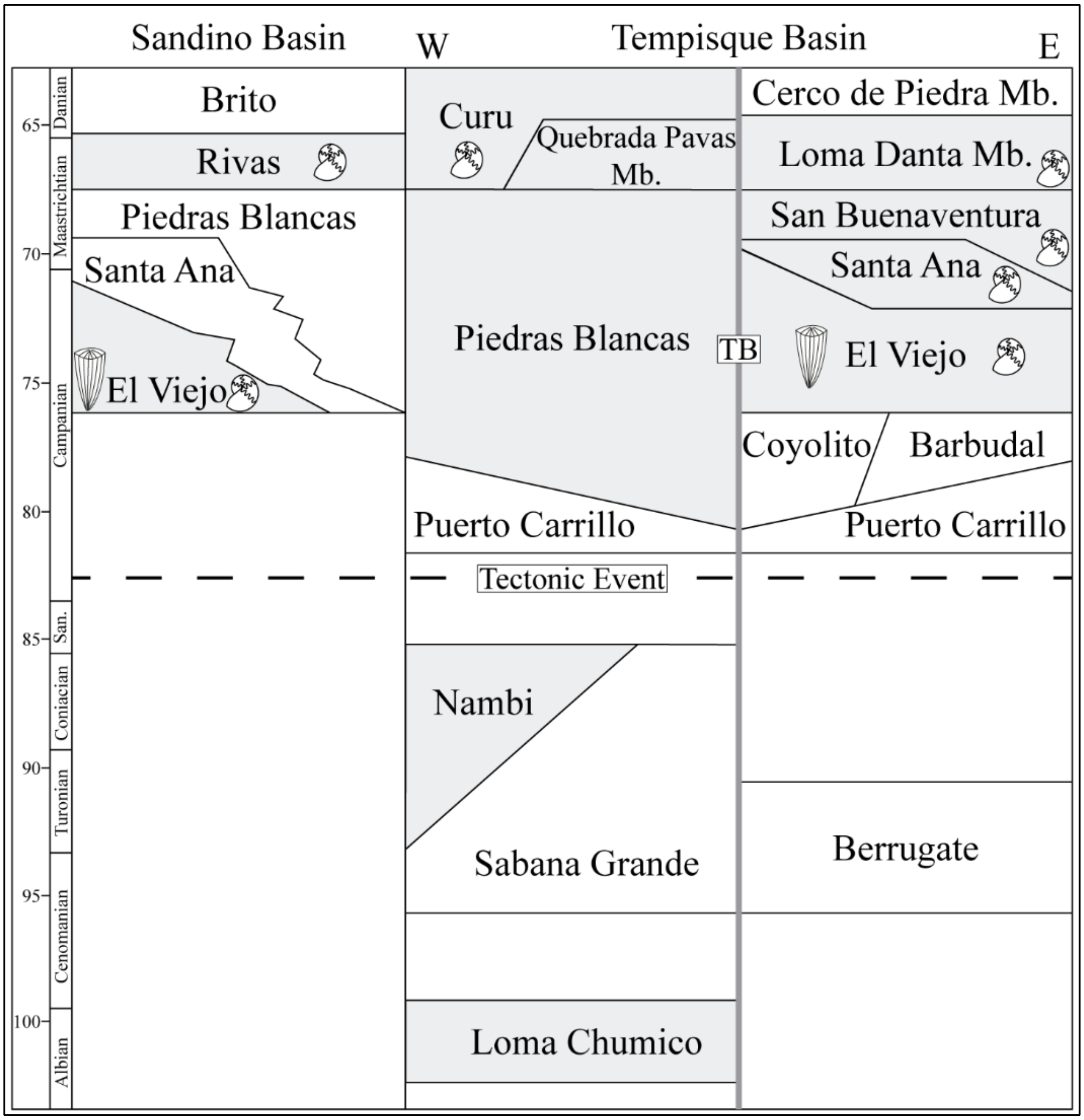

Text-fig. 3. Stratigraphic units mentioned in this manuscript (modified from Flores, 2003, Denyer et al., 2014, Aguilar and Denyer, 2019). Gray shading indicates units with non-rudist molluscan fossils studied in the manuscript. Ammonite symbols indicate units with updated biostratigraphic data. Rudist symbols represent the El Viejo Formation, the “rudist bed” marker layer in his study. The thick gray line with TB represent a tectonic boundary inside the Tempisque Basin.

MATERIALS AND METHODS

DATA COLLECTION

Existing faunal and locality data for 51 fossil-bearing localities of Late Cretaceous age were compiled from published literature, ECG collections, and shared unpublished data from active researchers in this area (K. Flores, T. Aguilar) (Appendix 2). Additional fieldwork in December 2022 and December 2023 provided more complete faunal and stratigraphic records from sites not previously studied, or those that needed updated/more detailed information.

Previous and newly collected specimens were photographed for later identification. The field fossil relative abundance and orientation were noted (including specimens not collected), as well as taphonomic condition, sedimentary structures, and composition and grain size of beds. Sedimentological data was used to place faunal assemblages into paleoenvironmental context and document geological history of the area. All newly collected specimens were reposited in the paleontology collections at ECG.

Stratigraphic field data were used to reconstruct several local and composite stratigraphic logs with ~ 50 cm resolution. True thicknesses of stratigraphic units were calculated in Adobe Illustrator CC 2018 (Adobe Inc., 2017) from maps created in ArcMap 10.4 (ESRI, 2016). Relevant sedimentary structures and fossil assemblages are included in these logs. Fieldwork and literature research resulted in 30 updated and revised stratigraphic sections (Appendix 1, Appendix 3). Stratigraphic logs were grouped according to similarities in sedimentology and geographical proximity. This resulted in subdivisions in the northern, central southwest and southern subareas. Log C15, while being close to the southwest subarea, is correlated with the southern subarea because of similarity in facies. Loma Chumico Formation outcrops are patchy due to tectonic activity.

The determination of sediment environments was based on the combination of lithology, grain size, sedimentary structures and taphonomic characteristics observed from the fauna. Relative sea level could be inferred as shallow if there were coarse sediments and/or associated to rudist reefs in life position, since they are typical of very shallow environments (Sanders and Pons, 1999). Deeper relative sea level could be inferred by the combination of finer grained lithologies and the presence of fauna that preferred deeper offshore environments. These observations were compared and contrasted with facies models developed for carbonate and siliciclastic platforms of the Lower Gosau Group (Coniacian-Early Campanian of Austria (Sanders et al., 1997; Sanders and Pons, 1999), the Chiapas Central Depression of Mexico (Early Campanian-Latest Maastrichtian) (Michaud and Fourcade, 1989; Pons et al., 2016a) and the Guinea Corn Formation of Jamaica (Latest Maastrichtian) (Mitchell, 2002). These three facies models include several rudist-bearing levels, which have different environmental interpretations according to the taphonomy of rudist bivalves.

High resolution photos of existing and newly collected fossil taxa were taken using a Cannon DX3200 camera and Samsung A51 and A53 cellphone cameras. Photos were compared to existing, identified species in ECG collections as well as published literature. Given the lack of formal study of these faunas previously, many identifications also benefited from discussion with experts in bivalves (T. Aguilar), gastropods (S. Kiel, H. Löser), and cephalopods (C. Ifrim, N. H. Landman).

Taxon identifications were made mainly at the genus-level, and species-level when possible. Relevant metadata such as age, locality, lithology, was compiled into a taxonomic dataset and used for statistical analyses (Table 2, Appendix 4).

STATISTICAL METHODS

For statistical analyses, data were filtered to the genus-level and restricted to assemblages of early Late Campanian to Early Maastrichtian age. This resulted in 98 genera from 24 localities (11 early Late Campanian, 6 Latest Campanian, 7 Early Maastrichtian). Hypothesis 1 (different paleo-communities existed and are associated with different paleoenvironments) was investigated by first using ordination techniques such as similarity indexes (SI) and derived techniques like non-metric multidimensional scaling (NMDS) (Fang et al., 2019) to explore relationships among localities using presence-absence fossil data in the context of sediment-derived paleoenvironmental data (Hammer and Harper, 2006).

Another exploratory technique used was Multivariate Correspondence Analysis (MCA). This technique quantifies differences and define groups of similar observations based of categorical datasets (i.e., age, lithology, locality, genus) (Kassambara, 2017). This was used in a multidimensional framework to compare fossil assemblages within the context of their respective lithology and age.

Hypothesis 2 (faunal migration is observable between the Tethyan and Pacific oceanic realms) was tested qualitatively by comparing the Costa Rican fauna with similar age faunas from other Caribbean localities (Cuba, Jamaica, Chiapas), California, Northern Peru, Gulf Coastal Plain and Mediterranean Tethys faunas.

All analyses were completed within the R programming language (R Core Team, 2020, version 4.0.2) and using the RStudio environment version 2022.7.2.576 (RStudio Team, 2022). Ordination, dissimilarity indices and MCA were computed using the packages: vegan (Oksanen et al., 2019), parallelDist (Eckert, 2018), and ggplot2 (Wickham, 2016), FactoMineR (Lê et al., 2008), factoextra (Kassambara and Mundt, 2020).

RESULTS

LOCALITY INFORMATION AND STRATIGRAPHIC SECTIONS

Stratigraphic and faunal data collected from 51 localities are detailed in Appendix 2, but several localities were not statistically analyzed due to data quality. Locality 42 was excluded because the fossil material from ECG museum collections were misplaced. Localities 27 and 29 were excluded because only rudist bivalves and corals were reported and these sites could not be visited for verification due to permitting issues. Six additional localities were excluded because no fossil material had been reposited in the ECG collection (Localities 2, 8, 33, 34, 45), or could not be visited due to lack of permits (Locality 25). This cleaning left a total of 42 fossiliferous localities with detailed stratigraphic data (Table 2). From these, 30 stratigraphic logs were constructed to describe the sediments and fauna of the study area; this represents 14 new stratigraphic sections, six existing sections updated during fieldwork, and 10 modified from existing literature (Appendix 1, Appendix 3).

Relative dates, determined by prior biostratigraphic analyses, span the early late Albian? to Early Maastrichtian (Text-fig. 5). However, only faunal assemblages from early Late Campanian to Early Maastrichtian (37 localities in total) were included in hypothesis investigations because these localities are the best studied and contain the highest abundance and diversity of fauna (19 early Late Campanian, 9 Latest Campanian, 9 Early Maastrichtian). Fossil abundance in these localities ranges from 1-9 individuals (24 localities), 10-20 individuals (seven localities), and greater than 40 individuals (two localities) (Table 2). All specimens are reposited at the ECG collection at the UCR.

The localities grouped into 30 stratigraphic logs were further divided into four subareas according to their geographic location and similarities in stratigraphy (Text-fig. 7. Appendix 1, Appendix 3).

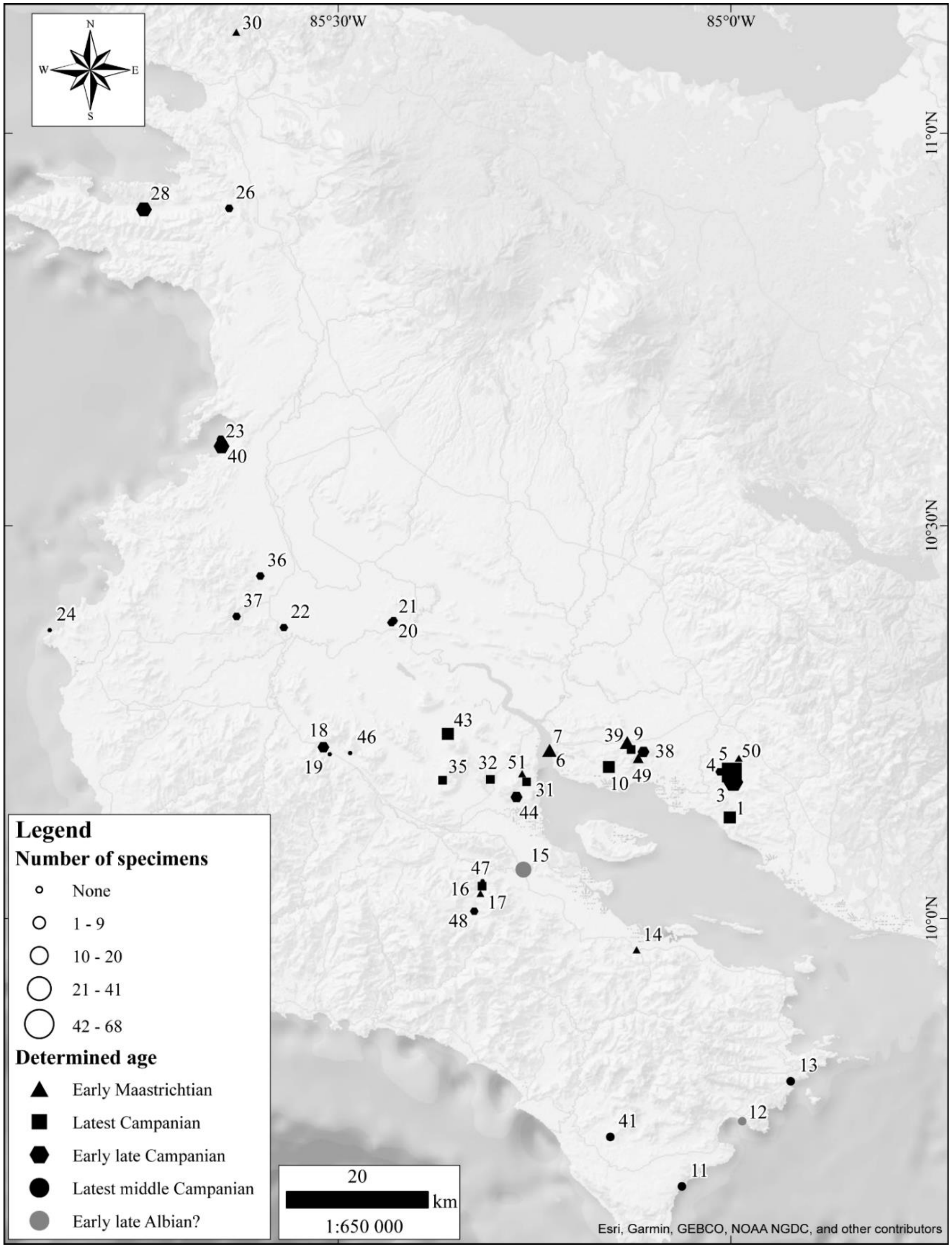

Text-fig. 4. Determined age for the studied localities and number of specimens reported and/or collected per locality. For complete information about the localities see Appendix 2.

Table 2. Summary of the 42 filtered localities.

Name	Age	Taxa	Specimens
1. Manzanillo quarry	Latest Campanian	11	11
3. Cerro Congo's abandoned quarry	Early Late Campanian	17	68
4. Unnamed ridge	Early Late Campanian	1	3
5. La Irma Quarry	Latest Campanian	29	57
6. N of Puerto Nispero (middle part)	Early Maastrichtian	6	33
7. N of Puerto Nispero (lower part)	Early Maastrichtian	2	9
9. E of Cerros Cerco de Piedra (2)	Latest Campanian	5	5
10. San Buenaventura	Latest Campanian	9	20
11. Montezuma	Latest Middle Campanian	1	4
12. Punta Pochote	Early Late Albian?	1	5
13. Playa Organos	Latest Middle Campanian	1	6
14. Jicaral	Early Maastrichtian	2	5
15. Loma Chumico	Early late Albian?	6	27
16. W of Santa Rita	Latest Campanian	1	2
17. Quebrada Pavas	Early Maastrichtian	1	1
18. Nambi	Early Late Campanian	1	10
19. Quebrada Honda de Nambi	Early Late Campanian	0	0
20. Top of Cerro Cebollin	Early Late Campanian	2	9
21. NE slope of Cerro Cebollin	Early Late Campanian	1	1
22. Fila Machete's abandoned quarry	Early Late Campanian	1	1
23. N point of Playa Panama	Early Late Campanian	2	8
24. Punta Conejo	Early Late Campanian	0	0

Table 2 (cont.)

26. Antigua Marmolina (old "marble" quarry)	Early Late Campanian	1	3
28. El Hachal hill	Early Late Campanian	4	30
30. Quebrada Cacao	Early Maastrichtian	1	9
31. N of Copal	Latest Campanian	4	1
32. Cerro Taburete	Latest Campanian	1	1
35. NW of Cerro Barra Honda	Latest Campanian	1	2
36. Castilla de Oro	Early late Campanian	3	1
37. Cerro Coyolar (Huevo Frito)	Early late Campanian	1	1
38. Los Almendros Quarry	Early late Campanian	13	13
39. Cerro Cebollin of Colorado	Early Maastrichtian	3	41
40. Bahia Monte del Barco	Early late Campanian	2	27
41. Cobano	Latest middle Campanian	2	8
43. Caballito	Latest Campanian	5	11
44. Across Copal's cemetery	Early late Campanian	5	10
46. Quebrada Chilamate	Early late Campanian	0	0
47. Rio Blanco, Tacanis	Early late Campanian	0	0
48. Rio Blanco Este	Early late Campanian	2	7
49. E of Cerros Cerco de Piedra (3)	Early Maastrichtian	1	20
50. Across Finca La Irma	Early Maastrichtian	2	2
51. Cerro Copal	Early Maastrichtian	1	1

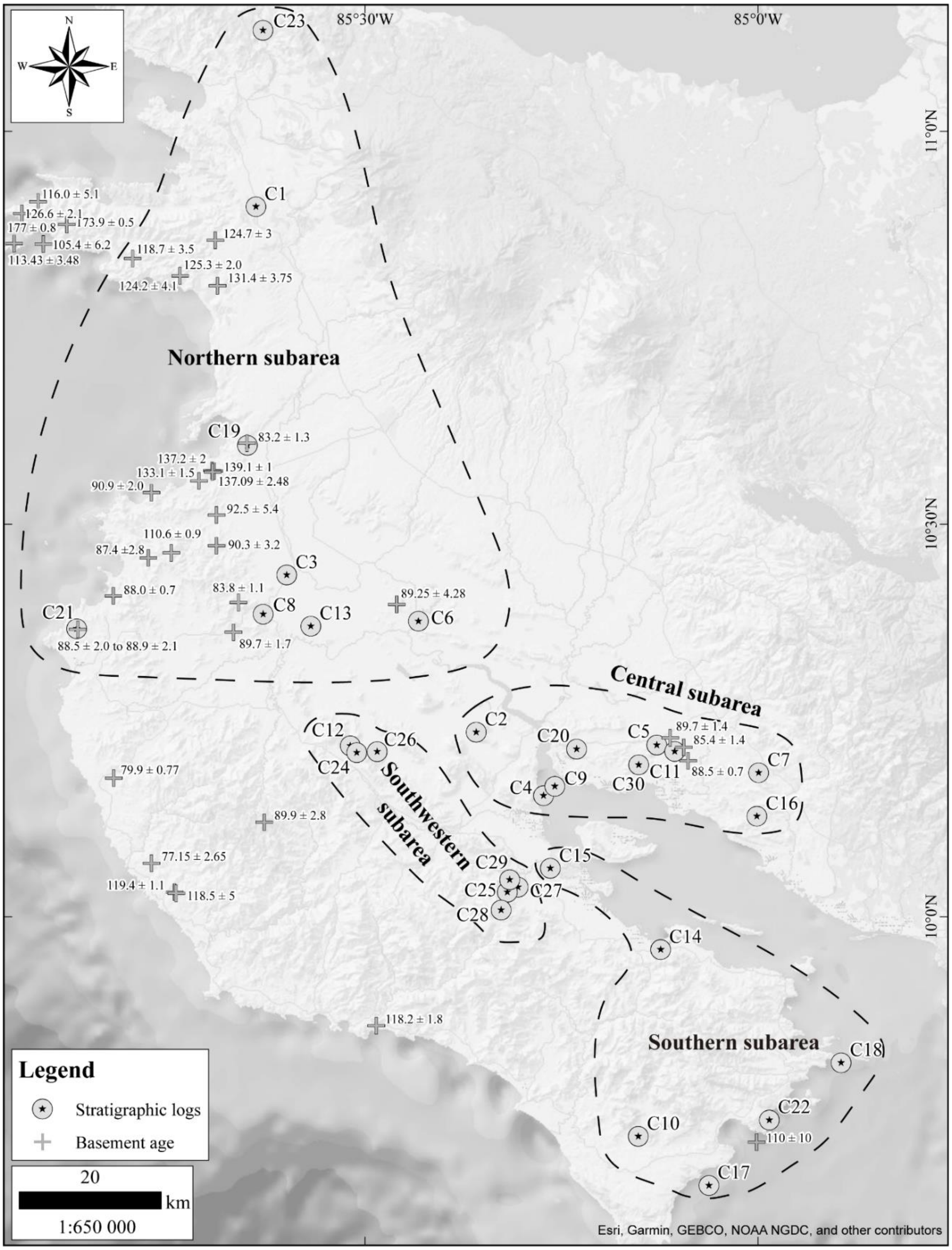

Text-fig. 5. Stratigraphic logs used in this study. For complete information about the stratigraphic logs, see Appendix 1 and 2. Basement ages after Whattam et al. (2016), Madrigal et al. (2016), Madrigal et al. (2015), Buchs et al. (2013), and references therein.

The southern subarea localities show little correlation with localities from other subareas, in part because the rudist bed (El Viejo Formation, early Late Campanian biomarker) is missing, making correlation more difficult. Only two localities yield ammonites (Localities 12, 14, Text-fig. 6D), but with no similarities to the ammonite faunas of the central subarea. Other localities only yield red foraminiferal mudstones with inoceramid prisms (Text-figs. 6A, 6C) or inoceramids in life position (Text-fig. 6B), and oysters growing on top of those prisms (Locality 41). However, no inoceramid molds were found, which limited taxon identifications to the family-level (Inoceramidae). These localities have silt or mud lithologies. Turbiditic deposits on top of white foraminiferal mudstones (Locality 15) yielded ammonite mold fragments and one belemnite rostrum. The age of these southern red foraminiferal mudstones was determined by stratigraphic position below tuffs dated as 76 Ma (Flores, pers. comm.).

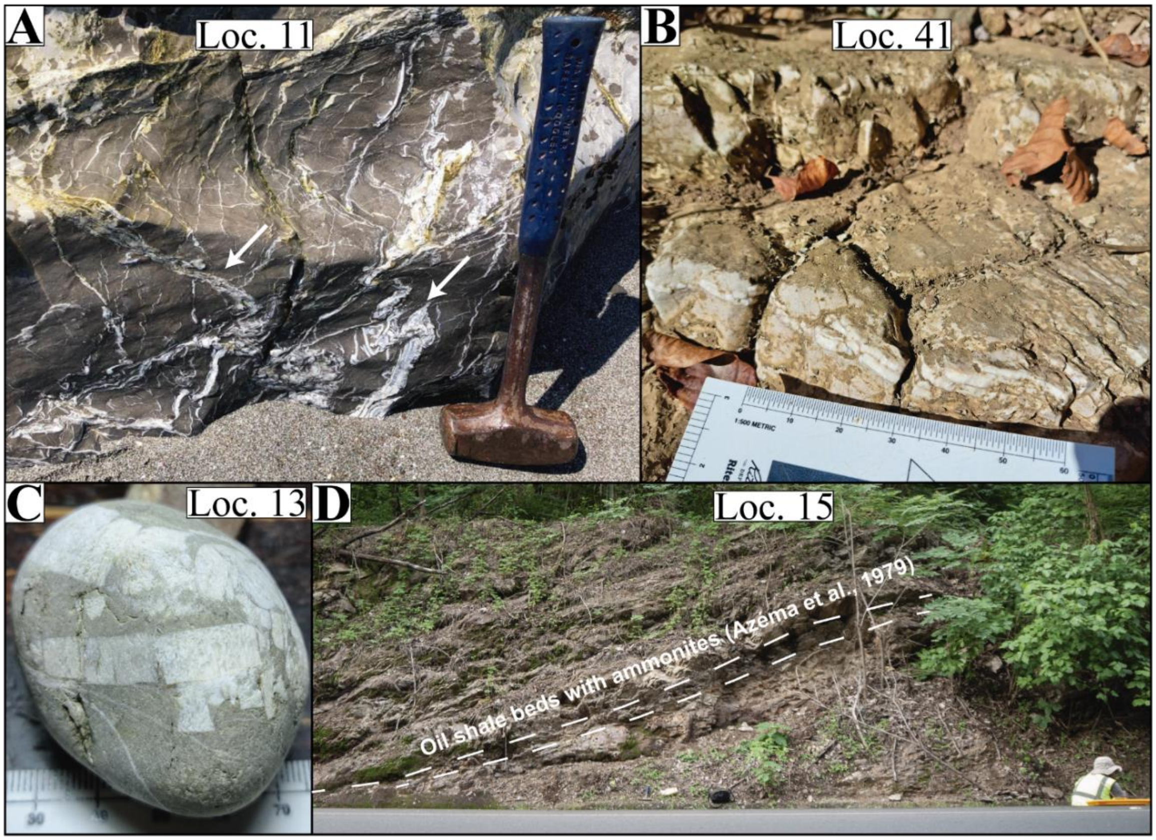

Text-fig. 6. Pre-early Late Campanian localities. A, Deformed mudstone beds with inoceramid prisms (white arrows) (Locality 11: Montezuma). B, Decimeter-long inoceramid bivalve in life position parallel to red mudstone beds (Locality 41: Cobano). C, Blocks of gray-reddish mudstone containing inoceramid prisms (Locality 13: Playa Organos). D, Part of the stratotype of Loma Chumico Fm. (Locality 15: Loma Chumico).

The rudist bed (El Viejo Fm., early Late Campanian biomarker) is present in the other three subareas (Text-fig. 8), which aids in log correlation. In localities of the central subarea where the rudist bed is found, there is evidence of tectonic uplift beneath it (Text-figure 7). This evidence can be viewed as continental deposits or fan delta breccia (Text-figs. 7A-B), or as a carbonate paleosoil (Text-figs. 7C-D). In the southwestern and northern subareas, the rudist bed is found above the basement, and the matrix sediment contains clasts derived from it. On section C7 (Colorado), the fan delta deposits are situated above submarine tuff levels dated at 78 Ma (Flores, pers. comm.).

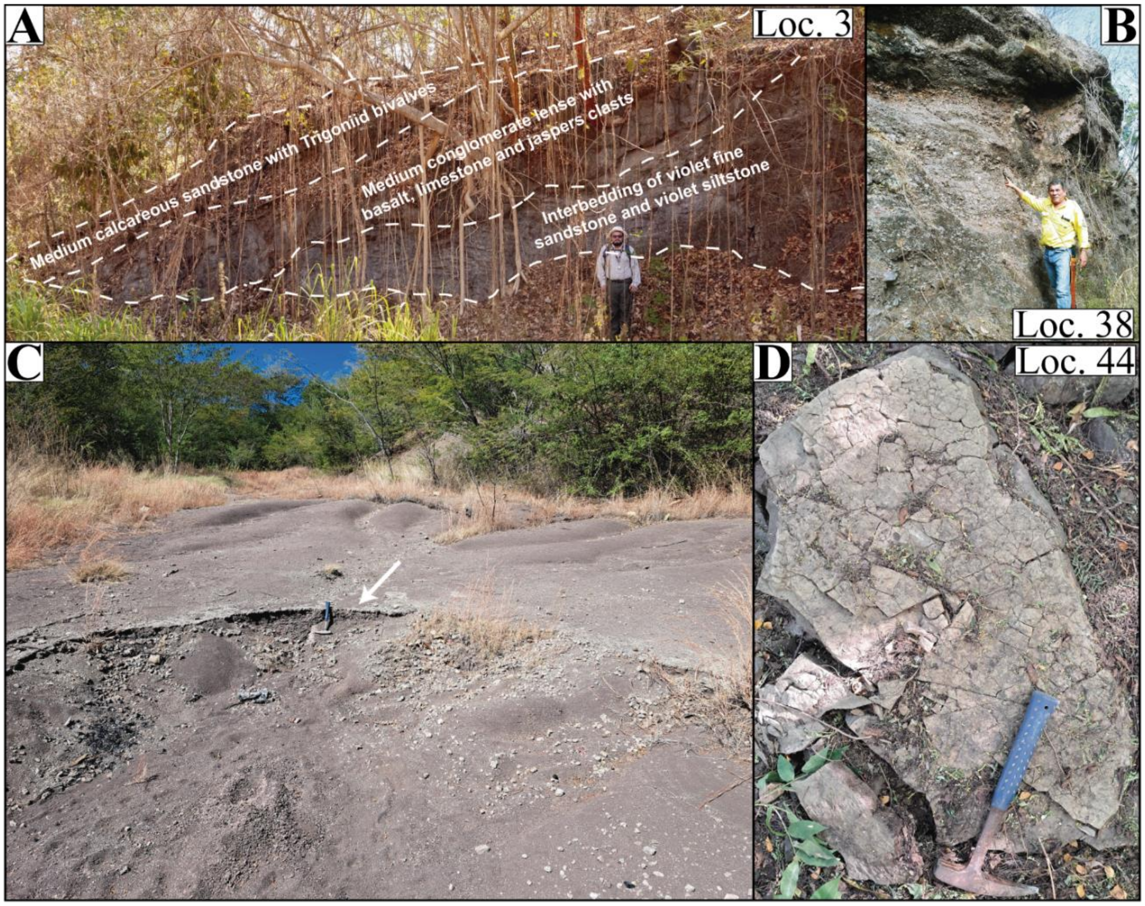

Text-fig. 7. Evidence of early Late Campanian tectonic uplift. A, Floodplain deposits and river channel beneath Locality 3 (Cerro Congo’s quarry). B, Violet basaltic breccia, fan delta deposits, below Locality 38 (Los Almendros Quarry). C, Paleosol level between violet foraminiferal mudstones (Cerro Sombrero, stratigraphic log C9 in Appendix 1). D, Block of paleosoil between interbedding of coarse and fine sandstones beneath Locality 44 (Copal’s cemetery).

Above the continental deposits, the paleosols or the basement, the rudist beds event is found throughout the rest of the subareas. Some localities have rudist reefs growing in life position (Text-fig. 2A, 2C, 2D), while others show toppled isolated rudists (Text-fig. 2B) or more extensive reworking. Lithology in these sections is highly variable, including medium calcareous sandstones (Text-fig. 8A), conglomeratic rudstones (Text-fig. 2B), rudist framestone into a rudstone matrix (Text-figs. 2A, 8B), beds of medium basaltic conglomerates (Text-figs. 2C-D, 8C), and coarse conglomerate lenses interbedded with interbedding of coarse and fine sandstones (Text-fig. 8D). The age of this rudist level is constrained to the early Late Campanian based on the presence of *Nostoceras hyatti* Stephenson, 1941 biozone in Locality 38. Also, lateral correlation was made with C9, where the paleosol is overlain by foraminiferal red mudstones containing 75 Ma hornblende tuffs (Flores, pers. comm.).

Following up section, most subareas show finer-grained lithologies. In the northern subareas, these deposits do not contain molluscan fauna. In the southwestern subarea, red foraminiferal mudstones yield inoceramid prisms levels and inoceramids in life position, but incomplete preservation makes generic identification difficult. Inoceramid prisms have been dated using Sr-isotopes as Latest Campanian (Weber, 2013). However, in the eastern part of the central subarea, these deposits yield abundant molluscan fossils, mostly in blue gray medium-fine sandstones to siltstones of the San Buenaventura Formation (Localities 1, 5, 9, 10, 49, Text-fig. 9). These deposits show dm-to-m thick-to-massive beds, and fossils are found as float in debris piles. These localities are biostratigraphically dated as Latest Campanian on the basis of *Pseudokossmaticeras brandti* (Redembatcher, 1873), *Baculites leopoliensis* Nowak, 1908 and *Pachydiscus* cf. *neubergicus neubergicus* biozones identified. The western half of the central subarea shows more complex lateral variations, with Locality 31 yielding *Glyptoxoceras retrosrsum* (Schlüter, 1872), also found in Locality 10.

Text-fig. 8. Early Late Campanian associated fauna to the rudist bed marker layer. A, Fine calcareous sandstone with trigoniid bivalves (Locality 3: Cerro Congo's quarry). B, Nerineid gastropod *Parasimploptyxis epelys* (Woodring, 1952) found between rudist and coral framestone (Locality 20: Top of Cerro Cebollin). C, Nerineid gastropod *Parasimploptyxis epelys* (Woodring, 1952) found in medium calcareous conglomerates (Locality 40: Bahia Monte del Barco). D, Fossiliferous coarse conglomerate lens with imbrication between interbedding of coarse and medium sandstones (Locality 44: Copal's cemetery).

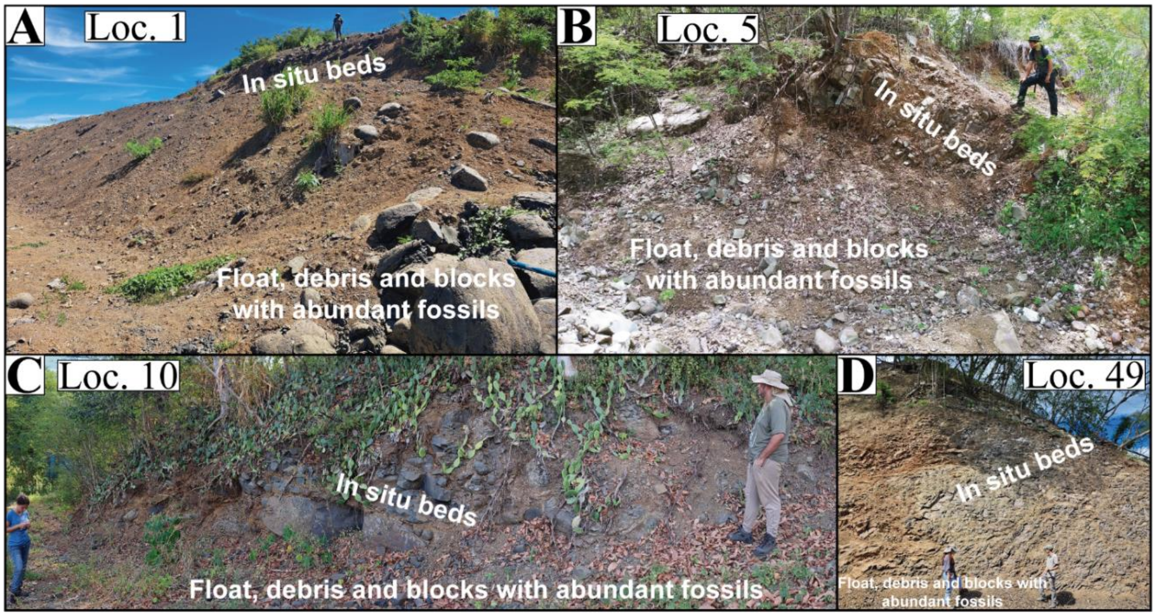

Text-fig. 9. Latest Campanian deposits of San Buenaventura Fm., most fossils are found as float in the debris. A, Blue gray fine sandstones-siltstones (Locality 1: Manzanillo quarry). B, Blue gray dm-m-thick medium sandstones (Locality 5: La Irma Quarry). C, Stratotype of San Buenaventura Fm., blue gray decimeter-thick medium to fine sandstones (Locality 10: San Buenaventura). D, Massive fractured blue gray medium sandstones near the top of the unit (Locality 49: E of Cerros Cerco de Piedra (3)).

On top of the previous deposits, in the northern, southwestern and southern subareas, there are coarse turbiditic deposits (Astorga 1987, 1997). These turbidites yield very few fossiliferous localities (namely Localities 15 and 30) that are likely Early Maastrichtian given their stratigraphic position on top of the Late Campanian-Early Maastrichtian Piedras Blancas Formation (Denyer et al., 2014; Aguilar and Denyer, 2019). In the central subarea, there are carbonate beds formed mainly by algal wackestones that can appear as a thick carbonate platform with coral reefs and nerineid gastropods (Localities 6, 7 and 51, Text-fig. 10A), or as decimeter-long and thick limestone lenses with small acteonellid and nerineid gastropods surrounded by shales and calcareous turbidites (Localities 39 and 50, Text-figs. 10B, 10D). One locality shows instead the development of calciturbidites with five beds of inoceramid prisms in life position (Locality 49, Text-fig. 10C). These carbonate deposits are Early Maastrichtian based on the presence of nerineid gastropods similar to *Plesioptygmatis* sp. and the coral *Marcelohelia* sp. (Chesnel et al., in prep.).

Text-fig. 10. Early Maastrichtian. A, Nerineid gastropod *Plesioptygmatis?* sp. between algal wackestones (Locality 6: Puerto Nispero (middle part)). B, Decimeter-thick limestone lens with corals, acteonellid and nerineid gastropods interbedded with white gray shales and mudstones (Locality 39: Cerro Cebollin of Colorado). C, Calciturbidites with five inoceramid prisms in life position and hornblende tuff levels (Locality 49: E of Cerros Cerco de Piedra (3)). D, Turritellid gastropod fragment (left white arrow) and coral colony (right white arrow) in algal wackestone lens (Locality 50: Across Finca La Irma).

Since in subduction zones sedimentary sections show extensive lateral variation, correlation between different sections have extra difficulty. However, by associating macrofauna and inferring relative sea level changes, correlations can be done between different subareas (Text-fig. 11). Sections in the central subarea show the most diverse molluscan faunas that show time and facies change. Southern sections are not included since neither the tectonic uplift, nor the rudist beds are detected.

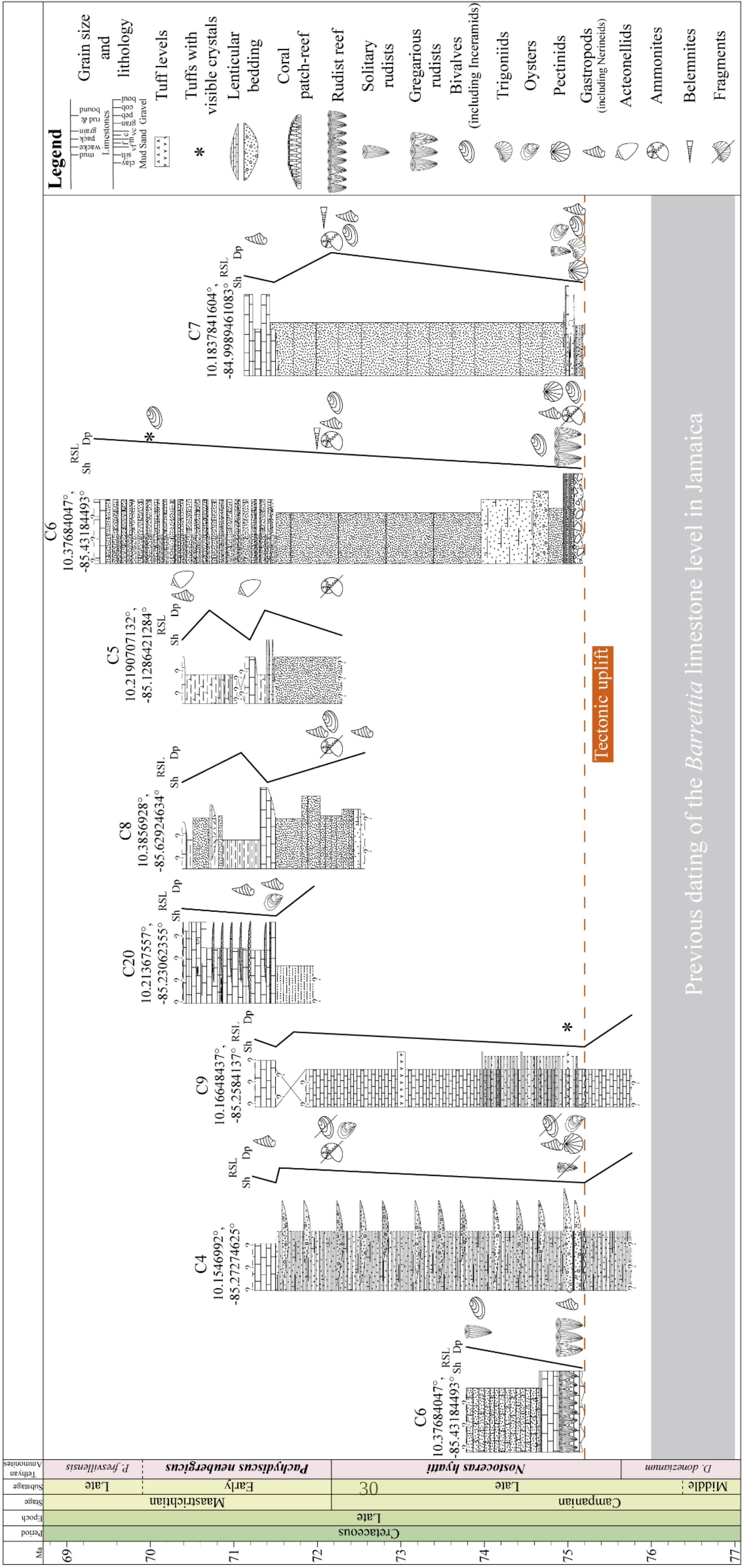

Ma
69
70
71
72
73
74
75
76
77
Period
Cretaceous
Epoch
Late
Stage
Maastrichtian
Campanian
Substage
Late
Early
Late
Middle
Tethyan Ammonites
P. fresvillensis
Pachydiscus neubergicus
Nostoceras hyatti
D. donezianum
C6
10.37684047°,
-85.43184493°
C4
10.1546992°,
-85.27274625°
C9
10.16648437°,
-85.2584137°
C20
10.21367557°,
-85.23062355°
C8
10.3856928°,
-85.62924634°
C5
10.2190707132°,
-85.1286421284°
C6
10.37684047°,
-85.43184493°
C7
10.1837841604°,
-84.9989461083°
Sh
RSL
Dp
Tectonic uplift
Previous dating of the Barrettia limestone level in Jamaica
Legend
Grain size and lithology
clay
silt
vf f m c vc
gran
peb
cob
boul
Mud
Sand
Gravel
mud
wacke
pack
grain
rud & bound
Limestones
Tuff levels
Tuffs with visible crystals
Lenticular bedding
Coral patch-reef
Rudist reef
Solitary rudists
Gregarious rudists
Bivalves (including Inceramids)
Trigoniids
Oysters
Pectinids
Gastropods (including Nerineids)
Acteonellids
Ammonites
Belemnites
Fragments

Text-fig. 11. Chronostratigraphic correlation and relative sea level (RSL) change in key stratigraphic logs.

The central, southwestern and northern subareas show evidence of tectonic uplift, followed by a relative sea level rise, in which the early Late Campanian rudist bed marker layer is detected. Up-section, sea level rise appears to continue in the three subareas during the latest Campanian. The northern and southern subareas show a change to coarse turbiditic sedimentation in the Early Maastrichtian (Astorga 1987, 1997) with very few molluscan fossils. The southwestern and central subareas show a relative sea level drop, which allowed the carbonate platform sedimentation in the central subarea. The southwestern subarea shows the onset of medium conglomerate sedimentation with mega-ripples and reworking of older rocks, and very few molluscan fossils.

TAXONOMIC IDENTIFICATION AND FINAL DATASET

A total of 478 specimens stored at the ECG paleontology collection or collected during fieldwork have been databased and georeferenced (a small number of specimens were photographed in the field but left uncollected). This resulted in 147 different taxa determined; 63 taxa were identified at a species level, 53 at genus level, and 27 at family level or above. Metadata associated with each specimen includes georeferenced locality, abundance, reported age, stratigraphic and lithology (Appendix 4).

Fauna recovered from localities older than Late Campanian included three morphospecies of small ammonites previously reported as *Neokentroceras* sp. by Azema et al. (1979) (Text-figs. 12-4, 12-5). This identification places them as early late Albian in age. The lack of visible sutures in the specimens makes it difficult to identify specimens beyond genus- or family-level affinities and the genera reported have long durations. In contrast, ammonite biozone data conflicts with radiolarian age reports (Andjic et al., 2019), indicating additional work is needed to better understand this fauna. Notably, this study found the first observation of encrusting oysters on inoceramid prisms, something commonly reported in the Coniacian-Early Campanian of Kansas (Hattin, 1986).

Text-fig. 12. Pre-early Late Campanian mollusks. 1, *Gaudryceras* sp., CF-1119 (Locality 15: Loma Chumico). 2-3, Acanthoceratidae indet., CF-1115 (Locality 15: Loma Chumico). 4, *Neokentroceras?* sp., CF-1467 (Locality 15: Loma Chumico). 5, *Neokentroceras?* sp., CF-3515 (Locality 15: Loma Chumico). 6, *Ostrea* sp. living attached to an Inoceramid prism (Locality 41: Cobano). Scale bars = 1 cm.

Fauna associated with the rudist bed is the most diverse and abundant. The presence of *Nostoceras hyatti* Stephenson, 1941 (Text-figs. 13-1 to 13-6) supports an early Late Campanian age for this fauna. Within the rudist bed several bivalves showed paleobiogeographic affinities to Jamaica, Cuba, Puerto Rico (like the rudist bivalves), including *Notoscabrotrigonia?* sp. (Aguilar and Denyer, 2002) (Text-figs. 13-7, 13-8), *Veniella jamaicensis* Trechmann, 1927 (Text-fig. 13-9), *Neithea* sp. (Text-figs. 13-10, 13-11), and *Trochoceramus?* sp. (Text-figs. 13-12, 13-13). Important paleobiogeographic gastropods include *Gyrodes* sp. (Text-figs. 13-14, 13-15), *Parasimploptyxis epelys* (Woodring, 1952) (Text-figs. 13-16, 13-17), *Parasimploptyxis* sp. B (Text-figs. 13-18, 13-19) and *Acteonella* sp. (Text-fig. 13-20). The presence of autochthonous solitary and gregarious or toppled rudists, in addition to this particular assemblage of bivalves and gastropods, supports a very shallow marine environment less than 15 m deep (Aguilar and Denyer, 2002). The presence of *Nostoceras hyatti* most likely indicates reworking from an offshore environment via flotation of dead ammonites to the shore (Hoffmann et al., 2021). *N. hyatii* is the Tethyan biomarker for the latest ammonite zone of the Campanian (Blaszkiewicz, 1980), whose base is determined around 75.4 Ma (Voigt et al., 2012).

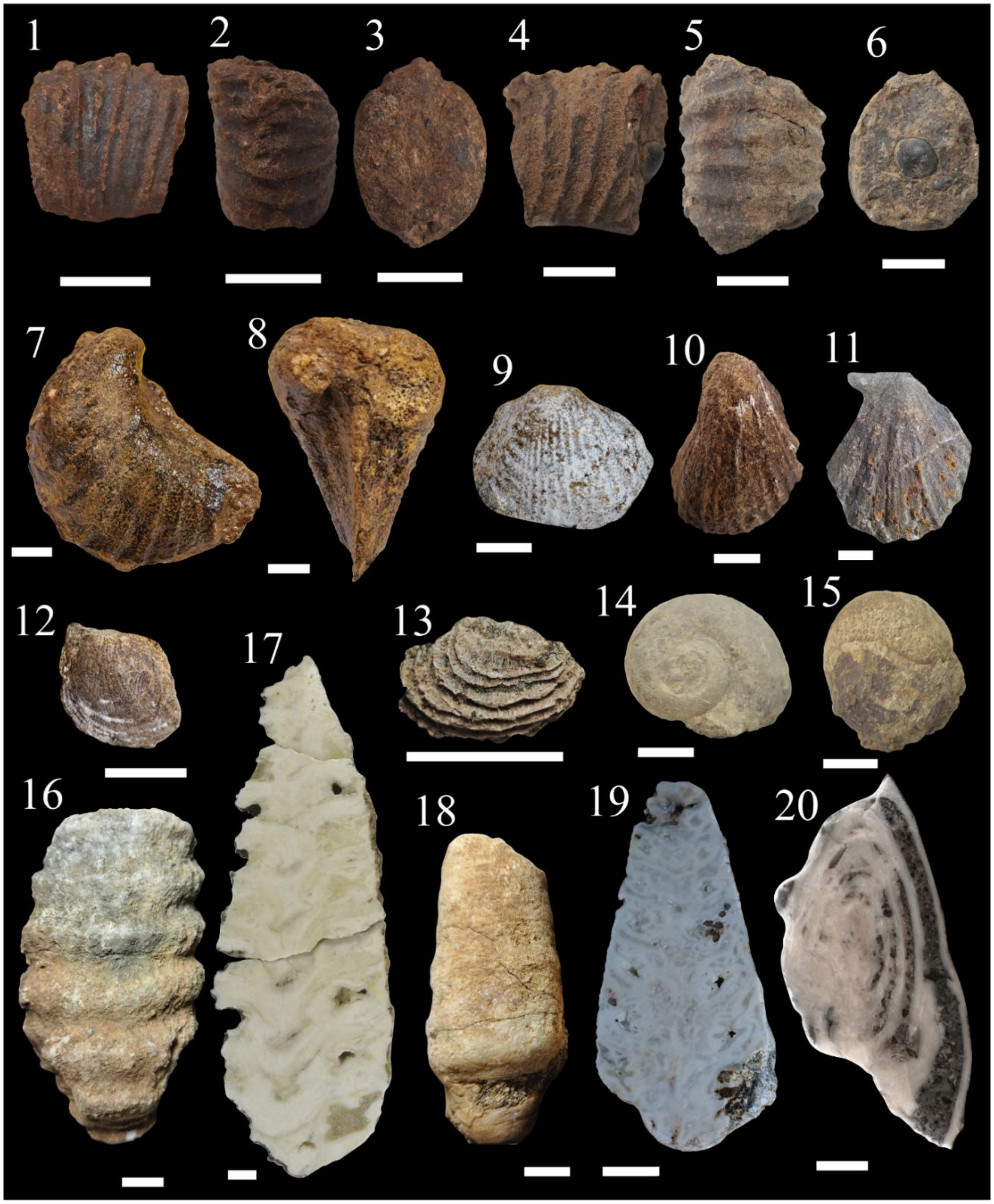

Text-fig. 13. Early late Campanian mollusks associated with the rudist level. 1-6, *Nostoceras hyatti* Stephenson, 1941, CF-3960 (1-3), CF-4507 (3-6) (Locality 38: Los Almendros Quarry). 7-8, *Notoscabrotrigonia?* sp., CF-4231 (Locality 3: Cerro Congo's quarry). 9, *Veniella jamaicensis* (Trechmann, 1927), CF-4230 (Locality 38). 10, *Neithea* sp. A, CF-4508 (Locality 38) 11, *Neithea* sp. C, CF-5770 (Locality 3). 12, *Trochoceramus?* sp. CF-4508 (Locality 38). 13, *Trochoceramus?* sp. (Locality

44: Copal’s cemetery). 14-15, *Gyrodes* sp., CF-3954 (Locality 38). 16-17, *Parasimploptyxis epelys* (Woodring, 1952), CF-6098 (Locality 20: Top of Cerro Cebollin). 18-19, *Parasimploptyxis* sp. B (Locality 40: Bahia Monte del Barco). 20, *Acteonella* sp. A (Locality 22: Fila Machete). Scale bars = 1 cm.

Above the rudist bed, in Localities 5, 9, 10, the environment changed. Latest Campanian localities have more abundant cephalopods (Text-fig. 14). Biostratigraphic age is determined by the presence of the ammonites *Pseudokossmaticeras brandti* (Redembatcher, 1873) (Text-fig. 14-4), *Baculites leopoliensis* Nowak, 1908 (Text-fig. 14-12), *Glyptoxoceras retrorsum* (Schlüter, 1872) (Text-figs. 14-8 to 14-10), and *Pachydiscus* cf. *neubergicus neubergicus* (Text-figs. 15-5 to 15-7). This age agrees with the planktonic foraminifera age reported by Calvo (1998) near Locality 49.

Other relevant ammonites from Localities 1, 5 and 10 include *Neophylloceras surya* (Forbes, 1846) (Text-fig. 14-1), *Gaudryceras* sp. (Text-figs. 14-2, 14-3), *Solenoceras* sp. (Text-fig. 14-11), and *Scaphites* sp. (Text-fig. 14-19). Locality five is notable given the presence of five morphospecies; three of which are shown in Text-figs. 14-13 to 14-18). Two remarkable findings are the first reports of (1) Late Cretaceous ammonite jaws in the Caribbean Province (at least one from the Scaphitidae) (Text-figs. 14-20, 14-21) and (2) post-Turonian belemnites in the Caribbean Province (*Belemnitella americana* (Morton, 1830)) (Text-figs. 14-22, 14-23).

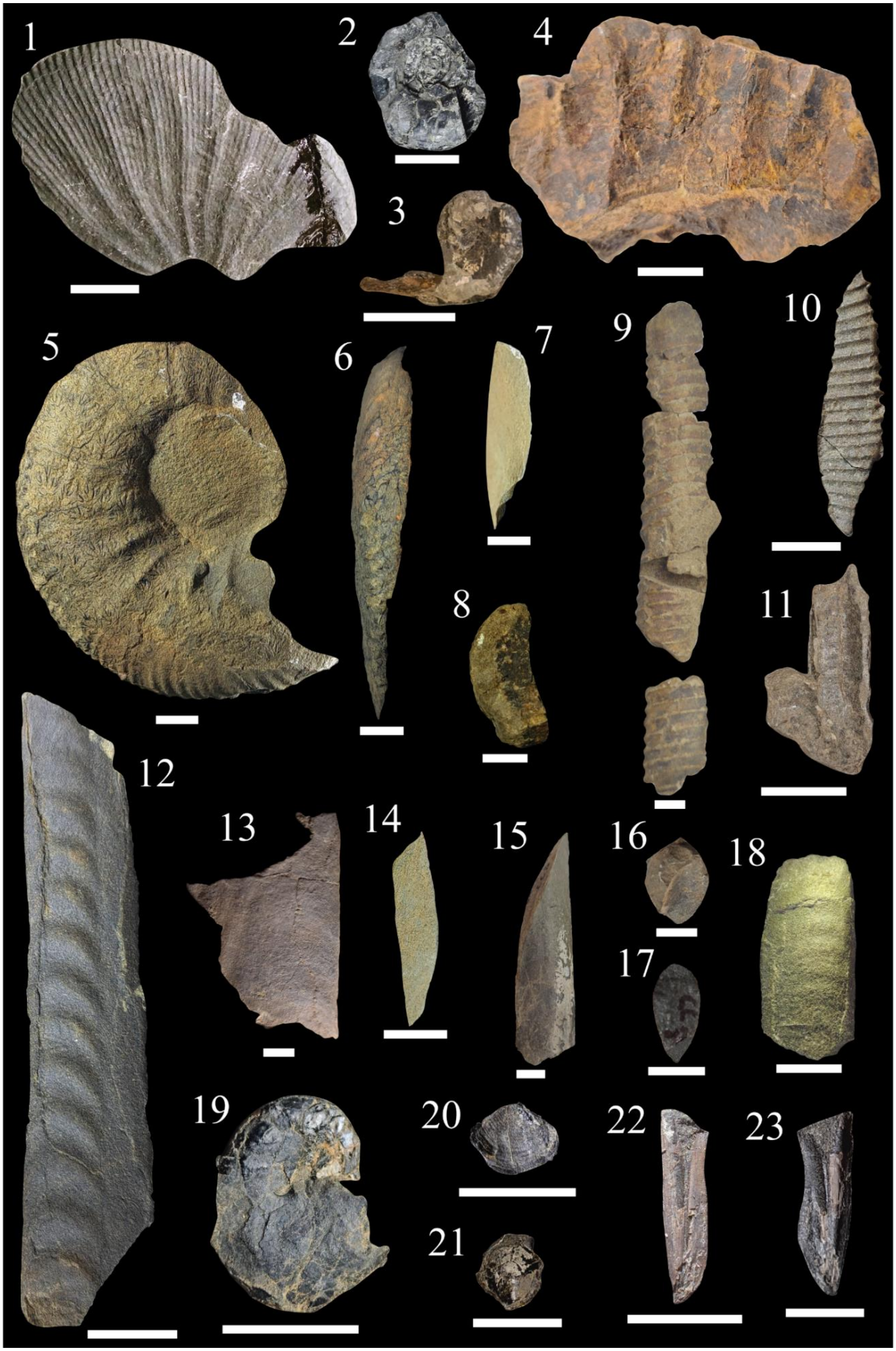
1
2
4
3
10
5
6
7
9
8
11
12
13
14
15
16
18
17
19
20
22
23
21

Text-fig. 14. Latest Campanian cephalopods. 1-6, *Neophylloceras surya* (Surya, 1846), CF-6126 (Locality 5: La Irma Quarry). 2, *Gaudryceras* sp. A (Locality 1: Manzanillo). 3, *Gaudryceras* sp. B (Locality 9: E of Cerros Cerco de Piedra (2)). 4. *Pseudokossmaticeras brandti* (Redembatcher, 1873), CF-3393 (Locality 10: San Buenaventura). 5-7, *Pachydiscus* cf. *neubergicus* (Locality 5). 8-10, *Glyptoxoceras retrorsum* (Schlüter, 1872), CF-599 (8-9) (Locality 31: N of Copal), 10 (Locality 10). 11, *Solenoceras* sp. (Locality 10). 12, *Baculites leopoliensis* Nowak, 1908 (Locality 5) 13-14, *Baculites* sp. frontward ribs (Locality 5). 15-16, *Baculites* sp. smooth 1 (Locality 5). 17-18, *Baculites* sp. weak ribs 1 (Locality 5). 19, *Scaphites* sp. (Locality 1: Manzanillo). 20, Scaphitidae jaw (Locality 1). 21. Ammonite jaw (Locality 1). 22-23 *Belemnitella americana* (Morton 1830). Scale bars = 1 cm.

Overall, bivalves and gastropods form a minority of the latest Campanian molluscan faunas (Text-figs. 15-1 to 15-9). Important bivalves for paleobiogeographic interpretations are represented by *Acila* sp. (Text-figs. 15-2, 15-3), *Macrocallista?* sp. (Text-fig. 15-3), *Mytilus?* sp. (Text-fig. 15-4), *Neithea* sp. (Text-fig. 15-5), *Cataceramus goldfussianus?* (d'Orbigny, 1847) (Text-fig. 15-6), and *Cataceramus* sp. (Text-fig. 15-7).

The Early Maastrichtian relevant fauna in paleobiogeographic terms is represented by *Plesioptygmatis?* sp. (Text-fig. 15-10), *Acteonella* sp. (Text-fig. 15-11), and *Acteonella duckettsensis* Sohl and Kollmann, 1985 (Text-fig. 15-12).

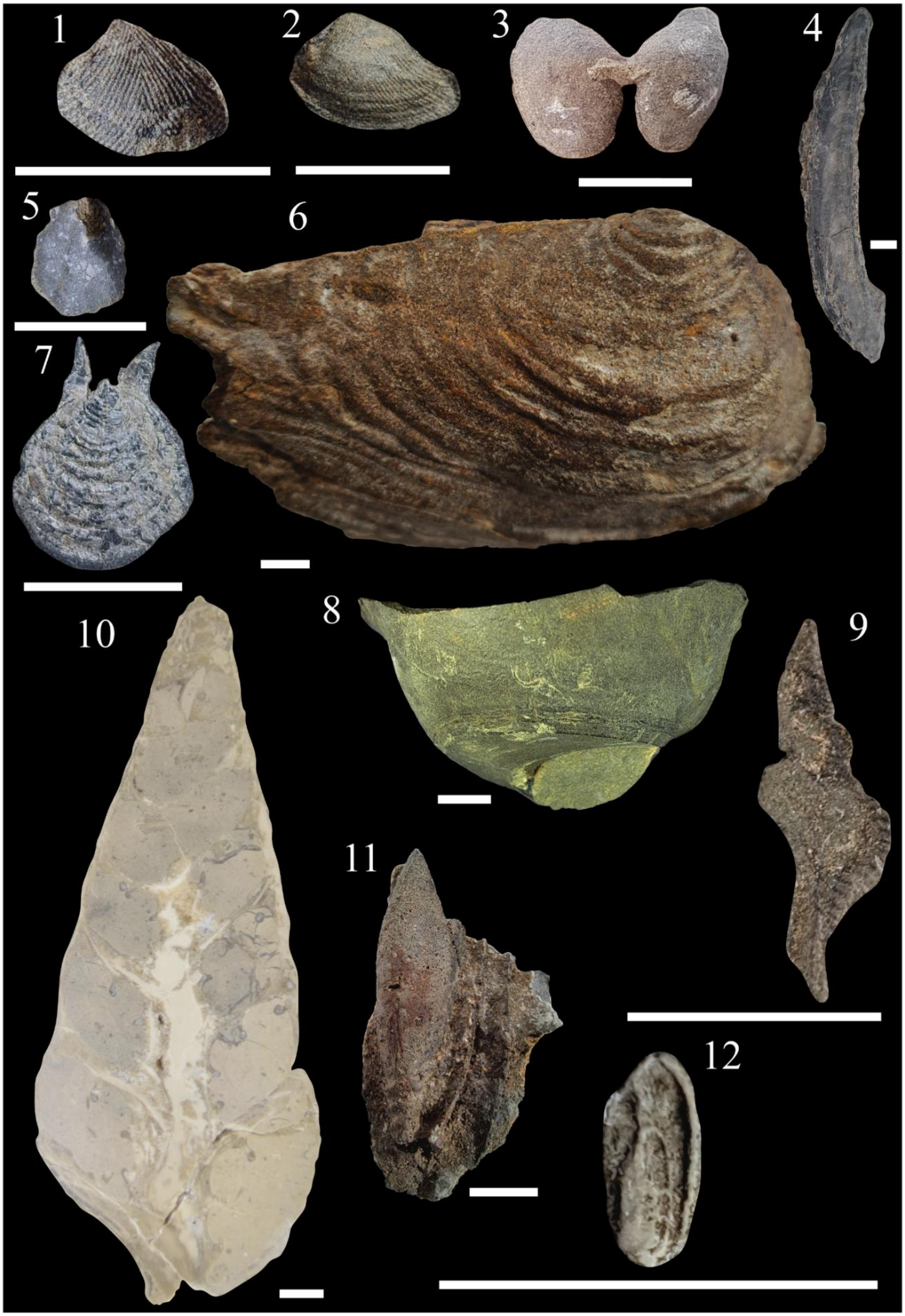
1
2
3
4
5
6
7
8
9
10
11
12

Text-fig. 15. Latest Campanian bivalves and gastropods (1-9), Early Maastrichtian gastropods (10-12). 1, *Acila* sp. A (Locality 5: La Irma Quarry). 2, *Acila* sp. B (Locality 1: Manzanillo). 3, *Macrocallista?* sp. B (Locality 5). 4, *Mytilus?* sp. (Locality 5). 5, *Neithea* sp. B (Locality 5). 6. *Cataceramus goldfussianus?* (d'Orbigny, 1847), CF-2293 (locality 43: Caballito). 7, *Cataceramus* sp. A (Locality 1). 8, *Terebra?* sp. (Locality 5). 9, *Fusinus* sp. (Locality 5). 10, *Plesioptygmatis?* sp. (Locality 6: Puerto Nispero (middle part)). 11, *Acteonella* sp. D, CF-2071 (Locality 39: Cerro Cebollin of Colorado). 12, *Acteonella duckettsensis* Sohl and Kollmann, 1985 (Locality 6). Scale bars = 1 cm.

STATISTICAL ANALYSES

After identifying the taxa, I performed an analysis based on dissimilarity indices and NMDS analyses were used to qualitatively explore potential clustering of fossil assemblages by different metadata metrics; each point in Text-fig. 16 reflects a single locality and distance between points is based taxonomic diversity and abundance similarity. These analyses are useful to identify potential clusters of localities that may be grouped by age, lithology, paleoenvironment, etc. (Fang et al., 2019). The NMDS plots (Text-figs. 16A-B) show one cluster containing the early Late Campanian rudist beds localities, with a second less clear cluster. The Raup-Crick index shows the second cluster is made of the Latest Campanian localities, while the Early Maastrichtian localities are spread out between and outside the clusters (Text-fig. 16A). The Ochiai index shows the Early Maastrichtian localities closer to the cluster of Latest Campanian ones (Text-fig. 16B).

The MCA plots show three different clusters associated by biostratigraphic age (Text-fig. 16C). However, MCA plotted by lithology is not very clear (Text-fig. 16D). The early Late Campanian localities (Text-fig. 16C) show a wide variety of facies (Text-fig. 16D). This indicates wide lateral variation of sedimentary environments that nonetheless share more similar taxa when compared to other time bins. The Latest Campanian cluster shows a dominance of calcareous fine sandstones, while the Early Maastrichtian cluster shows a dominance of algal wackestone facies (Text-figs. 16C-D). This supports the above results that assemblage similarity is more structured by age than paleoenvironment (assessed as by lithology). The Dim1 could be interpreted as representing relative sea level, with the early Late Campanian cluster representing very shallow environments dominated by rudist reefs (Text-figs. 16C-D). Latest Campanian localities show a deeper open shelf environment dominated by cephalopods (Text-figs. 16C-D). The Early Maastrichtian cluster represents a shallowing of the relative sea level, getting closer to the shore (Text-figs. 16C-D), but with a different shallow fauna compared to the early Late Campanian cluster.

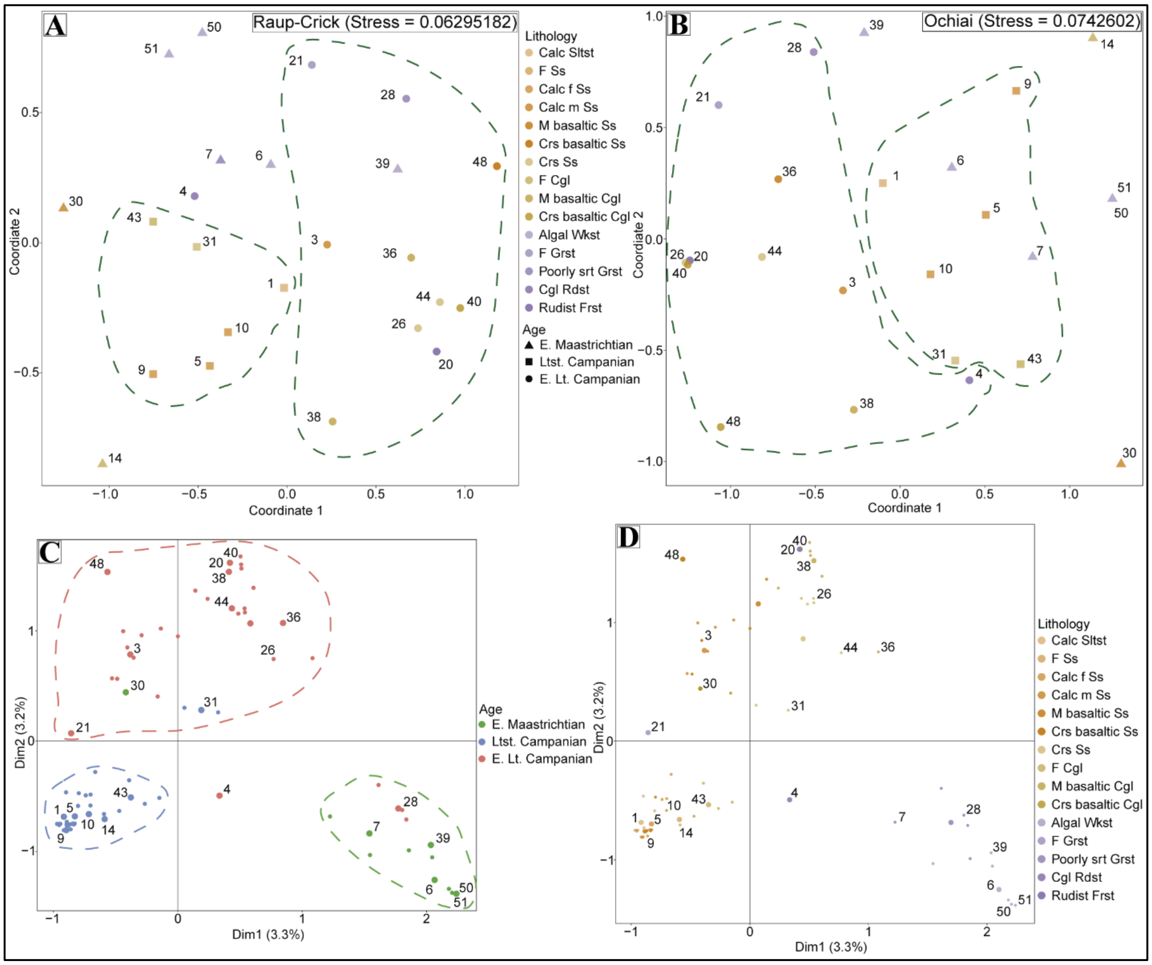

Text-fig. 16. Plots of the first two principal dimensions of NMDS analysis based on the Raup-Crick (A) and Ochiai (B) dissimilarity indexes. Plots of the first two principal dimension of MCA based on genus, locality, age, lithology labeling age (C) and lithology (D). Wkst = wackestone, Calc = calcareous, f = fine, Ss = sandstone, Sltst = siltstone, Crs = coarse, Cgl = conglomerate, Rdst = rudstone, Grst = grainstone, srt = sorted, Frst = framestone, E = Early, Ltst = Latest, Lt = Late.

DISCUSSION

This study reveals that Costa Rica contains a rich geologic and biologic record of Late Cretaceous molluscan faunas not clear from prior studies focusing on rudist bivalves (e.g., Pons, 2016). New sedimentological and taphonomic data presented here changes the environmental interpretation of most fossil localities, which were previously interpreted as slope deposits containing reworked shallow water deposits (Rivier, 1983; Astorga, 1987; Denyer et al., 2014). Whereas this work cannot conclusively explain faunal migrations and paleobiogeographic transition between the eastern and western Tethys regions, the analyses presented here provide support for more detailed testing of these hypotheses. Moreover, filling the knowledge gap in molluscan paleobiogeography with these data provide a solid baseline for continued studies in the paleobiogeography and paleoceanography of Tethyan tropical region, including better understanding interactions between the Caribbean Tethys, Pacific Ocean, Mediterranean Tethys, and Gulf Coastal Plain. This is important for understanding dispersal and migration patterns in several marine groups just prior to a major extinction event. Then we could understand extinction and survival patterns observed by the event.

PALEOENVIRONMENTAL PATTERNS

Starting with a major tectonic uplift during the early Late Campanian, relative sea level rose and created shallow platform areas around basement islands or structural highs (Seyfried and Sprechmann, 1985). Rudist reefs developed on those platforms, depending on depositional conditions and abundant molluscan communities thrived in this environment, such as trigoniid bivalves, big oysters, and nerineid gastropods (Text-fig. 17A). This is shown in the northern and central subareas. Rudists are scarce in the southwestern subarea and absent in the southern subarea, which could indicate deeper platform environments. As time progressed through the Latest Campanian, relative sea level rose again and drowned the rudist reefs, leading to assemblages characteristic of open shelf faunas dominated by cephalopods (Text-fig. 17B). This is noticeable in all subareas.

By the Early Maastrichtian, relative sea level dropped in the southwestern and central subareas, which allowed the return of reefs (this time composed mainly of corals) and shallow water fauna such as nerineid gastropods (Text-fig. 17C).

By combining the stratigraphic correlations with the statistical exploration of collected faunal assemblages I was able to explore two hypotheses: (1) different region-scale paleo-communities existed within the Late Cretaceous Costa Rican fauna that are controlled by different paleoenvironments (e.g., shallow-water rudist reef vs. open shelf systems); (2) faunal migration was observable between the Tethyan and Pacific oceanic realms. These analyses, unsurprisingly, suggest that specific faunal assemblages concentrate in different paleoenvironments; this supports that Hypothesis 1 should be further explored with more detailed quantitative tests. For example, the statistical exploration supports time interval as an important distinction between faunal assemblages, regardless of the environment compared to fauna from other ages; potential reasons for this should be investigated further (Text-fig. 16).

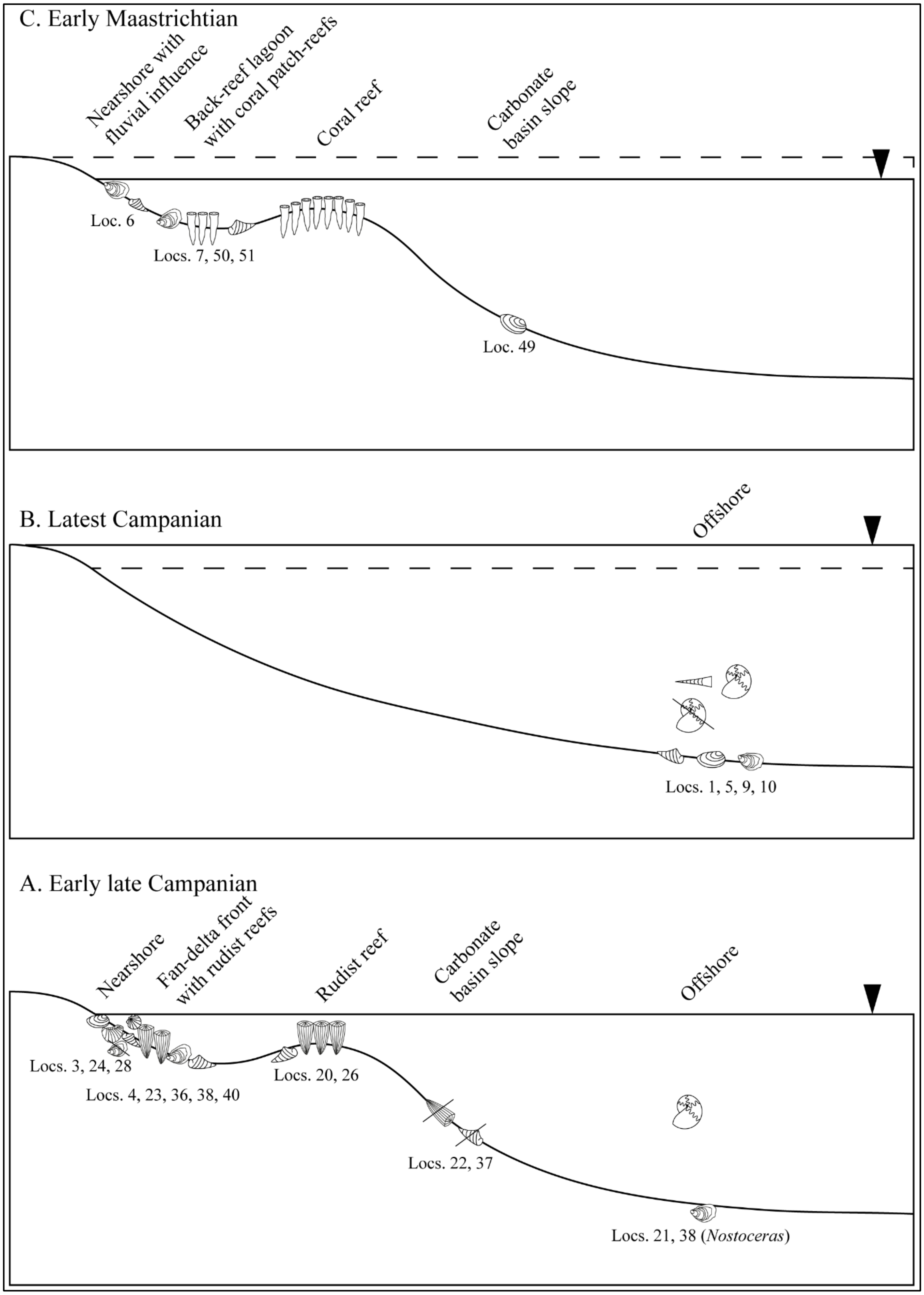
C. Early Maastrichtian
Nearshore with fluvial influence
Back-reef lagoon with coral patch-reefs
Coral reef
Carbonate basin slope
Loc. 6
Locs. 7, 50, 51
Loc. 49
B. Latest Campanian
Offshore
Locs. 1, 5, 9, 10
A. Early late Campanian
Nearshore
Fan-delta front with rudist reefs
Rudist reef
Carbonate basin slope
Offshore
Locs. 3, 24, 28
Locs. 4, 23, 36, 38, 40
Locs. 20, 26
Locs. 22, 37
Locs. 21, 38 (*Nostoceras*)

Text-fig. 17. Facies model profile of some studied localities showing fauna reported on them (legend for fossil groups after Text-fig. 12, locality information in Appendix 2). Black triangle represents relative sea level. Dashed line shows relative sea level change compared to the previous age. A, Early late Campanian. B, Latest Campanian. C, Early Maastrichtian.

The early Late Campanian rudist-bearing localities show interesting changes in faunal patterns, namely between Localities 23/40 and 38. Both localities are dominated by medium to coarse calcareous conglomerates with clasts derived from basement erosion. Rudist reefs grow in life position with some bouquets found toppled, which indicates a very shallow and high-energy environment, such as Sanders and Pons (1999) describe in the Gosau Group (Turonian-Early Campanian) in Austria. However, in Locality 38, there are only two levels of rudist reefs, and the conglomerate beds are much thicker compared to those in Locality 40. In Locality 40, rudists form several reef levels (Pons et al., 2016b). This suggests that rudist reefs could rapidly colonize the substrate in siliciclastic-dominated environments, and even keep up with the siliciclastic sedimentation rate (Sanders and Pons, 1999). Consequently, the lack of rudists at Locality 38, could reflect siliciclastic input that was too high in comparison to Locality 40.

Where rudist reefs are well-developed, the non-rudist fauna is dominated entirely by nerineid gastropods. Where rudists could not keep up to form reef levels, molluscan fauna is much more diverse, with very few nerineid gastropods. Kollmann (2014) indicated nerineid gastropods only inhabited unconsolidated sediments, with grainstone being the preferred substratum for mass-occurrences of nerineids. This could mean that well-developed rudist reefs may create the grainstone substrate, due to wave destruction of the rudists and corals, in which nerineids then prosper.

Relative sea level continued to rise during the latest Campanian, as observed by the facies change from shallow water deposits (e.g., rudist and coral framestone) to offshore deposits (e.g., fine blue-gray sandstone) dominated by cephalopods, with associated gastropods and bivalves (Text-fig. 17B). By the Early Maastrichtian, the central subarea shows a relative sea level drop without evidence of tectonic uplift as observed by the resurgence of carbonate platforms. However, these platforms are very muddy compared to the early Late Campanian and dominated by elevator coral patch-reefs with associated nerineid gastropods and oysters (Text-fig. 17C). The lack of rudist bivalves in the Early Maastrichtian platforms could be related to a lack of suitable habitat; muddy substrates in general do not usually preserve rudists, as shown in the Early Maastrichtian Cardenas Formation in San Luis Potosi, Mexico (Götz and Mitchell, 2009). The base of the Cardenas Formation consists of marl and clay sediments interpreted as open shelf deposits, in which the rudist *Laluzia armini* Götz and Mitchell, 2009 was able to colonize a soft substrate with low sedimentation rates (Götz and Mitchell, 2009). Götz and Mitchell (2009) also indicate that this environment is not the preferred one by rudist bivalves.

Moreover, Early Maastrichtian gastropods differ in environmental preferences compared to those in the early Late Campanian (Text-figs. 16A-B). Early Late Campanian nerineids were found in a wide variety of environments, from foreshore deposits (Loc. 3) to coastal deposits dominated by coarser sedimentation (Locs. 23, 36, 38, 40) to pure carbonate platforms with well-developed rudist reefs (Locs. 20, 26). This preference for coarser grained environments has not been reported in Campanian nerineids, of which the paleobiology was last revised by Kollmann (2014). However, by the Early Maastrichtian nerineids were restricted to algal wackestone facies interpreted as lagoonal. The findings of this study and further work could help expand this topic further, particularly by comparison to the better characterized Campanian nerineids from the Mediterranean Tethys.

Another group of paleobiogeographic interest, the inoceramid bivalves, showed no environmental preference. Prisms and complete specimens are found in very shallow deposits during the early Late Campanian (Locs. 3, 38, 44), as well as in open platform deposits during the Latest Campanian (Locs. 1, 17, 42), and in high energy platform slope deposits during the Early Maastrichtian (Loc. 49).

PALEOBIOGEOGRAPHIC PATTERNS

These data represent the largest and highest-resolution set of faunal occurrences of marine invertebrates of Central America (both taxonomically and spatiotemporally). During the Late Cretaceous, the Nicoya region of Costa Rica was situated at the southern tip of the North American continent and attached to the MCOT terrain in the coast of Nicaragua and Honduras (Flores and Gazel, 2020) (Text-figs. 1, 18). This location, at the constriction of Tethyan waters circulating between North and South America could have plausibly supported a "mixing pot" of faunas from different paleobiogeographic realms (e.g., cosmopolitan, Caribbean, Mediterranean Tethys, North Pacific, North America). In this way, Costa Rican faunal assemblages and their stratigraphic transitions can provide key evidence of biogeographic changes related to sea level, ocean currents, and tectonic processes just prior to the end-Cretaceous mass extinction.

In early Late Campanian faunas, rudist and non-rudist assemblages are associated with the neighboring Caribbean Province, with similar taxa found in Jamaica, Cuba, Chiapas and Puerto Rico (Pons et al., 2016b). For example, the nerineid gastropod *Parasimploptyxis epelys* (Woodring, 1952) is found in Cuba (Woodring, 1952), the bivalve *Veniella jamaicensis* (Trechmann, 1927) is found in the Early Maastrichtian of Jamaica and northern Peru (Dhont and Jaillard, 2005) and the bivalve *Notoscabrotrigonia?* sp. is present in Cuba (Cooper, 2015) (Text-fig. 19); acteonellids, such as *Acteonella* sp. and *Trochacteon* sp., are also present in other Caribbean Province localities. This was expected, since nerineid and acteonellid gastropods are generally found associated with rudist reefs (Sohl and Kollmann, 1985; Kiel, 2002; Kollmann, 2014).

Taxa indicative of the Tethyan Realm include the gastropods *Gyrodes* sp. and *Neithea* sp. The presence of *Nostoceras hyatti* also shows an affinity with the Tethyan Realm, since it is an important biomarker for the Late Campanian globally (Blaszkiewicz, 1980; Küchler and Odin, 2001; Voigt et al., 2012). The inoceramids found in the shallow early Late Campanian deposits seem to be cosmopolitan taxa, but the lack of umbo preservation makes species identification intractable.

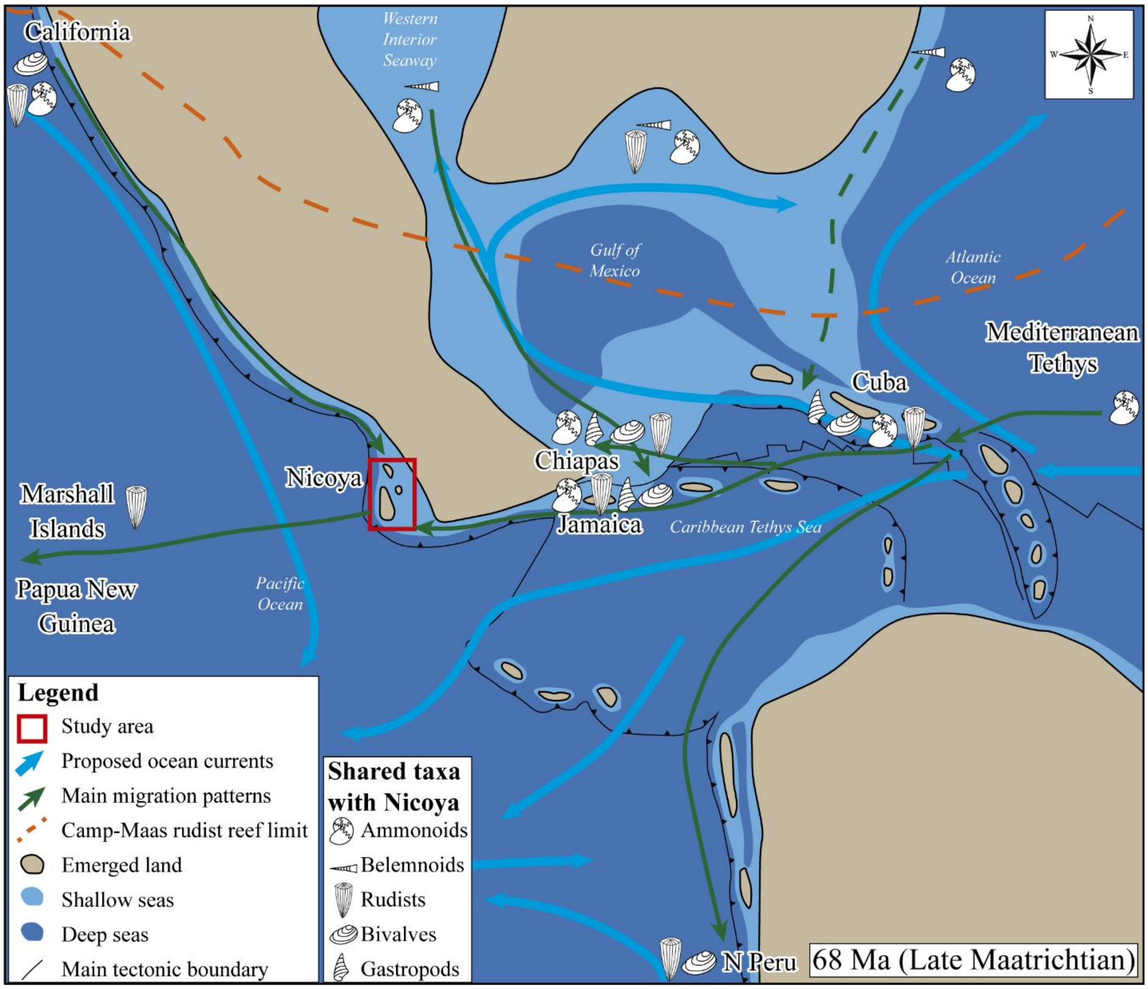

Text-fig. 18. Paleogeographic reconstruction of Middle America at 68 Ma (modified from Flores, 2009, Flores and Gazel 2020, Gazel et al. 2021) showing the tectonic setting of Nicoya and migration patterns of the fauna found in this study. Proposed oceanic currents after Johnson et al. (2002), Zimmerman et al. (2023).

Latest Campanian offshore faunas show more complex paleobiogeographic affinities. Some ammonites observed are common in the Mediterranean Tethys, such as *Neophylloceras surya* (Forbes, 1846), *Baculites leopoliensis* (Nowak, 1908), *Glyptoxoceras retrorsum* (Schlüter, 1872), *Pseudokossmaticeras brandti* (Redembatcher, 1873), *Pachydiscus* cf. *neubergicus neubergicus,* and *Gaudryceras* sp.; *G.* cf. *retrorsum* has also been reported in Jamaica (Wiedmann and Schmidt, 1993). However, unlike the Late Campanian of the Mediterranean Tethys, these faunas show an unusual diversity of baculitids. For example, only one *Baculites* species is recorded the Late Campanian of Aquitaine, France (Kennedy, 1986). This increased diversity suggests an affinity with northern Pacific localities, where the fauna is similar to those from Japan, Canada and California. In contrast, *Baculites leopoliensis* is the most common baculite in Late Campanian deposits of Europe (Klinger and Kennedy, 2001); further global comparisons of baculite diversity (including evenness) will better describe their paleobiogeographic affinities.

Notably, this study uncovered some unique occurrences of the cephalopods *Scaphites* sp. and *Belemnitella americana* (Morton, 1830). Scaphitid ammonites are rare in the Campanian-Maastrichtian Tethyan Realm; e.g., Kennedy (1986) reported six scaphitid species in the Campanian-Maastrichtian of Aquitaine, southern France. Scaphitids are more common in the Boreal Realm of Europe and the Western Interior Seaway (WIS), Atlantic and Gulf Coastal Plains (ACP and GCP, respectively) of North America (Monks, 2000; Landman et al., 2015).

Taphonomically, it is also remarkable to find ammonite jaws in the offshore Latest Campanian deposits (Loc. 1, Text-fig. 14-20, 14-21). This work is the first report of Late Cretaceous ammonite jaws in the Caribbean region writ large, let alone with preservation quality high enough to attribute these jaws to scaphitid ammonites. Ammonite jaws are generally difficult to find, and this provides an insight for future research on the ammonite paleobiology and taphonomy of Caribbean Tethys faunas, since most of Late Cretaceous jaws have been found in the Mediterranean Tethys (i.e., Kennedy, 1986), Japan (Tanabe and Fukuda, 1987), the WIS (Kruta et al., 2011), and ACP (Landman et al., 2007).

Belemnites have not previously been found in post-Turonian deposits of the Caribbean Province. *B. americana* ranges from Late Campanian-Early Maastrichtian throughout the WIS, ACP, and GCP of North America (Christensen, 1997a). Although far from common, both taxa do suggest some migration of North American cephalopod faunas into the Caribbean Tethys and then the Nicoya region (Text-fig. 18).

Latest Campanian gastropods and bivalves are similar to cosmopolitan faunas, such as *Cataceramus goldfussianus?* (d'Orbigny, 1847) and *Neithea* sp. However, the bivalve *Acila* sp. look very similar to specimens from the Late Campanian-Early Maastrichtian of California (Squires and Saul, 2006). This suggests potential distribution of faunas from temperate California into the Nicoya region along the Pacific coast of North America (Text-fig. 18).

Early Maastrichtian carbonate deposits containing the nerineid *Plesioptygmatis?* sp., and acteonellid *Acteonella duckettsensis?* (Sohl and Kollmann, 1985) suggest an affinity with assemblages found in Cuba, Jamaica, and San Luis Potosí in Mexico (Text-fig. 18). Even though rudists were not found in the Early Maastrichtian deposits, the presence of Caribbean Province nerineids and acteonellids during this time support migration potential between the Caribbean Tethys and the Pacific Ocean (Text-fig. 18).

Taken together, these observations support Hypothesis 2 – that Costa Rican assemblages represent a mixture of faunas from either side of the Americas – and suggest that dispersal between and Pacific and Atlantic Oceans was frequent in the Latest Cretaceous. The paleobiogeographic signals found here may also inform reconstructions of paleoceanographic conditions, e.g., paleocurrent directions, that would have permitted dispersal corridors (Johnson, 1999, Johnson et al., 2002). For example, Kiel (2002) presents a comprehensive record of the paleobiogeography of several gastropod clades (Archaeogastropoda, Neritimorpha, Caeonogastropoda, Heterostropha) that was used to support a hypothesized land bridge across restricting dispersal through the Caribbean Tethys at this time. In contrast, this work supports open passages as proposed by Johnson et al. (2002) rudist reef data and Flores and Gazel (2020) tectonic models. The previous information gap in the Pacific coast of the Americans between California and northern Peru impedes evaluation of his hypotheses. This work will help to fill this gap and enable higher resolution and more accurate faunal reconstructions, following Johnson et al. (2002).

Prior work on Caribbean rudists has led to some more detailed reconstructions. For example, Skelton and Wright (1987) proposed east-to-west island-hopping from the Caribbean through the Pacific Ocean to Oman (Text-fig. 18). Camoin et al. (1995) report the presence of Caribbean rudists and larger foraminifera as far as the Marshall Islands. Alternatively, Philip (1998) proposes west-to-east migration of rudists due to the first appearance of supposed Caribbean endemics in Oman. However, many more studies support east-to-west current directions: Johnson et al. (2002), using reef taxa including both corals and rudists, proposed the existence of the Gulf Stream during Campanian-Maastrichtian times, leading to ocean currents moving east-to-west across the Caribbean into the Pacific and Oman (Text-fig. 18) and other branch going northwards into the Gulf of Mexico and the WIS, as well as a current from California southward to the Tropical Pacific (Johnson et al., 2002) (Text-fig. 18); Christensen (1997b) proposed migration of the family Belemnitellidae across the North Atlantic to the GCP and WIS. Ward et al.

(2012) showed that ammonite species along the Pacific Coast of North America (Canada to Baja California) represented a more mixed fauna than previously thought and proposed intermittent seawater connections between the Gulf of Mexico or Western Interior Seaway to the Pacific (Ward et al., 2012).

Further research into the Late Cretaceous non-rudist molluscan faunas of Central America and the Caribbean should analyze these paleobiogeographic patterns found in Costa Rica, also comparing it to the rudist paleobiogeographic data. This is important to test paleobiogeographic connections between different areas, and if the molluscan faunas of the Caribbean region were thriving just before the K-Pg mass extinction event.

CONCLUSIONS

Here I present the first detailed characterization of the Late Cretaceous non-rudist fauna of Costa Rica. These assemblages are described and placed in paleoenvironmental context using high resolution stratigraphic correlation and available geochronological dates from Sr-isotopes and non-published tuff ages (Flores, pers. comm.). After a major tectonic uplift in the early Late Campanian, relative sea level rise allowed the establishment of rudist reefs in a variety of environments, with associated abundant molluscan fauna. As sea level continued to rise, the sedimentation changed to offshore deposits dominated by cephalopod faunas, with secondary gastropods and bivalves. A subsequent drop in relative sea level supported a return to carbonate-dominated sedimentation, however no longer structured by rudist reefs, but instead as muddy platforms topped with coral-based reefs and abundant nerineid gastropods living in the agonal facies.

Across available time slices, the molluscan fauna shows affinities from several biogeographic provinces such as those in the Caribbean, the Mediterranean Tethys, North America, and California. Minimally this demonstrates broad ocean circulation between the western Tethys (Caribbean) and the Pacific Coast of North America. These results add an important piece in the puzzle of molluscan paleobiogeography during Late Cretaceous and open up several questions for further field collection and hypothesis testing. Continued study of the Nicoya region and surrounding areas fills an important gap in faunal and paleoenvironmental sampling between California and Northern Peru; this research supports circulation between the Atlantic and Pacific, and a "mixing pot" of different zones that were a launching point for faunas crossing the Pacific Ocean. Further work will benefit from additional sampling of Late Cretaceous outcrops in Central America and northern South America, as well as more quantitative analysis of faunal assemblage's similarities across regions within their paleoceanographic context.

REFERENCES

Adobe Inc. (2017). Adobe Illustrator CC 2018. Retrieved from https://adobe.com/products/illustrator

Aguilar, T., and Denyer, P. (2002). Primer hallazgo de Trigonias (Mollusca: Bivalvia) cretácicas de Costa Rica (Tortugal, Guanacaste): geología, estratigrafía y paleontología. *Revista Geológica de América Central*, *26*, 53-63. doi: https://doi.org/10.15517/rgac.v0i26.8530

Aguilar, T., and Denyer, P. (2019). Estratigrafía sedimentaria. In P. Denyer (Ed.), *Perspectiva geológica del noroeste de Costa Rica. Historia, evolución y cartografía* (pp. 43-100). Editorial de la Universidad de Costa Rica.

Andjic, G., Baumgartner, P., and Baumgartner-Mora, C. (2019). Collision of the Caribbean Large Igneous Province with the Americas: Earliest evidence from the forearc of Costa Rica. *Bulletin of the Geological Society of America*, *131*(9/10), 1555–1580. doi: https://doi.org/10.1130/B35037.1

Arroyo, M., Chavarria, F., Jarquin, E., and Madrigal, A. (2016). *Sedimentología y paleogeografía de las turbiditas del Maastrichtiano-Eoceno Inferior del sector noroeste, Guanacaste, Costa Rica* [Field Geology II report]. Universidad de Costa Rica.

Astorga, A. (1987). *El Cretácico Superior y el Paleógeno de la vertiente pacífica de Nicaragua meridional y Costa Rica septentrional: origen, evolución y dinámica de las cuencas profundas relacionadas al margen convergente de Centroamérica* [B.S. thesis]. Universidad de Costa Rica.

Astorga, A. (1997). El puente-istmo de América Central y la evolución de la Placa Caribe (con énfasis en el Mesozoico). *Profil*, *12*, 1-201.

Azema, J., Tournon, J., and Sornay, J. (1979). Presencia de amonites de Albiano superior en las formaciones del "Complejo de Nicoya". El yacimiento de la Loma Chumico, provincia de Guanacaste, Costa Rica. *Informe Semestral del Instituto Geográfico Nacional*, *1978*(2), 71-76.

Bandini, A., Baumgartner, P., Flores, K., Dumitrica, P., and Jackett, S. (2011). Early Jurassic to early Late Cretaceous radiolarians from the Santa Rosa Accretionary Complex (Northwest Costa Rica). *Ofioliti*, *31*(1), 1-35. doi: https://doi.org/10.4454/ofioliti.v36i1.392

Blaszkiewicz, A. (1980). Campanian and Maastrichtian ammonites of the Middle Vistula River valley, Poland: a stratigraphic-paleontological study. *Prace Instylulu Geologicznego*, *92*, 1-63.

Buchs, D., Pilet, S., Baumgartner, P., Cosca, M., Flores, K., Bandini, A. (2013). Low-volume intraplate volcanism in the Early/Middle Jurassic Pacific basin documented by accreted sequences in Costa Rica. Geochemistry, Geophysics, Geosystems, 14(5), 1552-1568. doi: https://doi.org/10.1002/ggge.20084

Calvo, C. (1998). Kretazische Subduktionsprozesse in Südzentralamerika. *Profil*, *15*, 1-161.

Camoin, G., Armaud Vanneau, A., Bergersen, D., Colonna, M., Ebren, P., Enos, P., and Ogg, J. (1995). 14. Anatomy and Evolution of the Inner Perimeter Ridge (Sites 874 and 877) of a Campanian–Maastrichtian Atoll-Like Structure (Wodejebato Guyot, Marshall Islands). In J. Haggerty, I. Premoli Silva, F. Rack, and M. McNutt (Eds.), *Proceedings of the Ocean Drilling Program, Scientific Results* (Vol. 144, pp. 887-893). Ocean Drilling Program Publications.

Christensen, W. (1997a). The Late Cretaceous belemnite family Belemnitellidae: Taxonomy and evolutionary history. *Bulletin of the Geological Society of Denmark*, *44*, 59-88. doi: https://doi.org/10.37570/bgsd-1998-44-04

Christensen, W. (1997b). Paleobiogeography and migration in the Late Cretaceous belemnite family Belemnitellidae. *Acta Palaeontologica Polonica*, *42*(4),451-495.

Cooper, M. (2015). On the Pterotrigoniidae (Bivalvia, Trigoniida): their biogeography, evolution, classification and relationships. *Neues Jahrbuch für Geologie und Paläontologie – Abhandlungen*, *277*(1). doi: 10.1127/njgpa/2015/0488

Dengo, G. (1962). *Estudio Geológico de la Región de Guanacaste, Costa Rica*. Imprenta del Instituto Geográfico.

Denyer, P., Aguilar, T., and Montero, W. (2014). *Cartografía geológica de la península de Nicoya: estratigrafía y tectónica*. Editorial de la Universidad de Costa Rica.

Dhont, A., and Jaillard, E. (2005). Cretaceous bivalves from Ecuador and northern Peru. *Journal of South American Earth Sciences*, *19*, 325-342. doi: https://doi.org/10.1016/j.jsames.2005.01.005

Eckert, A. (2018). *parallelDist: Parallel Distance Matrix Computation using Multiple Threads*. R package version 0.2.4. https://CRAN.R-project.org/package=parallelDist

ESRI. (2019). *ArcGIS Desktop: Release 10.4*. Redlands, CA: Environmental Systems Research Institute.

Fang, X., Burrett, C., Li, W., Zhang, Y., Zhang, Y., Chen, T., and Wu, X. (2019). Dynamic variation of Middle to Late Ordovician cephalopod provincialism in the northeastern peri-Gondwana region and its implications. *Palaeogeography, Palaeoclimatology, Palaeoecology*, *521*, 127-137. doi: https://doi.org/10.1016/j.palaeo.2019.02.015

Fischer, R., and Aguilar, T. (1994). Palaeontology of an evolving island arc. In H. Seyfried, W. Hellmann (Eds.), *Geology of an Evolving Island Arc* (Profil, Vol. 7, 329-343).

Flores, K. (2003). *Propuesta Tectonoestratigráfica de la región septentrional del golfo de Nicoya* [B.S. thesis]. Universidad de Costa Rica.

Flores, K. (2009). *Mesozoic oceanic terranes of southern Central America - Geology, Geochemistry and Geodynamics* [Ph.D. thesis]. Université de Lausanne.

Flores, K., and Gazel, E. (2020). A 100 m.y. record of volcanic arc evolution in Nicaragua. *Island Arc*, *29*(1), 1-14. doi: https://doi.org/10.1111/iar.12346

Galli-Olivier, C., and Schmidt-Effing, R. (1977). Estratigrafía de la cubierta sedimentaria supraofiolítica Cretácica de Costa Rica. *Revista de Ciencia y Tecnología*, *1*(1), 87-96.

Gazel, E., Flores, K., and Carr, M. (2021). Architectural and Tectonic Control on the Segmentation of the Central American Volcanic Arc. Annual Review of Earth and Planetary Sciences, 49, 485-511. doi: https://doi.org/10.1146/annurev-earth-082420-055108

Glaessner, M. (1960). Upper Cretaceous Larger Foraminifera from New Guinea. *Science reports of the Tohoku University. 2nd series, Geology. Special volume*, *4*, 37-44.

Götz, S., and Mitchell, S. (2009). The *Laluzia armini* (gen. et spec. nov.) ecosystem: understanding a deeper-water rudist lithosome from the Early Maastrichtian of Mexico. Facies, 55, 539-551. doi: 10.1007/s10347-009-0184-6

Hammer, O., and Harper, D. (2006). *Paleontological Data Analysis* (1ra ed.). Washington D.C.: Blackwell Publishing Ltd.

Hattin, D. (1986). Carbonate Substrates of the Late Cretaceous Sea, Central Great Plains and Southern Rocky Mountains. Palaios, 1(4), 347-367. doi: https://doi.org/10.2307/3514473

Hoffmann, R., Slaterry, J., Kruta, I., Linzmeier, B., Lemanis, R., Mironenko, A., Goolaerts, S., De Baets, K., Peterman, D., and Klug, C. (2021). Recent advances in heteromorph ammonoid palaeobiology. *Biological Reviews*, *96*, 576-610. doi: 10.1111/brv.12669

Johnson, C. (1999). Evolution of Cretaceous surface current circulation patterns, Caribbean and Gulf of Mexico. In E. Barrera, C. Johnson (Eds.), *Evolution of the Cretaceous Ocean-Climate System* (Geological Society of America Special Papers, Vol. 332, 329-343). doi: 10.1130/0-8137-2332-9.329

Johnson, C., Sanders, D., Kauffman, E., and Hay, H. (2002). Patterns and processes influencing Upper Cretaceous reefs. In W. Kiessling, E. Flügel, J. Golonka (Eds.), *Phanerozoic Reef Patterns* (Society for Sedimentary Geology Special Publication, Vol. 72, pp. 549-585). Society for Sedimentary Geology.

Kassambara, A. (2017). *Practical Guide To Principal Component Methods in R: PCA, M (CA), FAMD, MFA, HCPC, factoextra* (Vol. 2). STHDA.

http://www.sthda.com/english/wiki/practical-guide-to-principal-component-methods-in-r

Kassambara, A. and Mundt, F. (2020). *factoextra: Extract and Visualize the Results of Multivariate Data Analyses*. R package version 1.0.7. https://cran.r-project.org/web/packages/factoextra/index.html

Kauffman, E. (1973). Cretaceous Bivalvia. In A. Hallam (Ed.), *Atlas of Paleobiogeography* (pp. 353-383). Elsevier Scientific Publishing Company.

Kennedy, W. (1986). Campanian and Maastrichtian ammonites from northern Aquitaine, France. *Special Papers in Paleontology*, *36*, 1-145.

Kiel, S. (2002). Notes on the biogeography of Campanian-Maastrichtian gastropods. In M. Wagreichm (Ed.): *Aspects of Cretaceous Stratigraphy and Paleobiogeography* (Schriftenreihe der Erdwissenschaftlichen Kommission, Vol. 15, pp. 109-127). Österreichische Akademie der Wissenschaften.

Klinger, H., and Kennedy, W. (2001). Stratigraphic and geographic distribution, phylogenetic trends and general comments on the ammonite family Baculitidae Gill, 1871 (with an annotated list of species referred to the family). *Annals of the South African Museum*, *107*(1), 1-290.

Kollmann, H. (2014). The extinct Nerineoidea and Acteonelloidea (Heterobranchia, Gastropoda): a palaeobiological approach. *Geodiversitas*, *34*(3), 349-383. doi: http://dx.doi.org/10.5252/g2014n3a2

Kruta, I., Landman, N., Rouget, I., Cecca, F., and Tafforeau, P. (2011). The Role of Ammonites in the Mesozoic Marine Food Web Revealed by Jaw Preservation. Science, 331(6013), 70-72. doi: 10.1126/science.1198793

Küchler, T., and Odin, G. (2001). Upper Campanian-Maastrichtian ammonites (Nostoceratidae, Diplomoceratidae) from Tercis les Bains (Landes, France). In G. Odin (Ed.), *The Campanian-Maastrichtian Boundary* (Developments in Paleontology and Stratigraphy, Vol. 19, pp. 500-528). Elsevier Scientific Publishing Company. doi: https://doi.org/10.1016/S0920-5446(01)80052-2

Landman, N., Johnson, R., Garb, M., Edwards, L., and Kyte, F. (2007). Cephalopods from the Cretaceous/Tertiary boundary interval on the Atlantic Coastal Plain, with a description of the highest ammonite zones in North America. Part III. Manasquan River Basin, Monmouth County, New Jersey. Bulletin of the American Museum of Natural History, 303, 1-122. doi: https://doi.org/10.1206/0003-0090(2007)303[1:CFTTBI]2.0.CO;2

Landman, N., Goolaerts, S., Jagt, J., Jagt-Yazykova, E., and Machalski, M. (2015). Ammonites on the Brink of Extinction: Diversity, Abundance, and Ecology of the Order Ammonoidea at the Cretaceous/Paleogene (K/Pg) Boundary. In C. Klug, D., Korn, K. De Baets, I. Kruta, R. Mapes (Eds.), *Ammonoid Paleobiology: From* *macroevolution to paleobiogeography* (Topics in Paleobiology, Vol. 44, pp. 497-554). Springer-Verlag New York.

Lê, S., Josse, J., and Husson, F. (2008). FactoMineR: An R Package for Multivariate Analysis. Journal of Statistical Software, 25(1), 1-18. doi: https://doi.org/10.18637/jss.v025.i0

Madrigal, P., Gazel, E., Denyer, P., Smith, I., Jicha, B., Flores, K., Coleman, D., and Jonathan Snowg, J. (2015). A melt-focusing zone in the lithospheric mantle preserved in the Santa Elena Ophiolite, Costa Rica. *Lithos*, *230*, 189-205. doi: http://dx.doi.org/10.1016/j.lithos.2015.04.015

Madrigal, Pilar., Gazel, E., Flores, K., Bizimis, M., and Jicha, B. (2016). Record of massive upwellings from the Pacific large low shear velocity province. *Nature Communications*, *7*(13309), 1-12. doi: 10.1038/ncomms13309

Malavassi, E. (1961). Some Costa Rican Larger Foraminiferal Localities. *Journal of Paleontology*, *35*(3), 498-501.

Michaud, F., and Fourcade, E. (1989). Stratigraphie et paléogéographie du Jurassic et du Crétacé du Chiapas (Sud-Est du Mexique). *Bulletin de la Société Géologique de France, S8-5*(3), 639-650.

Mitchell, S. (2002). Palaeoecology of corals and rudists in mixed volcaniclastic^ carbonate small-scale rhythms (Upper Cretaceous, Jamaica). *Palaeogeography, Palaeoclimatology, Palaeoecology*, *186*, 237-259.

Monks, N. (2000). Functional morphology, ecology, and evolution of Scaphitaceae Gill, 1871 (Cephalopoda). *Journal of Molluscan Studies, 66*, 205-216.

Mora, S. (1978). *Estudio geológico de los Cerros Barra Honda y alrededores, Nicoya, Guanacaste, Costa Rica* [B.S. thesis]. Universidad de Costa Rica

NOAA National Geophysical Data Center. (2009). ETOPO1 1 Arc-Minute Global Relief Model. NOAA National Centers for Environmental Information. Accessed [April 5th, 2023].

Oksanen, J., Blanchet, F. G., Friendly, M., Kindt, R., Legendre, P., McGlinn, D., Minchin, P., O'Hara, R., Simpson, G., Solymos, P., Stevens, M. H., Szoecs, E., and Wagner, H. (2019). *vegan: Community Ecology Package*. R package version 2.5-6. https://CRAN.R-project.org/package=vegan

Philip, J. (1998). Biostratigraphie et paléobiogéographie des rudistes évolution des concepts et progrès récents. *Bulletin de la Societé Géologuique de France*, *169*(5), 689-708.

Philip, J., and Jaillard, E. (2004). Revision of the upper Cretaceous rudists from Northwestern Peru. Journal of South American Earth Sciences, 17, 39-48. doi: https://hal.archives-ouvertes.fr/hal-00101741

Pons, J., Vicens, E., Martinez, R., Garcia-Barrera, P., Nieto, I., Oviedo, A., Avendaño-Gil, M. (2016a). The Campanian-Maastrichtian rudist bivalves succession in the Chiapas Central Depression, Mexico. Cretaceous Research, 60, 210-220. doi: http://dx.doi.org/10.1016/j.cretres.2015.11.015

Pons, J., Vincens, E., and Schmidt-Effing, R. (2016b). Campanian rudists (Hippuritida, Bivalvia) from Costa Rica (Central America). *Journal of Paleontology, 90*(2), 211-238. doi: https://doi.org/10.1017/jpa.2016.27

Premoli Silva, I., Nicora, A., Amaud Vanneau, A., Budd, A., F. Camoin, G., and Masse, J. (1995). 50. Paleobiogeographic Evolution of Shallow-Water Organisms from the Aptian to the Eocene in the Western Pacific. In J. Haggerty, I. Premoli Silva, F. Rack, and M. McNutt (Eds.), *Proceedings of the Ocean Drilling Program, Scientific Results* (Vol. 144, pp. 887-893). Ocean Drilling Program Publications.

R Core Team (2020). *R: A language and environment for statistical computing*. R Foundation for Statistical Computing, Vienna, Austria. URL https://www.R-project.org/.

Rivier, F. (1983). Síntesis geológica y mapa geológico del área del bajo Tempisque, Guanacaste, Costa Rica. Research report, Universidad de Costa Rica.

RStudio Team (2022). *RStudio: Integrated Development Environment for R*. RStudio, PBC, Boston, MA URL http://www.rstudio.com/

Sanders, D., and Pons, J. (1999). Rudist formations in mixed siliciclastic-carbonate depositional environments, Upper Cretaceous, Austria: stratigraphy, sedimentology, and models of development. *Palaeogeography, Palaeoclimatology, Palaeoecology*, 148, 249-284.

Sanders, D., Kollmann, H., and Wagriech, M. (1997). Sequence development and biotic assemblages on an active continental margin: the Turonian-Campanian of the northern Calcareous Alps, Austria. *Bulletin de la Société Géologique de France, 168*(3), 351-372.

Schmidt-Effing, R. (1974). El primer hallazgo de amonites en América Central Meridional y notas sobre facies cretácicas en dicha región. Informe Semestral del Instituto Geográfico Nacional, 1974(1), 53-61.

Segura, A. (1945a). Apuntes sobre mármoles de Guanacaste. *Boletín del Museo Nacional*, *1*(1), 19-22.

Segura, A. (1945b). Rápidos apuntes sobre los mármoles del Guanacaste y otros aspectos geológicos. *Revista del Instituto de Defensa del Café de Costa Rica*, *15*(127), 337-347.

Seyfried, H., and Sprechmann, P. (1985). Acerca de la formación del Puente-istmo Centroamericano Neridional, con énfasis en el desarrollo acaecido desde el Campaniense al Eoceno. Revista Geológica de América Central, 2, 63-87. doi: https://doi.org/10.15517/rgac.v0i02.10482

Seyfried, H., and Sprechmann, P. (1986). Über die Frühgeschichte (Campan bis Eozän) der südlichen mittelamerikanischen Landbrücke. *Neues Jahrbuch für Geologie und Paläontologie-Monatshefte, 1*(1986), 38-55. doi: 10.1127/njgpm/1986/1986/38

Skelton, P., and Wright, V. (1987). A Caribbean rudist bivalve in Oman: island-hopping across the Pacific in the Late Cretaceous. *Paleontology*, *30*(3), 505-529.

Sohl and Kollmann, (1985). Cretaceous Actaeonellid Gastropods from the Western Hemisphere. *Geological Survey Professional Paper*, *1304*, 1-104. doi: 10.3133/pp1304

Squires, R., and Saul, L. (2006). Cretaceous *Acila (Truncacila)* (Bivalvia: Nuculidae) from the Pacific Slope of North America. *The Veliger*, *48*(2), 83-104.

Tanabe, K., and Fukuda, Y. (1987). The jaw apparatus of the Cretaceous ammonite Reesidites. *Lethaia*, *20*(1), 41-48. doi: https://doi.org/10.1111/j.1502-3931.1987.tb00758.x

Ulloa, F. (1977). *Aspectos de la geología de una parte este de la península de Santa Elena (desde Cuajiniquil a Santa Rosa de La Cruz, Guanacaste)* [B.S. thesis]. Universidad de Costa Rica.

Voigt, S., Gale, A., Jung, C., and Jenkyns, H. (2012). Global correlation of Upper Campanian– Maastrichtian successions using carbon-isotope stratigraphy: development of a new Maastrichtian timescale. *Newsletters on Stratigraphy*, *45*(1), 25-53. 10.1127/0078-0421/2012/0016

Ward, P., Haggart, J., Mitchell, R., Kirschvink, J., and Thomas Tobin, T. (2012). Integration of macrofossil biostratigraphy and magnetostratigraphy for the Pacific Coast Upper Cretaceous (Campanian–Maastrichtian) of North America and implications for correlation with the Western Interior and Tethys. *Bulletin of the Geological Society of America*, *124*(5/6), 957-974. doi: 10.1130/B30077.1

Weber, P. (2013). *Assessing sedimentary evolution by means of Sr-isotope ratios – 3 case studies on the Caribbean Plate (Cretaceous: Nicoya Peninsula, Costa Rica, Tertiary: Hess Rise, and La Désirade, Guadeloupe, France)* [Ph.D. thesis]. Université de Lausanne.

Whattam, S., Gazel, E., Yi, K., and Denyer, P. (2016). Origin of plagiogranites in oceanic complexes: A case study of the Nicoya and Santa Elena terranes, Costa Rica. Lithos, 262, 75-87. doi: http://dx.doi.org/10.1016/j.lithos.2016.06.017

Wickham, H. (2016). *ggplot2: Elegant Graphics for Data Analysis*. Springer-Verlag New York. doi: https://doi.org/10.1007/978-0-387-98141-3

Wiedmann, J., and Schmidt, W. (1993). Upper Cretaceous ammonites from Jamaica and their stratigraphic and paleogeographic implications. In R. Wright and E. Robinson (Eds.), *Biostratigraphy of Jamaica* (Geological Society of America Memoir, Vol. 182, pp. 77-92). Geological Society of America. doi: https://doi.org/10.1130/MEM182

Woodring, W. (1952). A *Nerinea* from Southwestern Oriente Province, Cuba. *Journal of Paleontology*, *26*(1), 60-62. doi: http://www.jstor.org/stable/1299770

Zimmerman, A., Johnson, C., Phillips, G., and Ehret, D. (2023). Taxonomy and paleobiogeography of rudist bivalves from Upper Cretaceous strata, Gulf Coastal Plain and Puerto Rico, USA. *Journal of Paleontology*, *97*(2), 318-340. doi: 10.1017/jpa.2022.104

APPENDIX 1.

Stratigraphic logs utilized in the study.

Legend for the stratigraphic logs

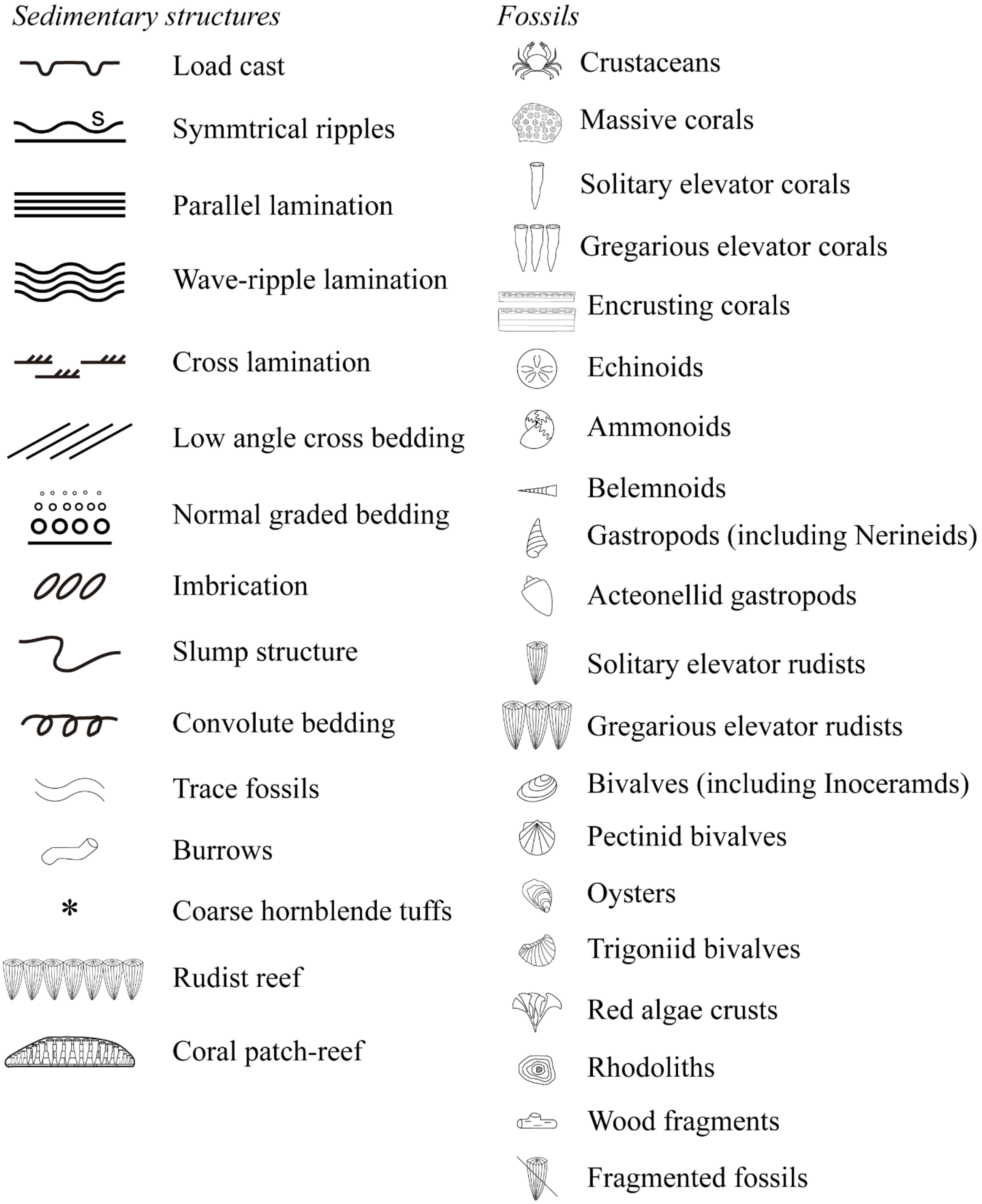

Esteban Lopez-Murillo

Stratigraphic section: C1 Antigua Marmolina

Coordinates of start: 10.896987/-85.63406

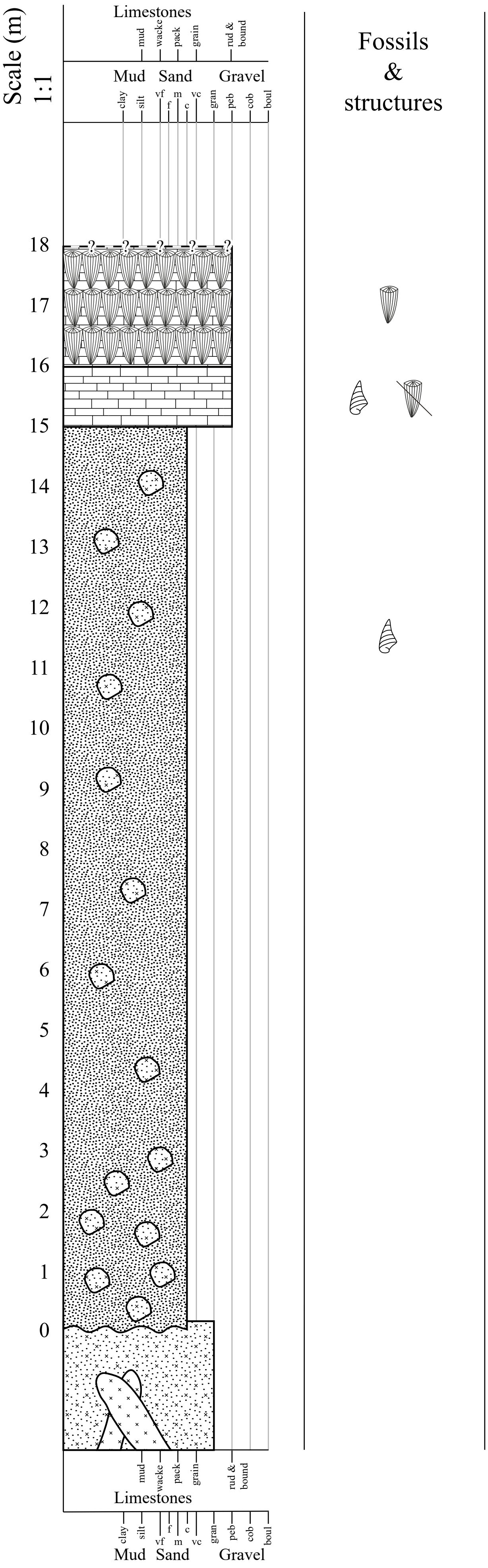

Description

2 m of massive radiolitid framestone with a foraminifer packstone matrix.

1 m of massive of rudstone with nerineid gastropds and diverse rudist shell fragments. 26. Antigua Marmolina: *Parasimploptyxis epelys* (Woodring, 1952), *Barrettia monilifera* Woodward,1862 (early late Campanian in Costa Rica).

15 m of coarse sandstone wth peridotite rounded lithoclasts and nerineid gastropod shells.

Santa Elena Nappe: massive serpentinized peridotites intruded by pegmatitic gabros (Hauterivian: 130 Ma) and by dolerites (Aptian: 120 Ma).

Esteban Lopez-Murillo

Stratigraphic section: C2 Caballito de Nicoya

Coordinates of start: 10.23533089/-85.3583425

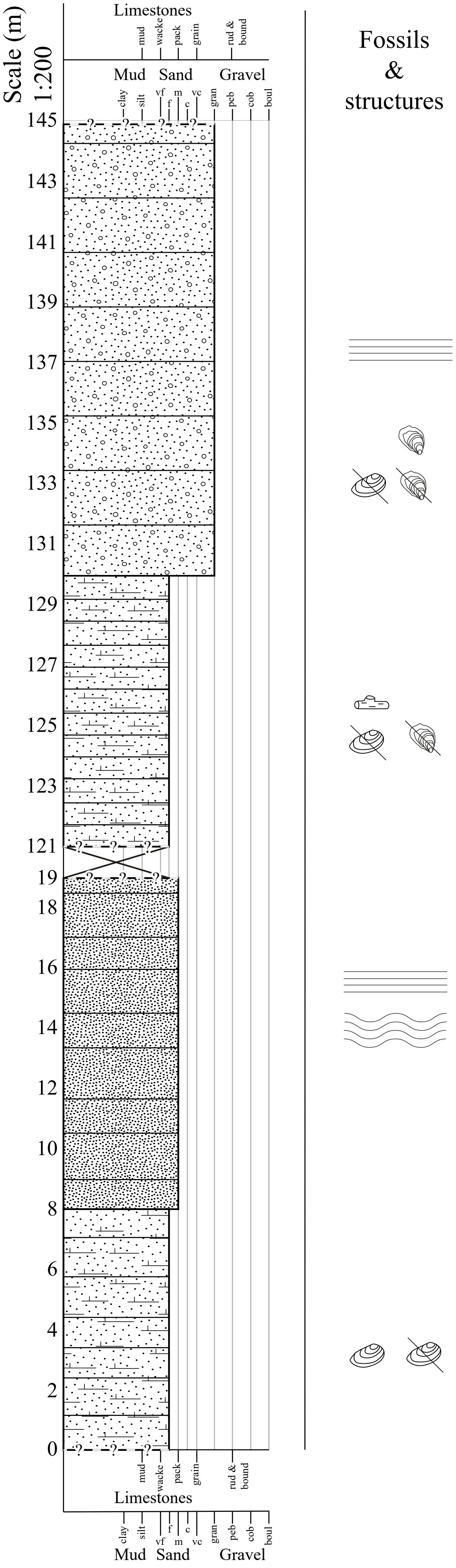

Description

15 m of dm-thick beds of fine conglomerate with mud clasts and cm-dm-long and cm-thick fine sandstone lenses.
43. 1.5 km W of Caballito: complete oyster valves and fragments, inoceramid prisms.

9 m of cm-thick fine calcareous sandstone with alligned wood fragments parallel to the bedding. It contains mud clasts.
35. NW of Cerro Barra Honda: dm-long cm-thick inoceramid prisms and fragments, complete oysters and fragments.

126 m not exposed.

11 m of cm-dm-thick beds of medium quartz sandstone.

8 m of cm-dm-thick beds of fine calcareous sandstone with inoceramid fragments.
43. 1.5 km W of Caballito: Complete inoceramid probably is from these facies.

Base unexposed.

Esteban Lopez-Murillo

Stratigraphic section: C3 Castilla de Oro

Coordinates of start: 10.43547312/-85.59921978

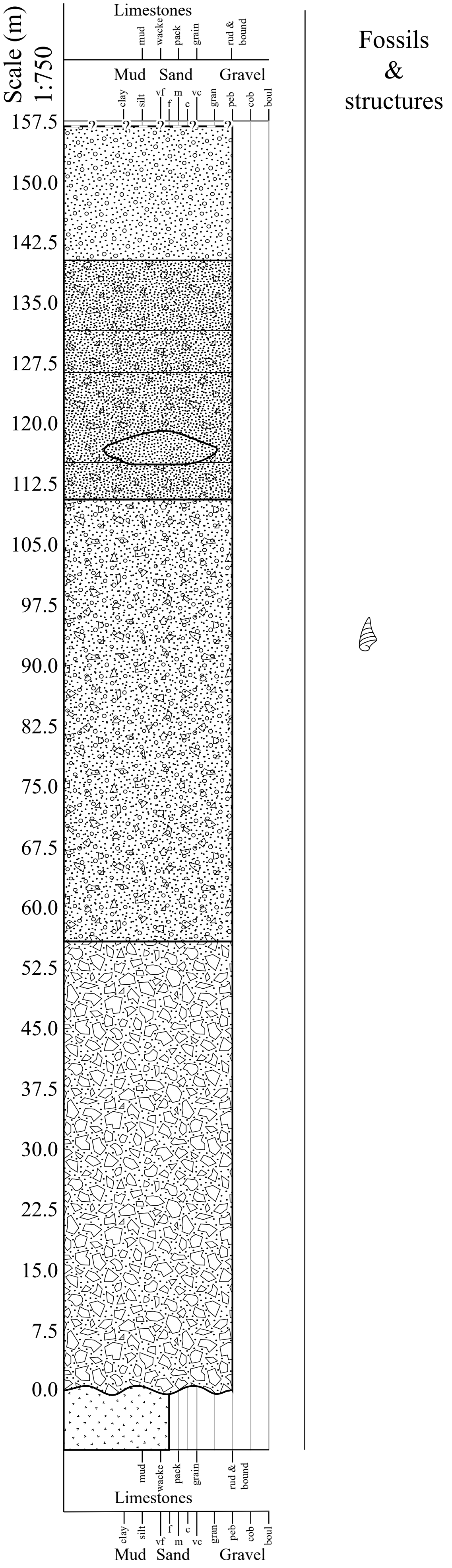

Description

16 m of massive beds of medium conglomerate with basaltic clasts (50%) and medium sandstone matrix (50%), poor sorting.

30 m of dm-m-thick amalgamated beds of medium breccia with basaltic clasts and 60% of medium sandstone matrix, poor sorting. It contains a dm-long and dm-thick medium sandstone lens.

36 m of massive beds of medium conglomerate-breccia with basalt and jasper clasts, medium sorting, almost no matrix.
36. Castilla de Oro: Nerineid gastropod.

48 m of massive beds of medium breccia with basalt clasts, bad sorting, almost no matrix.

Nicoya Complex (Turonian-Coniacian boundary: 89.7 Ma): massive weathered basalts.

Esteban Lopez-Murillo

Stratigraphic section: C4 Across Copal’s cemetery and N of Copal Coordinates of start: 10.1546992/-85.27274625

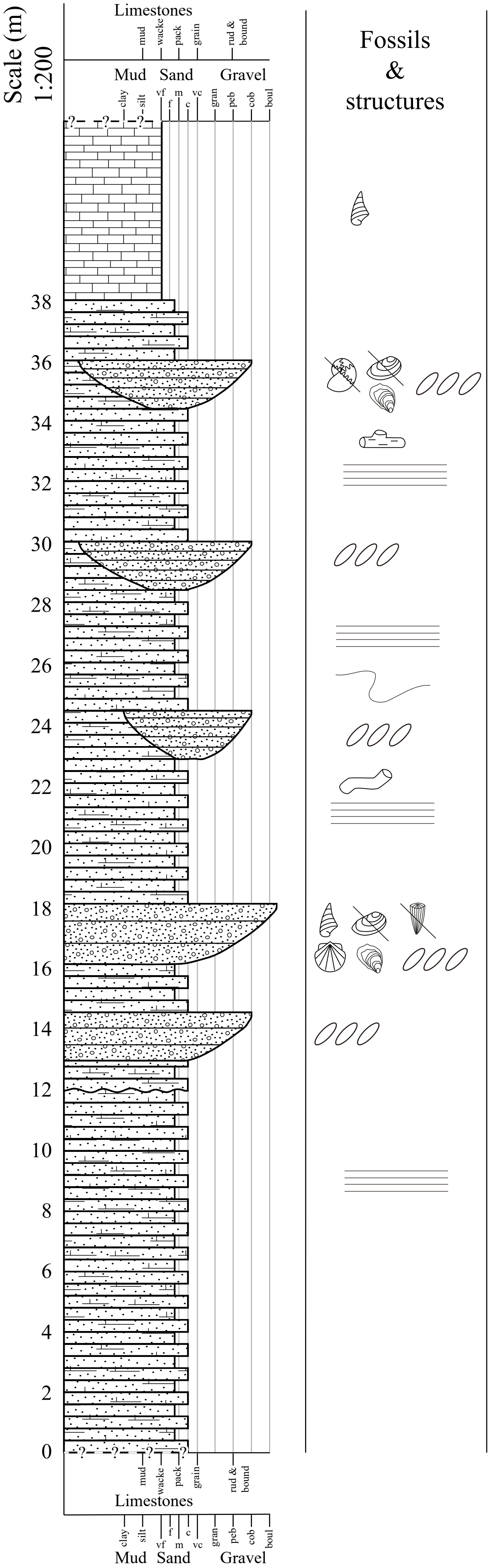

Description

Several dam of massive limestone. Blocks of wackestone the most abundant, less of floatstone.

51.Cerro Copal: small nerineid gastropod.

25 m of the interbedding of coarse and medium sandstone of the base with intrcalations of lenses m-thick and m-to-dm-long of medium to coarse conglomerate. Sinsedimentary folding observed in the interbedding of coarse and medium sandstone facies.

31. N of Copal: conglomerate and sandstone blocks inferred to be from the upper part of this sequence. Oysters, *Glyptoxoceras* sp., Inoceramidae indet. Some blocks contain abundant cm-wide-long allifgned wood fragments.

At 13 m, m-thick and m-to-dm-long lenses of medium to coarse conglomerate appear. The conglomeraes have dm-thick amalgamated bedding, bad sorting, matrix to clast support of grains. The clasts are made up of basalts, quartz, weathered tuff, jasper, green silicieous shale (Berrugate Fm. clasts). There are cm-thick and cm-long lenses of red mudstone with abundant planktonic foraminifera (lenses of the base of ïedras Blancas Fm.). Fossils found into the conglomerate lenses.

44. Across Copal’s Graveyard: *Pecten* sp., *Acteonella* sp., *Parasimpoptyxis* sp., Inoceramidae indet., *Endocostea* sp.

At 12 m, an interpreted subaerial erosion surface with paleosoil developed and mudcracks on top of the interbedding of coarse and medium calcareous sandstone facies.

13 m of interbedding of cm-thick beds of coarse sandstone with 20% reaction to HCl, with cm-thick beds of dark fine to medium sandstone. Sporadic cm-thick beds of fine cacalcareous sandtone in top of the medium sandstone beds.

Base not exposed.

Esteban Lopez-Murillo

Stratigraphic section: C5 Cerro Cebollin of Colorado

Coordinates of start: 10.2190707132/-85.1286421284

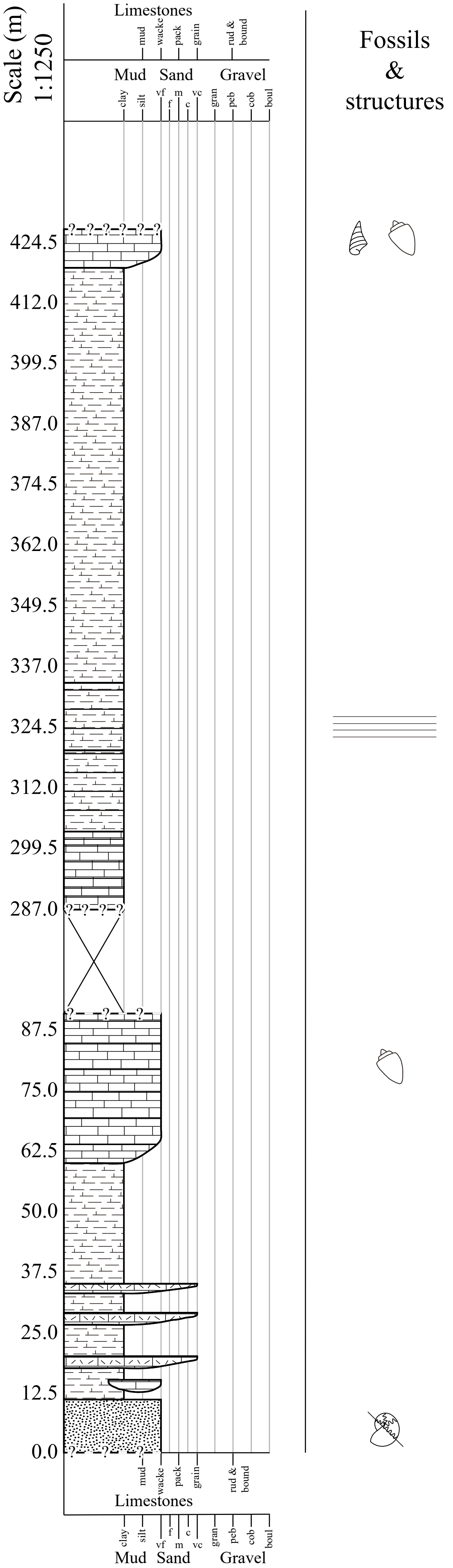

Description

8 m of dm-to-m-thick beds of limestone in a big lens. Facies include lithic grainstone at the base, overlied by wackestones, floatstones, and boundstones. Scleractinian corals, red algae (including rhodoliths), and gastropods.

86 m of massive gray calcareous shale.

14 m of dm-thick beds of rose to white-gray shales with amalgamated beds of white alligned bioclasts.

33 m of cm-to-dm-thick beds of terracotta red mudstones that change to rose calcareous shale.

196 m not exposed.

31 m of m-thick beds of limestone in a big lens, mainly wackestone and floatstone with Scleractinian corals and red algae.
39. Cerro Cebollin of Colorado: *Acteonella* sp., Nerineidae indet.

49 m of dm-thick beds of white gray calcareous shale, sometimes mudstone. There are several dm-thick m-long lenses of beds of lithic grainstone with red algae, glauconite and siliceous shale extraclasts.

11 m of massive blue-gray siltstone-very fine sandstone with crab and ammonite fragments.
Base not exposed.

Esteban Lopez-Murillo

Stratigraphic section: C6 Cerro Cebollin

Coordinates of start: 10.37684047/-85.43184493

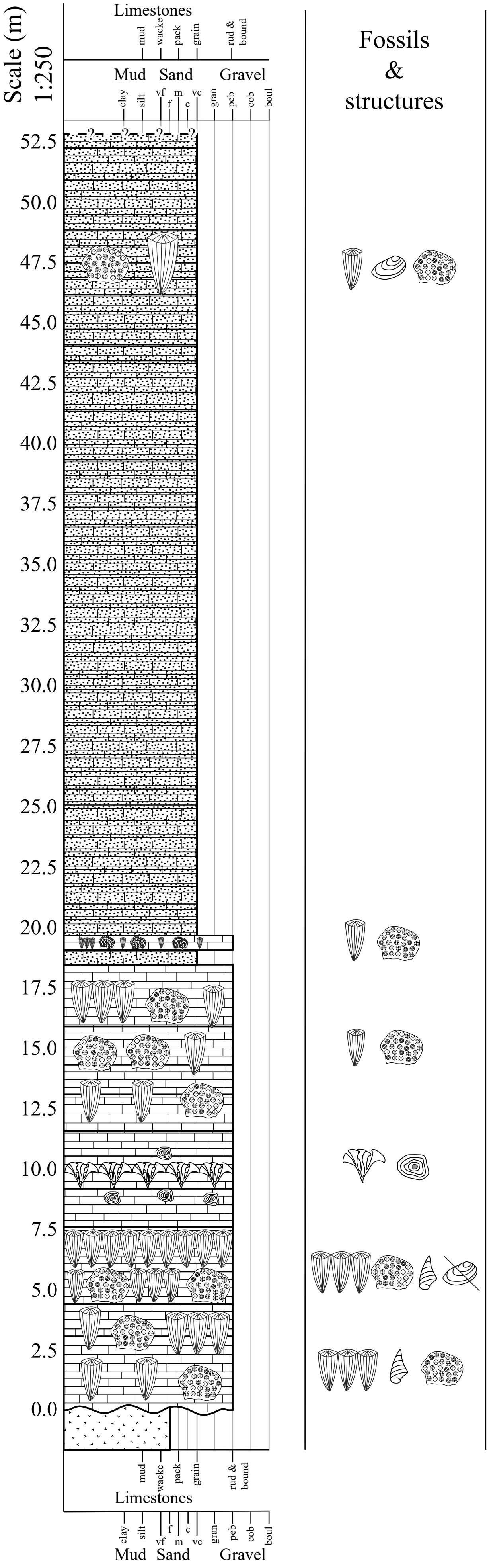

Description

33.3 m of cm-thick beds of fine grainstone.
21. NE slope of Cerro Cebollin: *Plicatula* sp.

0.6 m of hippuritid-coral bafflestone

0.6 m of fine grainstone

2.76 m of hippuritid-coral bafflestone

4 m of dm-m-thick beds of red algal bindstone with sparse rhodoliths.

3.2 m-dm-thick beds of rudist-coral framestone.
20. Top of Cerro Cebollin: *Inoceramus?* sp., *Parasimploptyxis epelys* (Woodring, 1952), *Barrettia monilifera* Wodward, 1862 (early late Campanian in Costa Rica).

4.4 m of dm-m-thick beds of bioclastic rudstone with some rudists, corals and Nerineids in life position. cm-dm-diameter basaltic clasts embedded in limestone matrix at the base.

Nicoya Complex (Turonian-Coniacian boundary: 89.25 Ma): massive weathered fractured basalts.

Esteban Lopez-Murillo

Stratigraphic section: C7 Cerro Congo

Coordinates of start: 10.1837841604/-84.9989461083

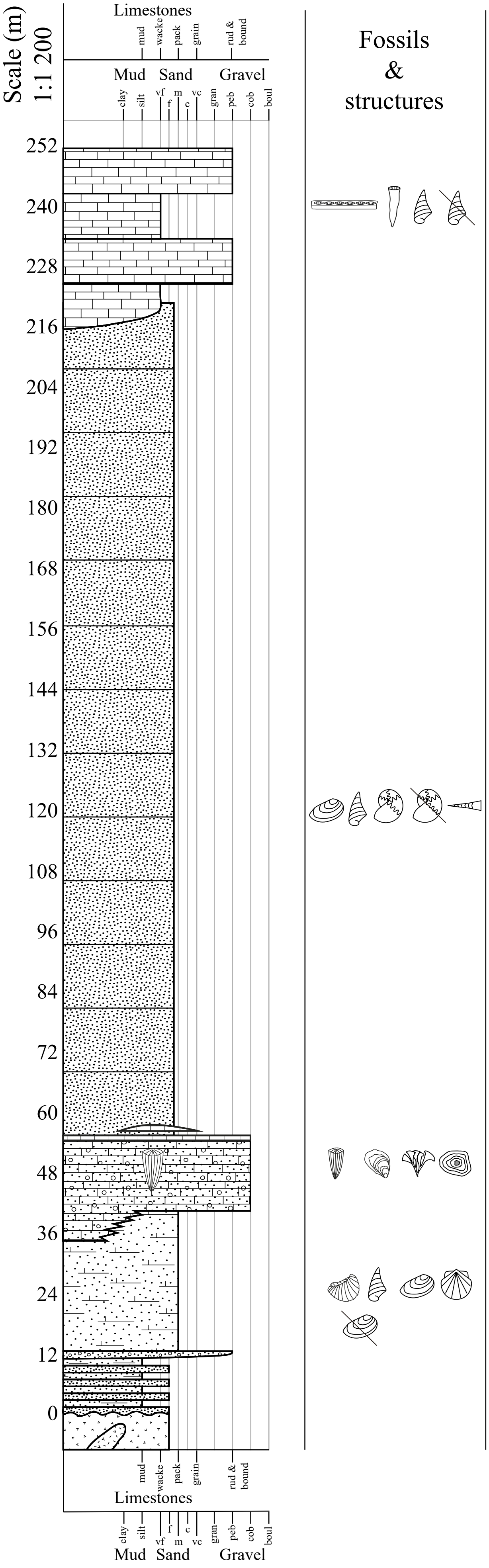

Description

36 m of lenticular carbonate platform containing massive m-dam-thick and long lenses of limestone. Mainly white-gray wackestones-floatsone. Intercalation of dm-m-thick intraclastic breccia beds. Rare bioclastic and oolithic grainstone beds. Isolated in-situ dm-m-large patch-reefs of bindstones of laminar Scleractinian corals. It contains *Euphyllia donatoi* Aguilar and Denyer, 2001, red algae (and rhodoliths), turritellid gastropods, other gastropods and solitary corals. Sparse bivalves, echinoderms, brachiopods, *Halimeda* sp., miliolids, small foraminifers. Interbedded with the previous facies.

50. Across Finca La Irma: small *Plesioptygmatis?* sp (early Maastrichtian).

166 m of dm-m-thick beds of massive blue-gray fine to medium slightly calcareous sandstone. It has frequent spheroidal weathering.

At base the sandstone is calcareous with m-thick and long lens-shaped bioclastic grainstone beds.

5. La Irma Quarry: *Baculites leopoliensis* Nowak, 1908, *Neophylloceras surya* (Forbes, 1846), *Pachydiscus* sp., 1 big gastropod, *Belemnitella americana* Morton, 1834, many small gastropods and bivalves (*Acila* sp., *Neithea* sp., *Pinna* sp.) (latest Campanian).

1 m of bioclastic grainstone.

21 m of m-thick massive medium conglomeratic, bioclastic and fossiliferous grainstone-rudstone with rhodoliths, basalt and jasper pebbles.

4. Unnamed ridge: giant oysters, *Barrettia monilifera* Woodward, 1862
(early late Campanian).

28 m of m-thick amalgamated cm-dm-thick beds of medium bioclastic and fossiliferous sandstone.

3. Cerro Congo's abandoned quarry: trigoniids, *Inoceramus*, gastropods and bivalves.

1,5 m of massive violet polymictic (basaltic-jasper) medium conglomerate. Canal-shaped erosive base.

11 m of interbedded cm-thick parallel beds violet fine laminated
sandstone and siltsone. Poorly lithified.

Nicoya Complex: massive weathered fractured basalts intruded by komatiitic lavas (earliest Coniacian: 89.25 Ma).

Esteban Lopez-Murillo

Stratigraphic section: C8 Cerro Coyolar (Huevo Frito)

Coordinates of start: 10.3856928/-85.62924634

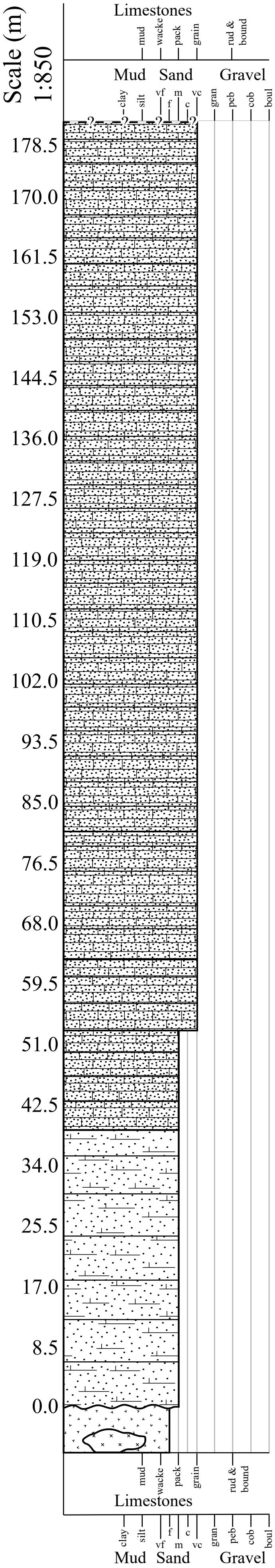

Fossils
&
structures

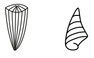

Description

100 m of dm-thick beds of bioclastic grainstone with jasper lithoclasts (5%) and bigger bioclasts (2%).

18 m of dm-thick parallel beds of bioclastic grainstone with a 1.5 m-thick bed of bioclastic grainstone with volcanic extraclasts.

10 m of dm-thick parallel beds bioclastic grainstone with a cm-long basalt extraclast and idiomorphic plagioclase crystal..

38. Cerro Huevo Frito (Coyolar): complete Nerineidae indet.

14 m of dm-thick parallel beds of bioclastic grainstone or medium bioclastic calcareous sandstone.

39 m of dm-thick parallel beds of medium bioclastic calcareous sandstone.

Nicoya Complex: massive weathered fractured basalts (Turonian-Coniacian boundary: 89.7 Ma) intruded by gabbros (Santonian-Campanian boundary: 83.8 Ma).

Esteban Lopez-Murillo

Stratigraphic section: C9 Cerro Sombrero

Coordinates of start: 10.16648437/-85.2584137

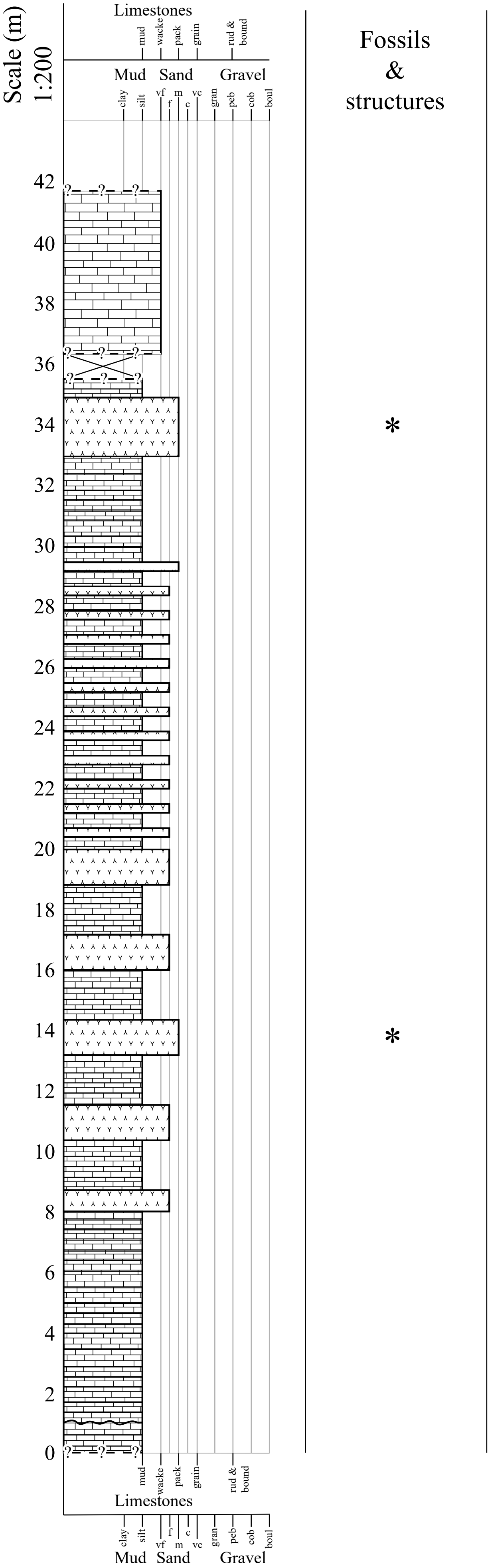

Description

5.4 m of massive cream wackestones.

5.5 m of dm-cm-thick beds of whitish gray mudstones, at the base there are lenses of red mudstones. There is a m-thick bed of hornblende tuff.

22 m of interbedding of cm-thick beds of red and violet mudstones and gray brown coarse to fine hornblende tuffs.

8 m of dm-cm-thick beds of red, brown reddish and violet mudstones.

At 1 m, subaerial erosion surface with paleosoil developed and mudcracks on top of the violet mudstones.

Base not exposed.

Esteban Lopez-Murillo

Stratigraphic section: C10 Santa Cecilia de Cobano

Coordinates of start: 9.72070165/-85.15209923

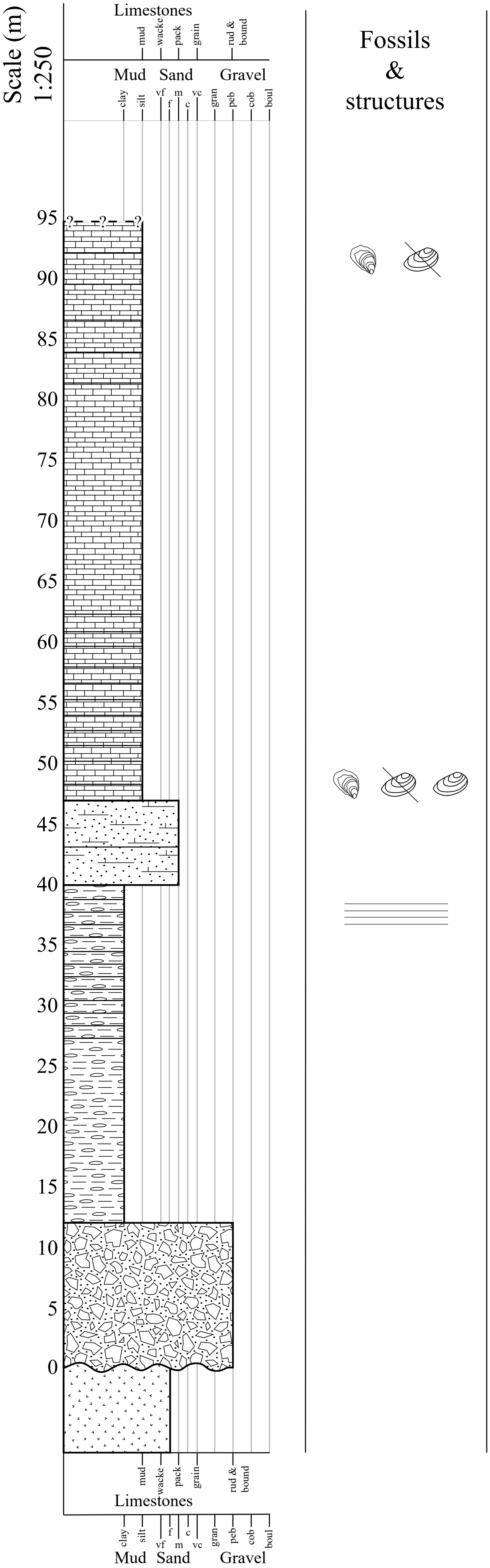

Description

48 m of red mudstones. At the base, cm-thick beds. In the middle, beds turn massive. In the upper part, dm-thick beds.

41. Cóbano: Entire inoceramid valves, inoceramid valve fragments, small oyster growing on top of inoceramid fragments.

7 m of m-thick beds of white medium sandstone with low reaction to HCl.

28 m of massive gray siliceous shale in the base. In the upper part, siliceous shales turn rose and in cm-thick beds.

12 m of massive medium breccia with basaltic and red and yellow jasper clasts (50), and medium sandstone marix (50%). Poor sorting.

Nicoya Complex (earliest middle Abian: 110 Ma): weathered breccified basalts.

Esteban Lopez-Murillo

Stratigraphic section: C11 Colorado de Abangares

Coordinates of start: 10.2108774092/-85.1058206473

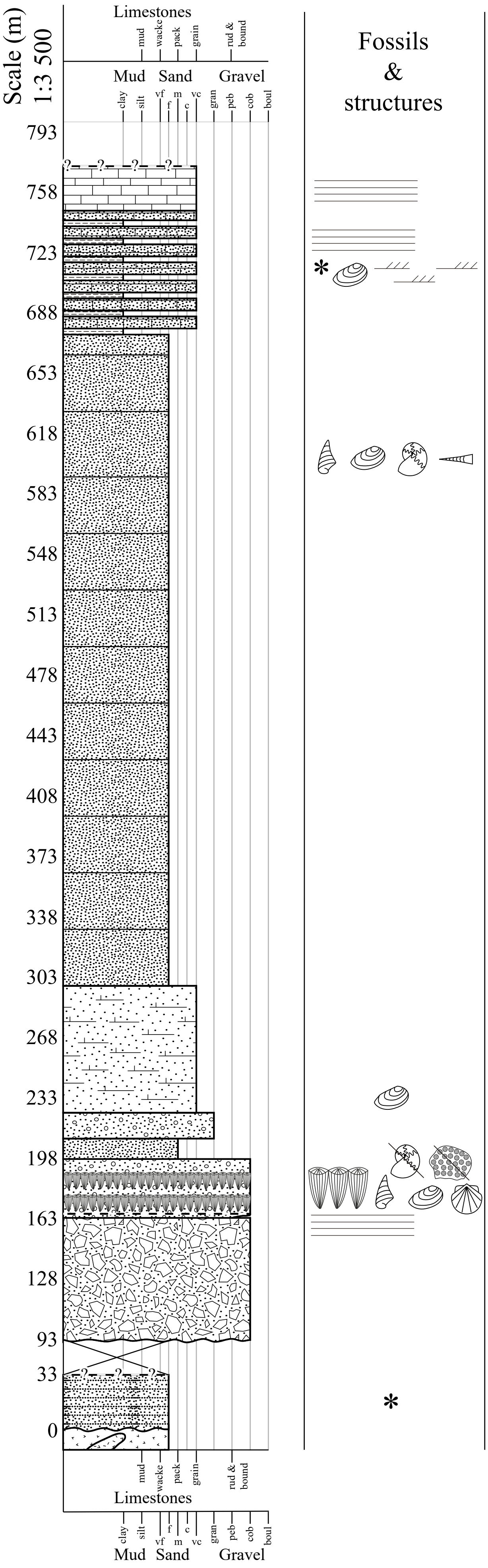

Description

26 m of massive beds of grainstone, packstone and wackestone with Scleractinian coral, rudist, *Inoceramus* and bivalve fragments.

72 m of intercalations of cm-thick beds of gray slightly calcareous shale and dm-thick beds of blue-gray biclastic grainstone. In the grainstone, there are several cm-thick laminae to beds of hornblende-rich tuff. In the middle, there are 5 beds of *Inoceramus* prisms in life position parallel to bedding, lying onto the grainstone beds.

49. E of Cerros Cerco de Piedra (3).

277 m of m-massive to dm-m-thick beds of greenish-gray fine sandstones with some greenish-gray calcareous shales. Spheroidal weathering is abundant.

Late Campanian.

8. E of Cerros Cerco de Piedra (1).

9. E of Cerros Cerco de Piedra (2): *Glypoxoceras* sp., *Gaudryceras* sp.

74 m of dm-m-thick beds packstone with macroforaminifers, lithoclasts and matrix.

15 m of dm-m-thick beds of conglomeratic vulcaniclastic sandstones with carbonate cement and macroforaminifers.

12 m of strongly weathered medium sandstone.

32 m of dm-m-thick beds of medium-coarse calcareous conglomerates with the same clast composition as below. It contains two levels with rudist close cluster reefs.

39. Tajo Los Almendros: inoceramid shells, nerineid gastropods, ammonite fragments and many other gastropods and bivalves (early late Campanian).

75 m dm-m-thick amalgamated beds of coarse basaltic violet breccia with low content of violet matrix. On top, three beds of medium conglomerate with basalt, jasper and green shale clasts, with laminated coarse sandstone. It gradually pases to the next unit.

60 m covered.

33 m of green-turquoise shales, followed by coarse to medium green sandstone (submarine ignimbrite), and cm interbedding of greenish-gray fine sandstones with greenish-gray to white calcareous shales.

Nicoya Complex: massive fractured weathered basalts intruded by komatiitic lavas (Turonian-Coniacian boundary: 89.25 Ma).

Esteban Lopez-Murillo

Stratigraphic section: C12 Nambi de Nicoya

Coordinates of start: 10.21805/-85.51832

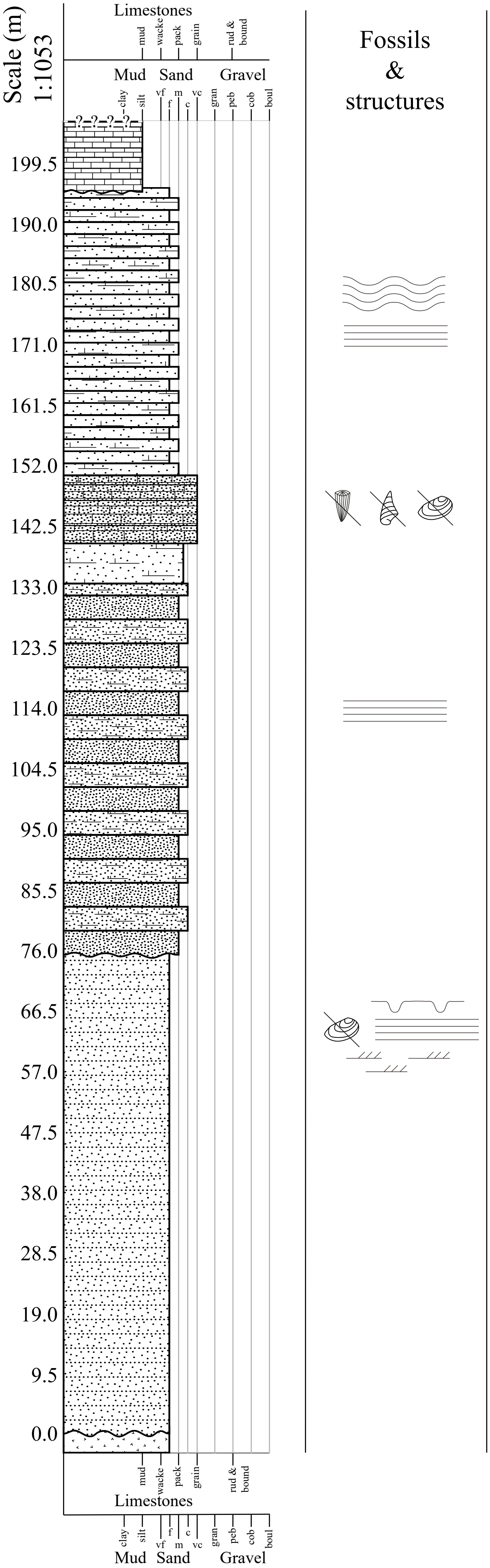

Description

100 m of cm-thick beds of red mudstones.

100 m of interbedding of cm-thick beds of calcareous dark gray to black medium and fine sandstone.

18 m of cm-dm-thick beds of gray grainstone or calcarenite.

10 m of very calcareous medium to coarse sandstone.

14 m of cm-dm-thick interbedding of dark gray medium sandstone and light gray very calcareous coarse sandstone.

39 m of super compacted dark gray fine sandstone. It has cm-thick beds, lenses and wedges of brown to reddish shales and very fine sandstone.
18. Nambi Curves roadcut: dm-long inoceramid prisms.

Nicoya Complex (Turonian-Coniacian boundary: 89.9 Ma): massive basalts.

Esteban Lopez-Murillo
Stratigraphic section: C13 Fila Machete

Coordinates of start: 10.37037223/-85.56854514

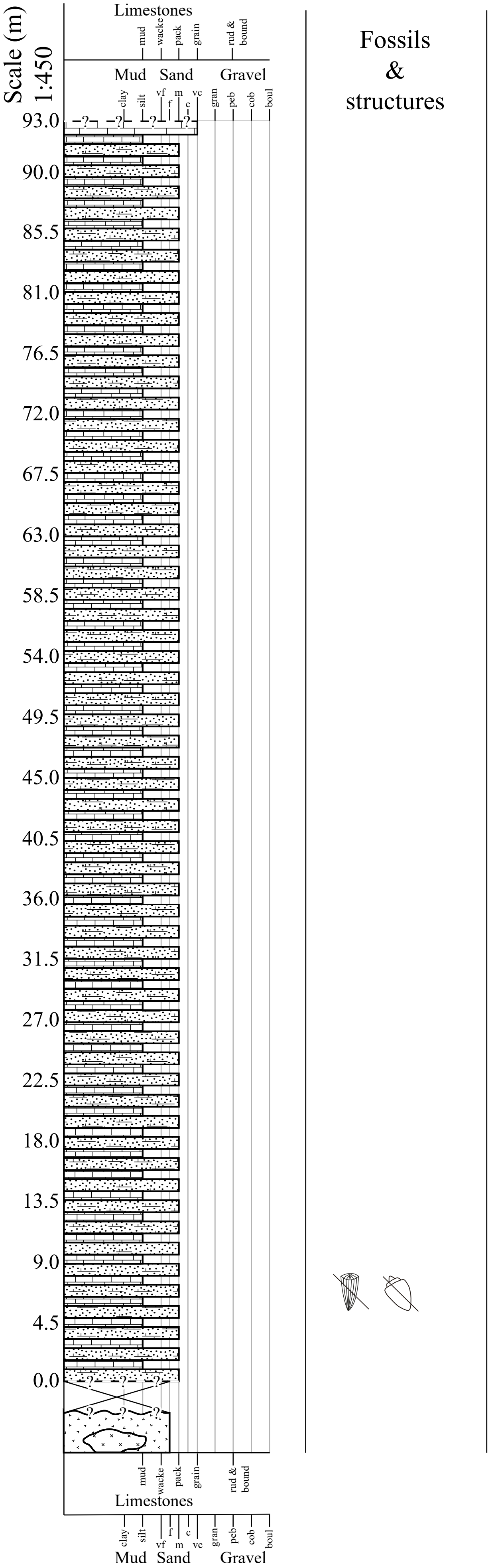

Description

1 m of bioclastic grainstone.

92 m of interbedded dm-thick beds of gray calcareous sandstones and cm-thick beds of fine mudstone.
22. Fila Machete’s abandoned quarry: rudist fragments and Actaeonellidae indet.

Unknown thickness of basaltic sandstones due to a lack of outcrops

Nicoya Complex: massive weathered fractured basalts (Turonian-Coniacian boundary: 89.7 Ma) intruded by gabbros (Santonian-Campanian boundary: 83.8 Ma).

Esteban Lopez-Murillo
Stratigraphic section: C14 Jicaral

Coordinates of start: 9.95851406/-85.12375691

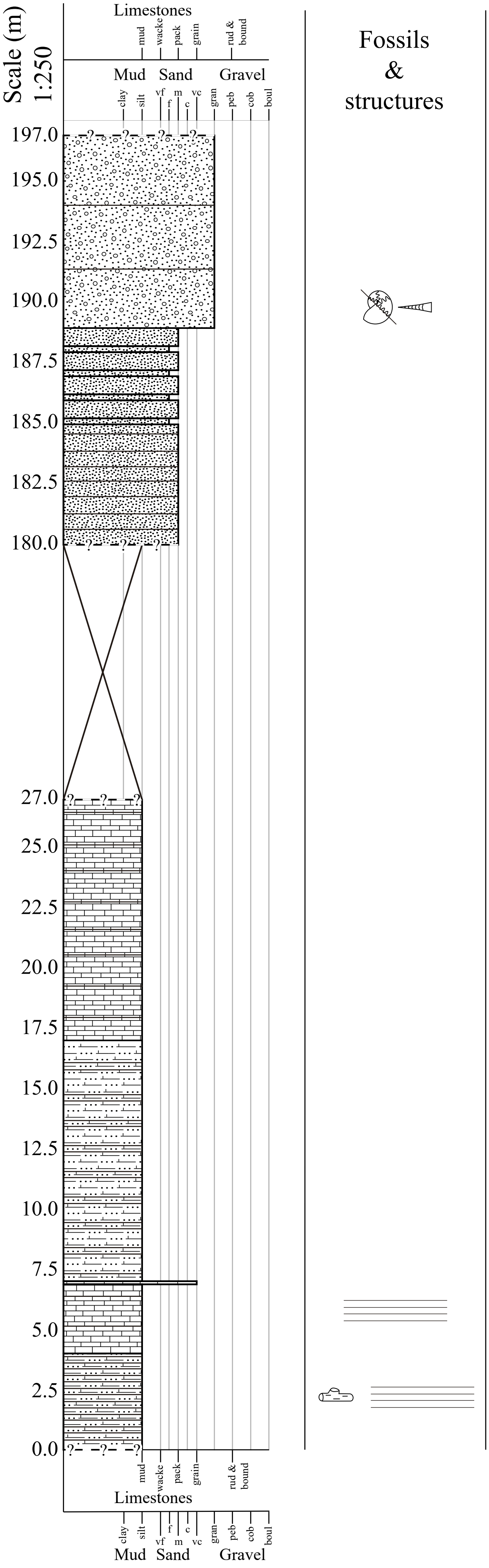

Description

8 m of m-thick beds of blue-gray fine conglomerate with small reaction to HCl. It has 85% of volcanic, volcanic minerals and sedimentary clasts, and 15% of medium sandstone matrix. Poor sorting, moderately rounded. Some clasts are up to 5 cm in diameter. It has cm-long lenses of blue-gray fine sandstone
14. Jicaral: belemnite rostrum, possible ammonite fragments.

4 m of interbedding of cm-thick beds of fine sandstone with dm-thick bed of medium sandstone with spheroidal weathering.

5 m of cm-thick beds of medium sandstone, white-gray color when wheatered. No reaction to HCl. Little spheroidal weathering, which becomes more abundant in the upper part.

153 m not exposed.

4 m of dm-m-thick beds of white mudstones.

4 m cm-dm-thick beds of calcareous siltsotnes.

0,13 m of white grainstone.

2,87 m of dm-m-thick beds of white mudstones.

4 m of cm-thick beds of blue-gray calcareous siltstone. It has spheroidal weathering, alligned organic matter prallel to bedding, and foraminifera.

Unknown base

Esteban Lopez-Murillo
Stratigraphic section: C15 Loma Chumico

Coordinates of start: 10.06203/-85.264026

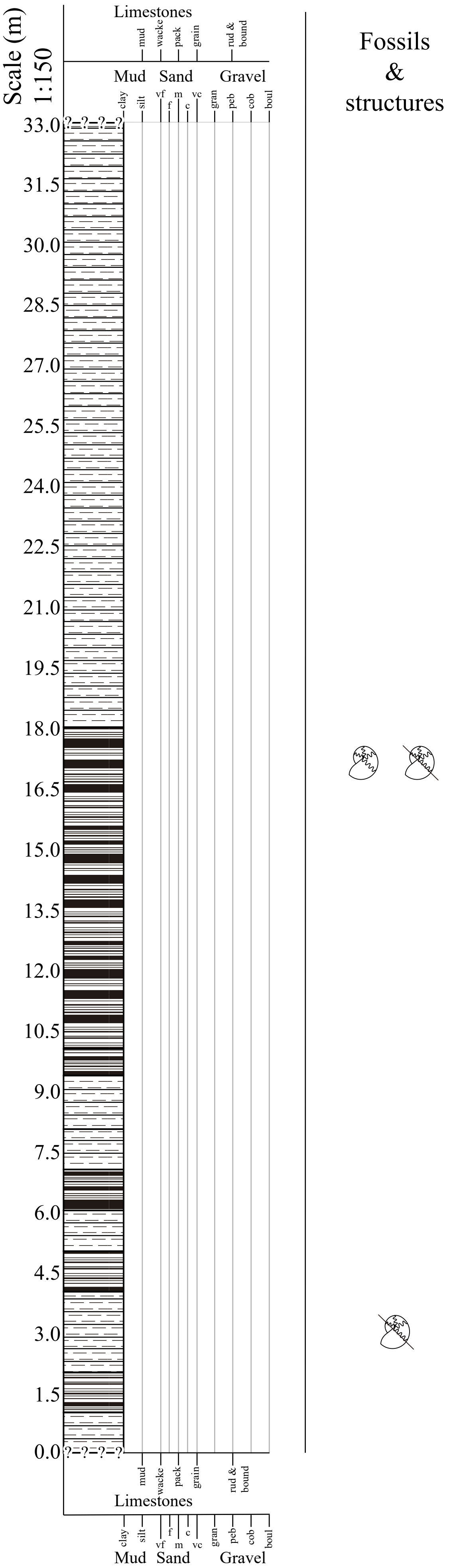

Description

15 m of cm-dm-thick beds of siliceous white grayish to yelowish shales with iron oxide rust.

9 m of cm-dm-thick beds of oil shale with white rust, some are silicified.
15. Loma Chumico roadcut: Acanthoceratidae indet., Gaudryceras sp., inoceramid prisms.

8 m of cm-dm-thick beds of siliceous white grayish to yelowish shales with iron oxide rust. Ocassional cm-dm-thick beds of oil shale with white rust, some are silicified. Sparse molds of ammonite fragments in the siliceous shales.

Unexposed base. 42. Rio Morote: Inoceramidae indet., probably from the coarse facies of the base.

Esteban Lopez-Murillo

Stratigraphic section: C16 E of Manzanillo

Coordinates of start: 10.1282508805/-85.0011369072

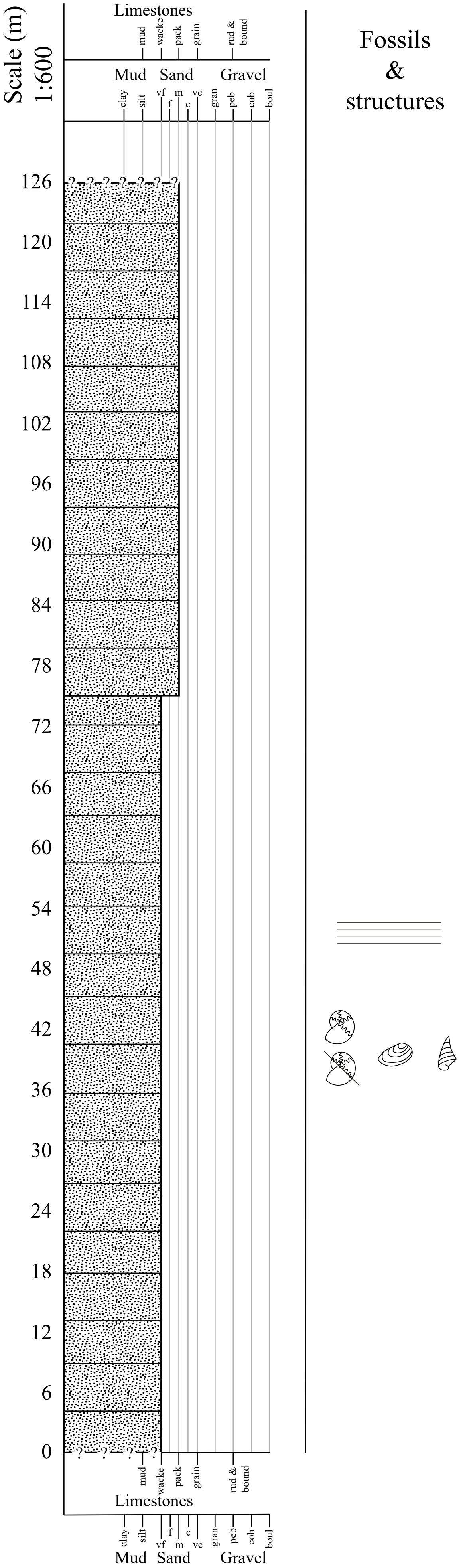

Description

126 m of dm-to-m-thick beds of fine calcareous sandstone to calcreous siltsone. On top, the sandstones become medium grained. Amalgamated bedding, weak parallel lamination.

1. E of Manzanillo: *Scaphites* sp., *Glyptoxoceras* sp., ammonite jaws, Gastropoda indet. 1, Gastropoda indet. 2, *Inoceramus* sp. 1, *Inoceramus* sp. 2, *Ostrea* sp., Inoceramid prisms (latest Campanian).

Esteban Lopez-Murillo
Stratigraphic section: C17 Montezuma

Coordinates of start: 9.658365/-85.062201

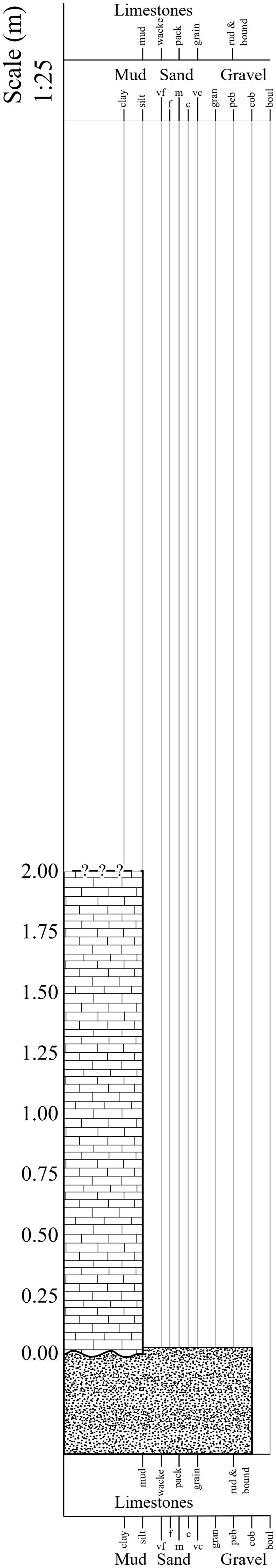

Fossils & structures

Description

2 m thick block of dark gray mudstone inserted into the breccia from below.
11. Montezuma: folded alligned inoceramid prisms.

Hialoclastitic basaltic breccia.

Esteban Lopez-Murillo
Stratigraphic section: C18 Playa Organos

Coordinates of start: 9.81451161/-84.89402525

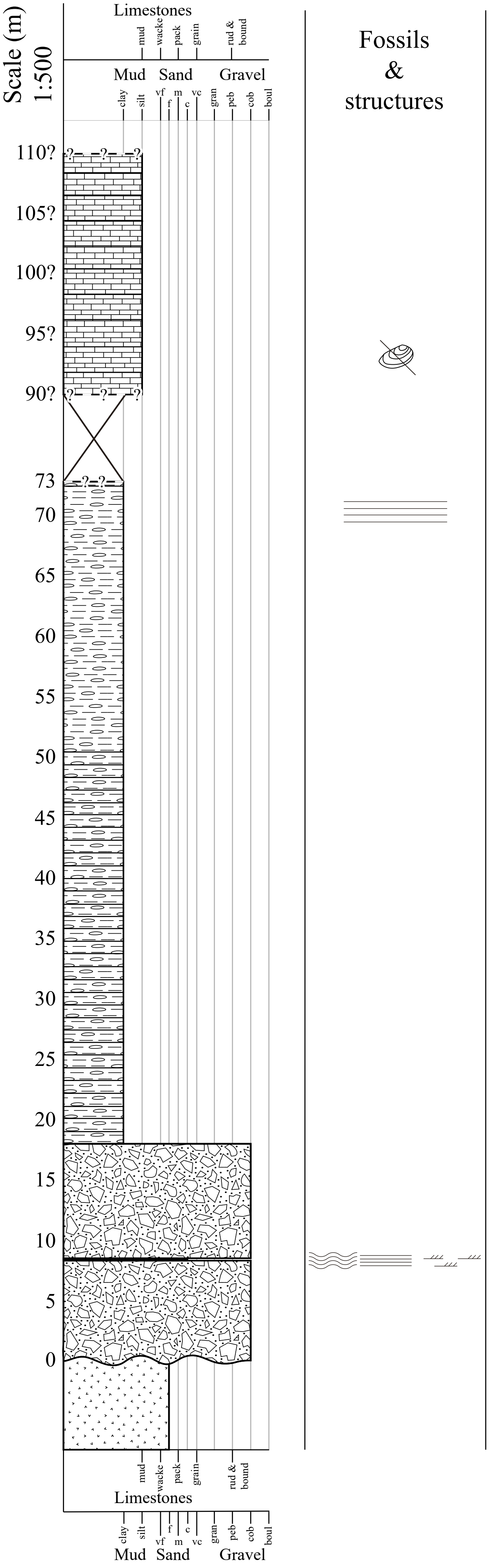

Description

Unknown thickness of red mudstones.
13. Playa Organos: inoceramid prisms.

Uknown thickness not exposed.

20 m of massive white-gray siliceous shales. While going upwards, shales turn rose. On top, they present parallel laminae.

35 m of interbedding of cm-dm-thick beds of siliceous reddish-brown, gray-white and green shales, sometimes in beds are lenticular. No reaction to HCl.

18 m of massive beds of green medium polymictic breccia with basaltic, gabbroic, and red, yellow and green jasper clasts (80%), with hyaloclastitic breccia (20%). There are megaclasts (m-diameter) of pillow basalts. No reaction to HCl.
Towards the top, there are 70 cm of interbedding of dm-thick beds of coarse and fine sandstone. No reaction to HCl.

Nicoya Complex (earliest middle Abian: 110 Ma): hyaloclastitic basalt breccia.

Esteban Lopez-Murillo

Stratigraphic section: C19 N point of Playa Panama

Coordinates of start: 10.6005499/-85.64936379

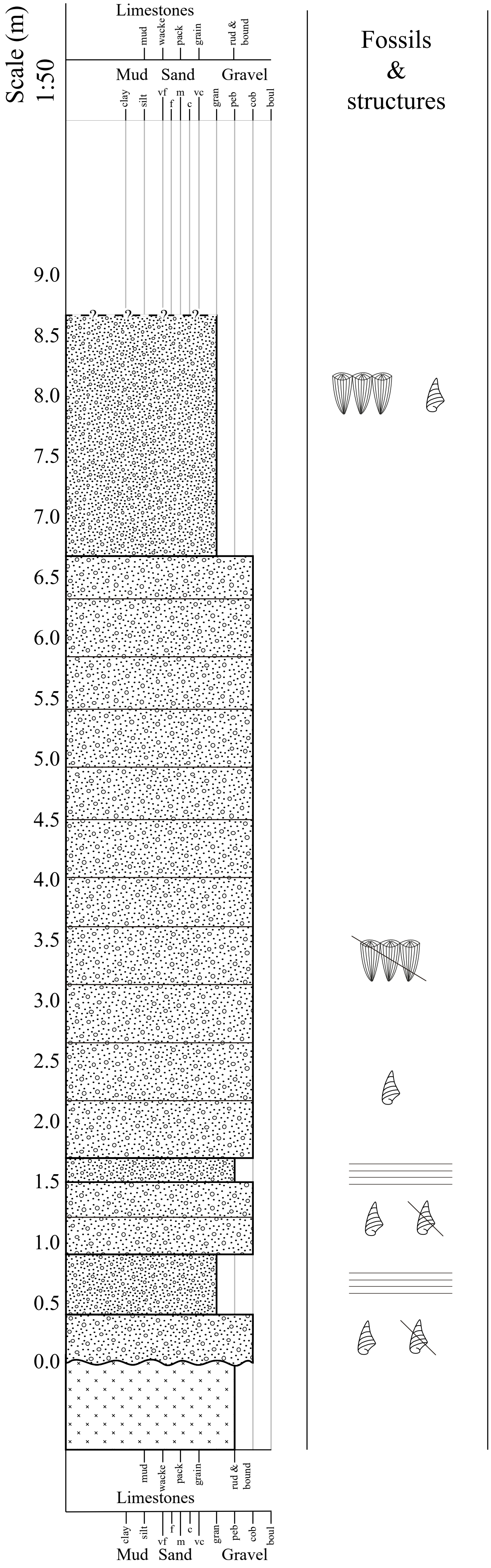

Description

23. N point of Playa Panama: blocks eroded from cliff. They come up from higher up in the sequence, m-long dm-thick rudist reefs with sparse colonial Scleractirian corals with encrusting red algae. Same 2 Nerineid gastropod species from the base. *Barrettia monilifera* Woodward, 1862 (early late Campanian).

2 m of fine calcareous conglomerate, same composition as beds below. Complete small nerineid gasropods. First appearance of small bouquets of *Alencasterites mooretownensis* (Trechmann, 1924) in life position.

10 m of dm-thick beds of coarse calcareous conglomerate, same composition as beds below. Complete nerineid gastropods in life position. First appearance of toppled small bouquets of *Alencasterites mooretownensis* (Trechmann, 1924).

0.6 m in two beds of coarse calcareous conglomerate, same composition as beds below. Complete nerineid gastropods in life position.

0,5 m of fine calcareous conglomerate, same composition as bed below.

0.4 m of coarse calcareous conglomerate, with 70% basaltic, jasper and gabbroic clasts, well rounded and spherical, poor sorting, 20% of coare sandstone matrix. Calcitic cement. Complete nerineid gastropods.

40. Bahía Monte del Barco: Complte nerineid gastropods and fragments.

Nicoya Complex (Santonian-Campanian boundary: 83 Ma): massive weathered gabbros.

Esteban Lopez-Murillo
Stratigraphic section: C20 N of Puerto Nispero

Coordinates of start: 10.21367557/-85.23062355

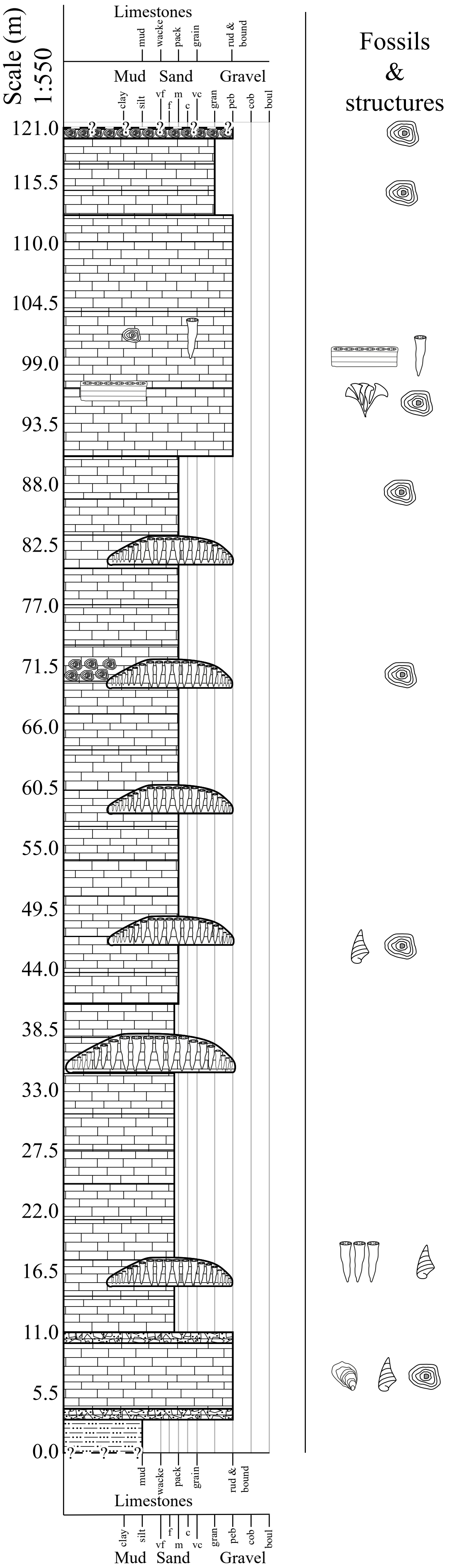

Description

7 m of dm-thick parallel beds of packstone-rudstone with dm-m-scale rhodolith beds.

22 m of m-thick to massive wackestone-packstone-rudstone. Common cm-dm-scale rhodoliths, solitary corals and scarse encrusting corals in life position.

50 m of dm-thick parallel beds of wackestone-packstone with dm-m-scale coral *E. donatoi* patch-reefs. Common rhodoliths and sparse rhodolith beds. Rare small gastropods. Scleractinian coral *Marcelohelia* sp. present (Maastrichtian).

30 m of dm-thick parallel beds of wackestone-packstone with dm-m scale *Euphyllia donatoi* Aguilar and Denyer 2001 patch-reefs.
06. N of Puerto Nispero (middle part): common dm long *Plesioptygmatis?* sp. between patch-reefs, *Rostellana* sp. (early Maastrichtian).

1 m of dm-m calcareous intraclastic breccia.
6 m of masive to dm-m-thick beds of bioclastic-lithoclastic packstone-grainstone. Sparse rhodoliths.
07. N of Puerto Nispero (lower part): small oyster patch-reefs, small *Plesioptygmatis?* sp.
1 m of dm-m calcareous intraclastic breccia.
3 m of massive-like weathered siltstone yielding *Rugoglobigerina rugosa* (Plummer, 1927) and *?Globotruncanella* sp. (late Campanian-early Maastrichtian).

Esteban Lopez-Murillo

Stratigraphic section: C21 Punta Conejo

Coordinates of start: 10.367278/-85.866607

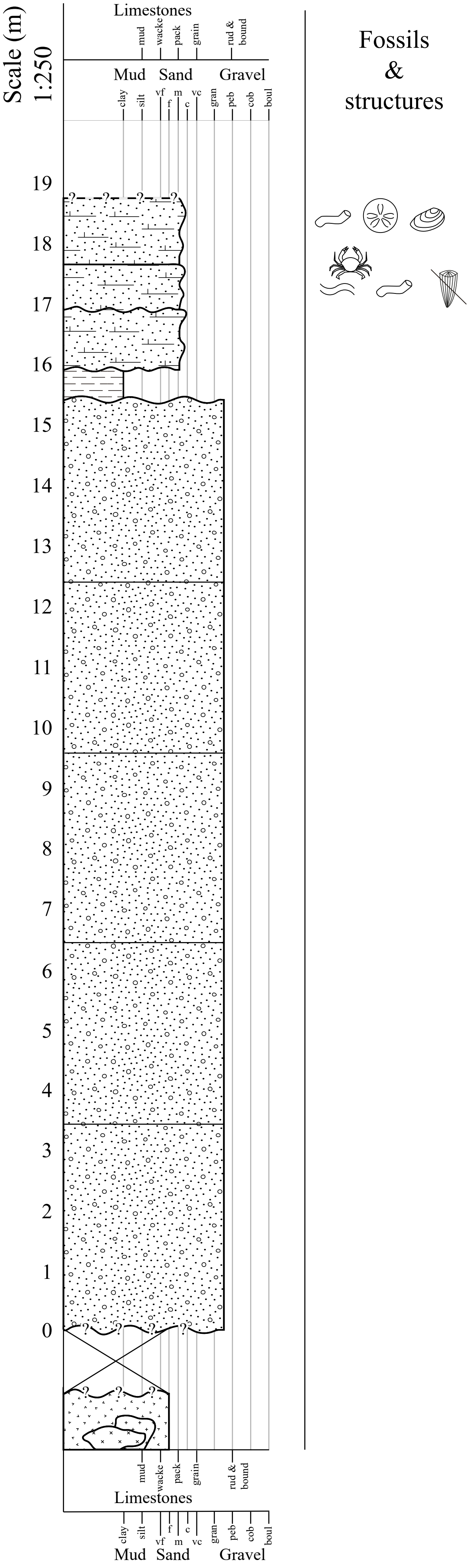

Description

33.3 m of 3 dm-m-thick beds of medium-coarse light-colored calcareous sandstone with good selection, clean and with abundant bioturbation (especially in the upper beds). It has some coarser material intercalations, and each bed finishes with a coarse bioclastic level (almost limestone). The intermediate bed has cm-diameter Thalassinoides and Ophiomorpha ichnofossils; the upper level has abundant bigger Thalassinoides burrows filled with hells and echinoid fragments and spines.
24. Punta Conejo: posible gastropods and bivalves.

0.5 m of red shales.

15-20 m of m-thick beds of medium conglomerate with basaltic clasts, and fine conglomerate with subangular gabbroic clasts, contact is by matrix or by clast, matrix is non-calcareous sand.

Unknown gap

Nicoya Complex: massive fractured basalts intruded by gabbros interbedded with plagiogranites and diorites (Turonian-Coniacian boundary: 88.9 Ma).

Esteban Lopez-Murillo

Stratigraphic section: C22 Punta Pochote

Coordinates of start: 9.741615/-84.985422

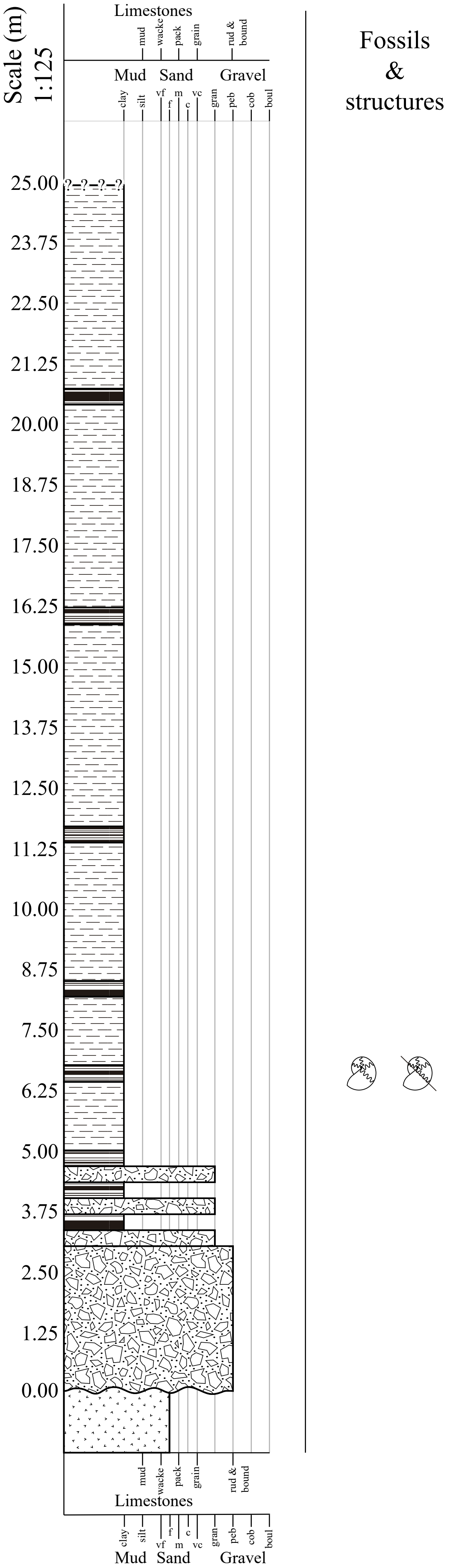

Description

20 m of cm-dm-thick beds of siliceous white grayish to yelowish shales with iron oxide rust. Ocassional cm-dm-thick beds of oil shale with white rust, some are silicified.
12. Punta Pochote: complete ammonites and fragments with nacareous layer.

2 m of interbedding of the bassaltic breccia from below with cm-dm-thick beds of oil shale with white rust, some are silicified.

3 m of basaltic breccia with subangular to subrounded mm-cm-long clasts.

Nicoya Complex (earliest middle Abian: 110 Ma): hyaloclastitic basaltic breccia.

Esteban Lopez-Murillo
Stratigraphic section: C23 Quebrada Cacao

Coordinates of start: 11.1288203/-85.62964014

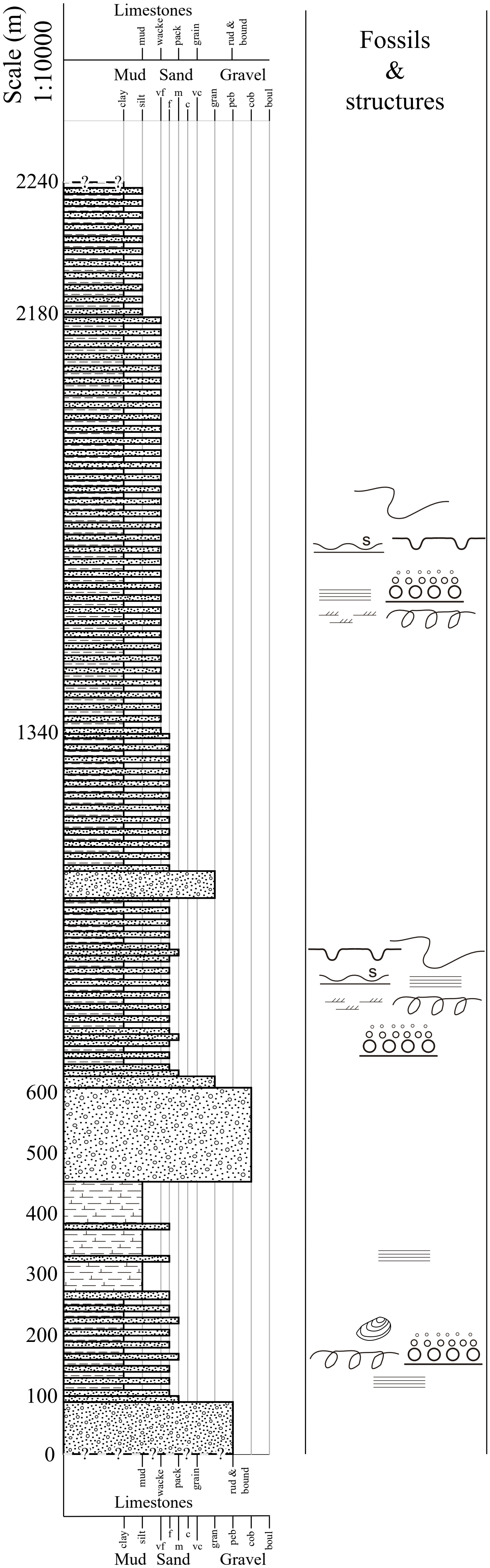

Description

1100 m of interbedding of cm-thick beds of medium sandstone to claystone. On top, the deposits becom interbeding of fine sandstone and claystone without coarse sandstone levels.

800 m of interbedding of dm-thick beds of medium sandstone, fine sandstone and claystone. Globotruncana sp. present (Maastrichtian), also Alveolina sp. (early Paleocene-Eocene).

150 m of almost massive coarse conglomerates.

200 m of parallel beds of mudstone with *Globotruncana rosetta*.

200 m of interbedding of dm-thick beds of medium sandstone, fine sandstone and claystone.
30. Quebrada Cacao: complete Inoceramids in life position.

92 m of fine conglomerate with bad sorting, floating, punctual or line contact between the clasts. Locally there are coarse sandstone lenses. Clasts of andesites, basalts, radiolarites, red and green jasper, sedimntary and limestone clasts, and opaque minerals.

Base not exposed.

Esteban Lopez-Murillo

Stratigraphic section: C24 Quebrada Chilamate

Coordinates of start: 10.21063883/-85.4841402

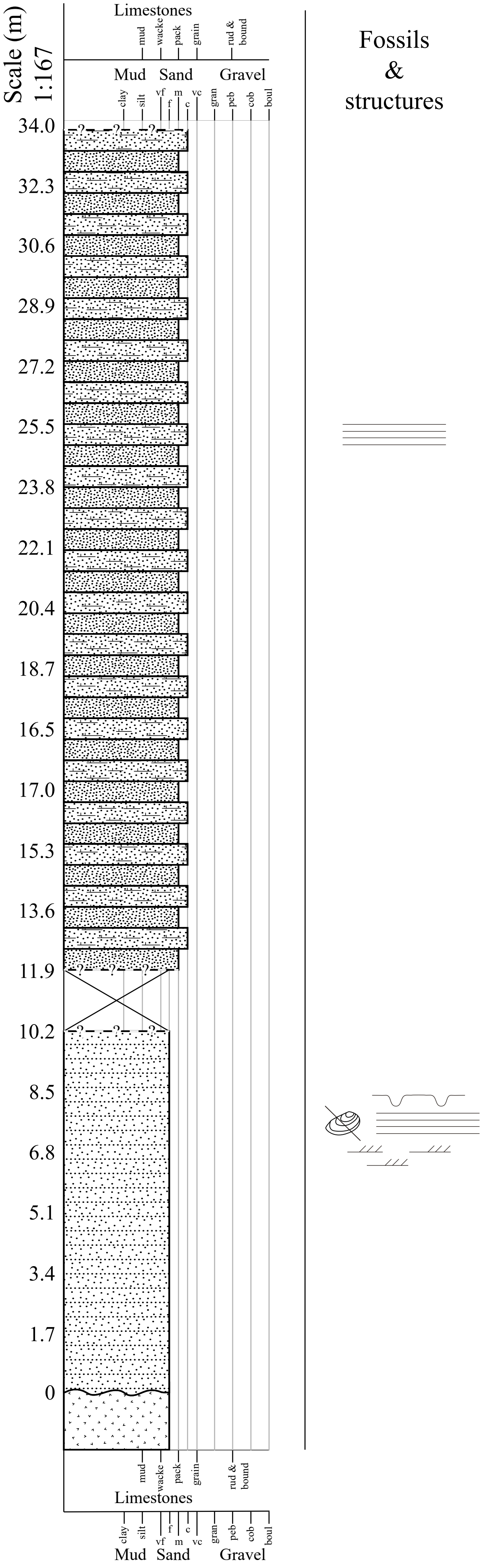

Description

23 m of cm-dm-thick interbedding of dark gray medium sandstone and light gray very calcareous coarse sandstone.

39 m of super compacted dark gray fine sandstone. It has cm-thick beds, lenses and wedges of brown to reddish shales and very fine sandstone.

46. Quebrada Chilamate: dm-long inoceramid prisms.

Nicoya Complex (Turonian-Coniacian boundary: 89.9 Ma): massive basalts.

Esteban Lopez-Murillo

Stratigraphic section: C25 Quebrada Grande, Tacanis

Coordinates of start: 10.04755728/-85.31568775

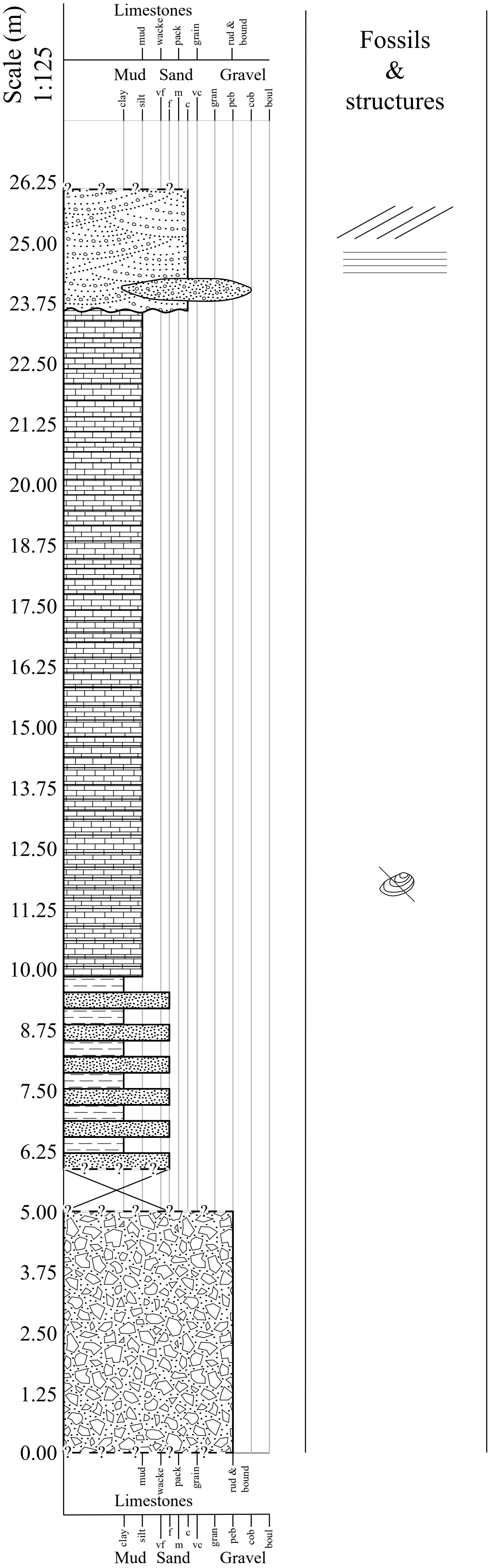

Description

2.5 m of calcareous medium and coarse sandstone. At the base it presents some conglomerate lenses with cm-long subangular to rounded clasts.

7.8 m dm-cm-thick whitish gray mudstones, it presents lenses of red mudstones at the base.

6 m of dm-cm-thick beds of red, brown reddish and violet mudstones.
16. W of Santa Rita: dm-long inoceramids in life position.

4 m of interbedding of cm-thick beds of fine sandstones and cm-thick beds of brown shales. Moderately altered.

5 m of breccia with cm-long angular clasts of siliceous white and yellowish shales, inside a crushed matrix. Very altered, possible fault zone.

Esteban Lopez-Murillo

Stratigraphic section: C26 Quebrada Honda, Nambi

Coordinates of start: 10.20918757/-85.51014715

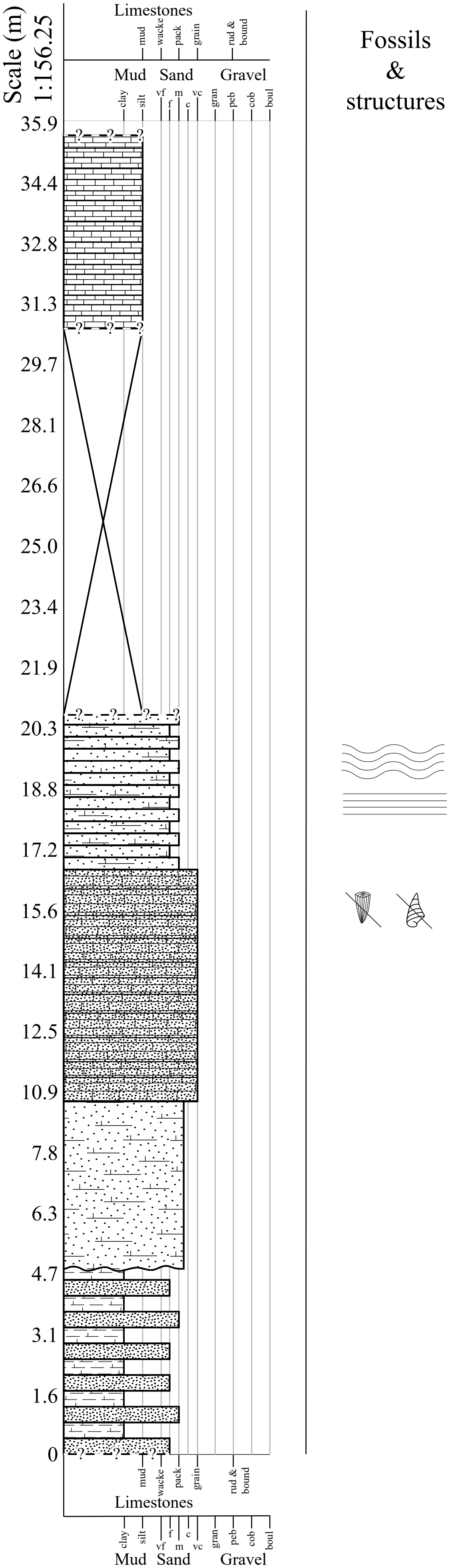

Description

5 m of dm-thick beds of cm-thick beds of red mudstones.

4 m of interbedding of cm-thick beds of calcareous dark gray to black medium and fine sandstone.

6 m of cm-dm-thick beds of gray grainstone or calcarenite.
19. Quebrada Honda, Nambi: cm-long Nerineid gastropod fragments.

3 m of of very calcareous medium to coarse sandstone.

5 m of interbedding of gray greenish and brown cm-thick beds of fine-medium sandstone, and brown calcareous shale with at least two beds of brown reddish mudstone.

Esteban Lopez-Murillo
Stratigraphic section: C27 Quebrada Pavas

Coordinates of start: 10.03167/-85.31867

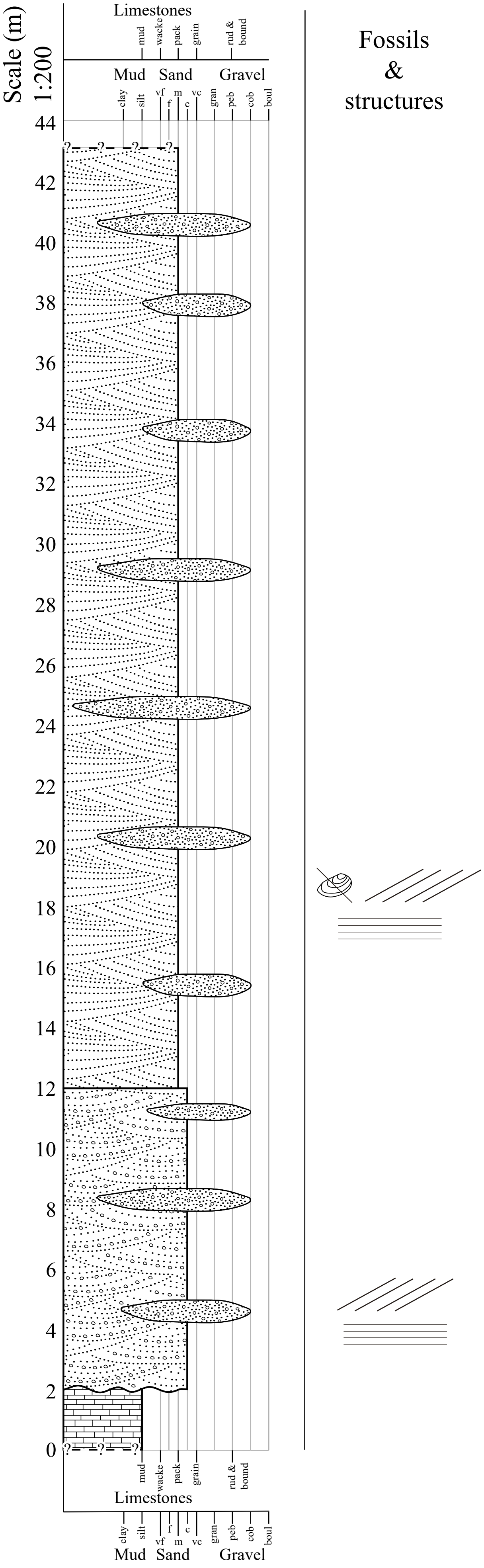

Description

31 m of medium-coarse sandstones with conglomerate lenses with subrounded clasts of basalts and mudstones.
17. Quebrada Pavas: dm-long inoceramid prisms (latest Campanian-early Maastrichtian).

10 m of m-dm-thick beds of medium-coarse sandstone with dm-cm long and thick lenses conglomerates, with cm-long subangular to subrounded clasts of basalts, radiolarites, siliceous shales, sandstones and mudstones. Mega cross-stratification.

2 m of very weathered red and white mudstones.

Esteban Lopez-Murillo

Stratigraphic section: C28 Rio Blanco Este

Coordinates of start: 10.00911774/-85.32654413

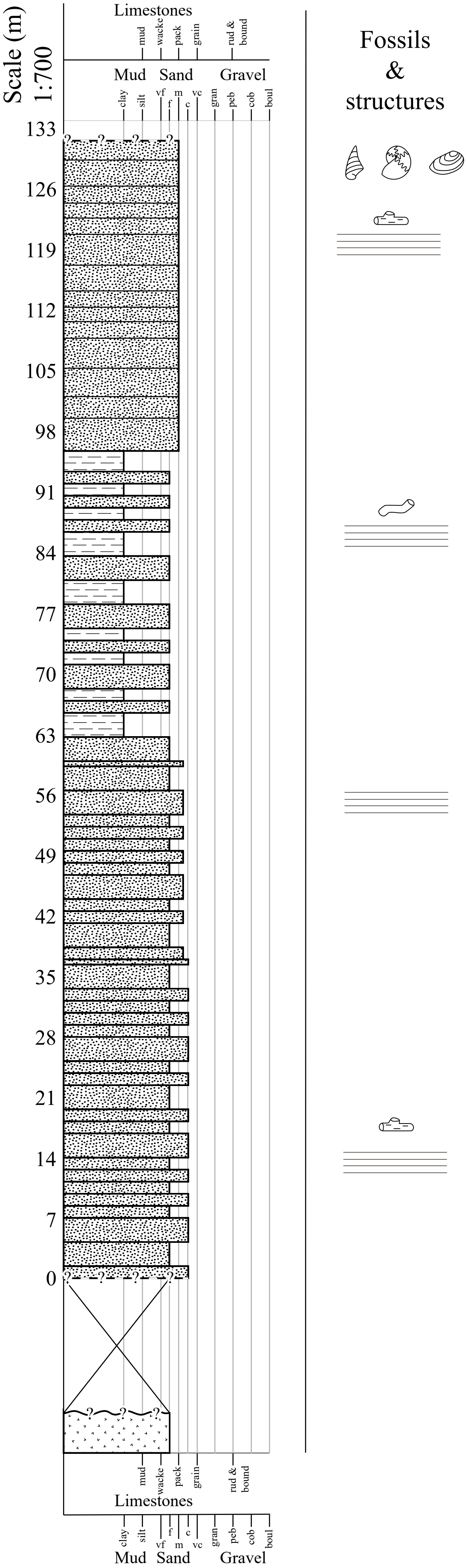

Description

36 m of dm-cm-thick beds of dark gray medium sandstone with small reaction to HCl. It has abundand cm-long wood fragments parallel to bedding.
48. Rio Blanco Este: *Terebra* sp., Gastropoda indet., silicified ammonites.

36 m of interbedding of dm-cm-thick beds of dark gray to black fine sandstone and cm-dm-thick beds of blue gray shale. No reaction to HCl.

23 m of interbedding of dm-cm-thick beds of dark gray to black fine sandstone and cm-dm-thick beds of dark gray to black medium-coarse sandsone with volcanic clasts. No reaction to HCl.

37 m of interbedding of dm-cm-thick beds of dark gray to black fine sandstone and cm-dm-thick beds of dark gray to black coarse sandsone with alligned cm-long wood fragments parallel to bedding and abudant plagioclase. No reaction to HCl.

Nicoya Complex (Valanginian-Turonian): massive basalts.

Esteban Lopez-Murillo

Stratigraphic section: C29 Rio Blanco, Tacanis

Coordinates of start: 10.04755728/-85.31568775

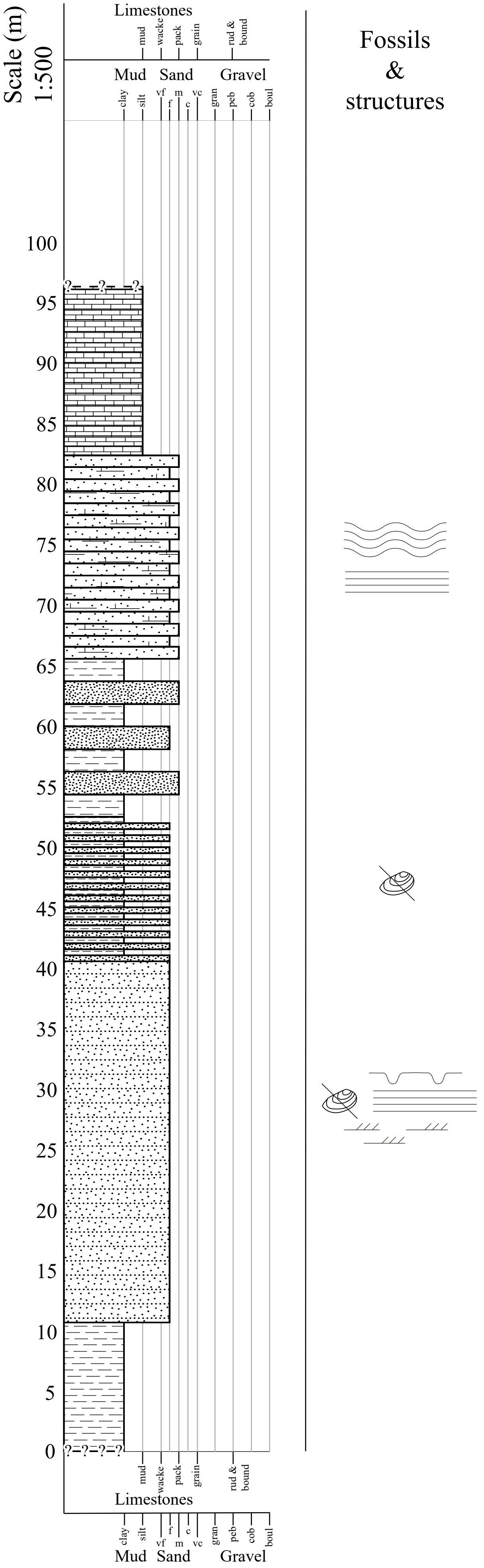

Description

14 m of cm-thick beds of red mudstones.

12 m of interbedding of black and brown reddish fine sandstones and brown reddish calcareous shales (partially silicified mudstones). Some locations have inoceramid prisms.

15 m of interbedding of cm-thick beds of calcareous dark gray to black medium and fine sandstone.

12 m of interbedding of black and brown reddish fine sandstones and brown reddish calcareous shales (partially silicified mudstones). Some locations have inoceramid prisms.

30 m of super compacted dark gray fine sandstone. It has cm-thick beds, lenses and wedges of brown to reddish shales and very fine sandstone.
47. Rio Blanco, Tacanis: dm-long inoceramid prisms.

11 m of cm-thick beds of green and brown siliceous shales.

Base not exposed.

Esteban Lopez-Murillo

Stratigraphic section: C30 San Buenaventura of Colorado Coordinates of start: 10.1939584787/-85.1516319815

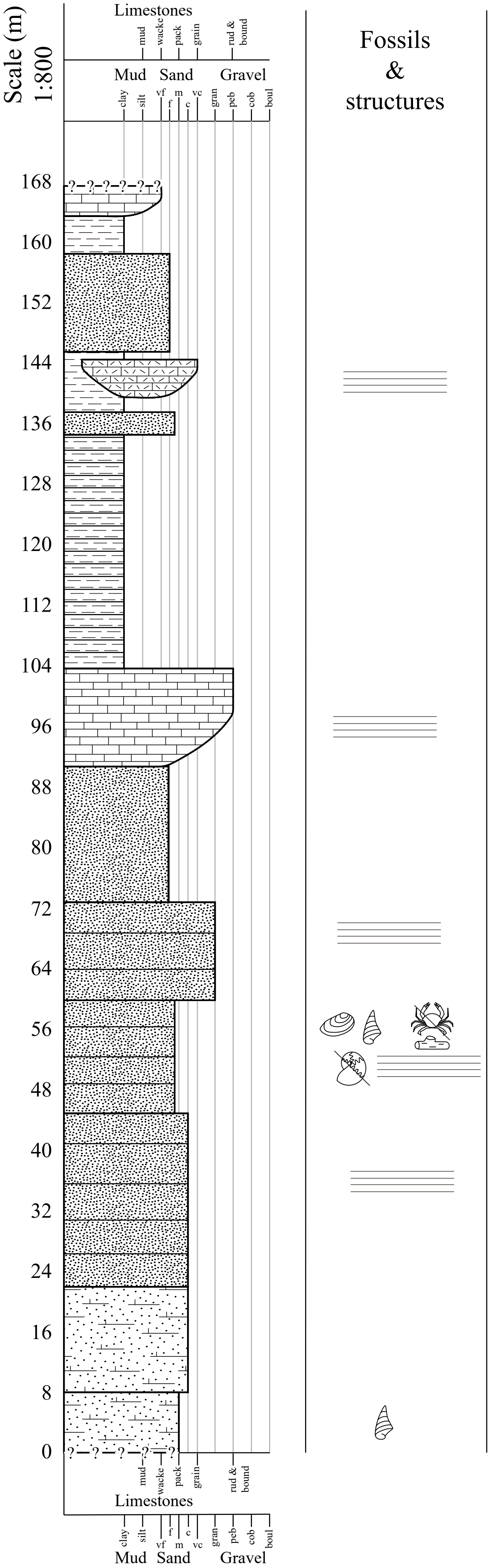

Description

4 m of massive white mudstone to wackestone with red algae.

5 m of massive friable terracotta brown shale with no reaction to HCl.

13 m of massive friable white fine sandstone with forams and 1 amphibole (2x1 mm).

8 m of cm-thick beds of red shale. There is a 5 m-thick m-long lens of lithic limestone with red algae, glauconite? and igneous rocks.
3 m of dm-thick beds of white gray fine to medium sandstone.

31 m of cm-thick beds of gray friable shale.

13 m of dm-thick beds of limestone. Platform that pinches out and reappers. Facies include lithic grainstone, calcareous breccia (other with rhodoliths), wackestone, boundstone. Scleractinian corals and red algae.

18 m of massive blue gray fine sandstone, friable and with spheroidal weathering.

17 m of dm-to-m-thick beds of fine conglomerate with volcanic clasts, wood, and *Ostrea* sp.

31 m of dm-to-m-thick beds of fine to medium sandstone. Wood fragments parallel to weak parallel bedding. Spheroidal weathering.
10. San Buenaventura: *Baculites* sp., *Glyptoxoceras* sp., *Pinna* sp., Inoceramidae indet., Gastropoda indet., *Pseudokossmaticeras brandti* (Redembatcher, 1873) (latest Campanian).

23 m of amalgamated dm-thick beds of coarse sandstone. Clasts of jasper, volcanic rocks, plagioclase, oxidized clasts, planktonic foraminifera.

14 m of massive blue-gray calcreous coarse sandstone with oxides and spheroidal weathering.

8 m of massive blue-gray calcreous medium sandstone with planktonic foraminifera. Crab parts and gastropods are also present. Spheroidal weathering
Base not exposed.

APPENDIX 2.

Fossil locality list.

Number	Name	Lat	Long	Stratigraphic unit	Age	Description	Specimens
1	Manzanillo quarry	10,1286	-85,0013	San Buenaventura Fm.	Latest Campanian	Massive friable gray shales	11
2	Czechs' Ammonite loc.	10,1275	-84,9972	San Buenaventura Fm.	Latest Campanian	Dark gray to blue-gray clay marls in dm to m beds	0
3	Cerro Congo's abandoned quarry	10,1838	-84,9989	El Viejo Fm.	Early late Campanian	Fossiliferous calcareous sandstone	68
4	Unnamed ridge	10,1845	-84,9997	El Viejo Fm.	Early late Campanian	Conglomeratic rudstone with basalt and jasper clasts, to rudstone	3
5	La Irma Quarry	10,1858	-84,9987	San Buenaventura Fm.	Latest Campanian	Dm to massive slightly calcareous blue-gray fine sandstones	57
6	N of Puerto Nispero (middle part)	10,2142	-85,2308	Puerto Nispero Fm.	Early Maastrichtian	Dm bedded wackestone with dasycladacean algae and microgastropods around a coral patch reef	33
7	N of Puerto Nispero (lower part)	10,2137	-85,2306	Puerto Nispero Fm.	Early Maastrichtian	Grainstone/rudstone with oyster reef patches, rhodoliths and intraclasts	9
8	E of Cerros Cerco de Piedra (1)	10,2060	-85,1150	San Buenaventura Fm. (lower)	Late Campanian	Calcareous fine sandstones and green gray shales, moderately weathered, with bivalve and ammonite fragments	0
9	E of Cerros Cerco de Piedra (2)	10,2150	-85,1270	San Buenaventura Fm. (upper)	Latest Campanian	Calcareous fine sandstones and green gray shales, moderately weathered, with bivalve and ammonite fragments	5
10	San Buenaventura	10,1930	-85,1551	San Buenaventura Fm.	Latest Campanian	Calcareous fine sandstones and green gray shales, moderately weathered, with bivalve and ammonite fragments	20
11	Montezuma	9,6584	-85,0622	Piedras Blancas Fm.	Latest middle Campanian	M blocks of red mudstones lying on the beach above the basalts	4

12	Punta Pochote	9,7416	-84,9854	Loma Chumico Fm.	Early late Albian?	Cm beds of oil shale	5
13	Playa Organos	9,7925	-84,9236	Piedras Blancas Fm.	Latest middle Campanian	Cm beds of white mudstone	6
14	Jicaral	9,9600	-85,1200	Curu Fm.	Early Maastrichtian	M thick beds of coarse blue gray sandstone	5
15	Loma Chumico	10,0620	-85,2640	Loma Chumico Fm.	Early late Albian?	Interbedding of cm beds of oil shale with cm beds of black siliceous shale and fine sandstones	27
16	W of Santa Rita	10,0411	-85,3167	Piedras Blancas Fm.	Latest Campanian	Cm beds of white mudstone	2
17	Quebrada Pavas	10,0317	-85,3187	Curu Fm. (Quebrada Pavas Mb.)	Early Maastrichtian	Cm to m beds of gray medium to coarse sandstones with conglomerate lenses	1
18	Nambi	10,2181	-85,5183	Nambi Fm. (lower)	Early late Campanian	Well compact dark gray fine sandstones interbedded with cm beds, lenses and wedges of brown to red shales of very fine sandstones	10
19	Quebrada Honda de Nambi	10,2092	-85,5101	Nambi Fm. (middle)	Early late Campanian	Cm to dm interbedding of gray calcarenites	0
20	Top of Cerro Cebollin	10,3768	-85,4318	El Viejo Fm.	Early late Campanian	Rudist and coral framestone	9
21	NE slope of Cerro Cebollin	10,3772	-85,4312	El Viejo Fm.	Early late Campanian	Fine gray grainstone with hippuritid bivalves and corals	1
22	Fila Machete's abandoned quarry	10,3704	-85,5685	Santa Ana Fm.	Early late Campanian	Interbedding of dm beds of gray calcareous sandstones and cm beds of mudstone	1
23	N point of Playa Panama	10,6020	-85,6491	El Viejo Fm.	Early late Campanian	M blocks of fossiliferous conglomerates with rudist patch reefs	8
24	Punta Conejo	10,3673	-85,8666	El Viejo Fm.	Early late Campanian	3 layers of medium to coarse sandstones	0
25	Arroyo Nisperal	10,8220	-85,6520	El Viejo Fm.	Early late Campanian	Peridotite-derived conglomerates with abundant sandy matrix	0

26	Antigua Marmolina (old "marble" quarry)	10,9044	-85,6385	El Viejo Fm.	Early late Campanian	12-15m section of coarse sandstone with peridotite rounded lithoclasts, then a massive limestone bed about 3 m thick (rudstone at the base)	3
28	El Hachal hill	10,9030	-85,7470	El Viejo Fm.	Early late Campanian	Fossiliferous limestone	30
30	Quebrada Cacao	11,1288	-85,6296	Rivas Fm. (basal)	Early Maastrichtian	Cm to dm beds of medium to coarse calcareous sandstones	9
31	N of Copal	10,1740	-85,2600	Curu Fm. (San Juan Conglomerates and Calcarenites)	Latest Campanian	Cm to dm beds of medium to coarse calcareous sandstones	1
32	Cerro Taburete	10,1770	-85,3061	Curu Fm.	Latest Campanian	Cm to dm beds of medium to coarse calcareous sandstones	1
33	Roblar SE	10,2150	-85,2910	Curu Fm.	Late Campanian-early Maastrichtian	Cm-thick beds of calcareous fine sandstone interbedded with cm-thick bed of medium calcareous sandstone	0
34	Roblar W	10,2210	-85,3010	Curu Fm.	Late Campanian-early Maastrichtian	Dm-thick beds of bioclastic grainstone with cross-bedding and dm-thick tuff laminae	3
35	NW of Cerro Barra Honda	10,1760	-85,3670	Curu Fm.	Latest Campanian	Cm to dm beds of medium to coarse calcareous sandstones	2
36	Castilla de Oro	10,4360	-85,5985	El Viejo Fm.	Early late Campanian	M blocks of basaltic conglomerate without matrix	1
37	Cerro Coyolar	10,3846	-85,6291	Santa Ana Fm.	Early late Campanian	Cm to dm beds of grainstones	1
38	Los Almendros Quarry	10,2121	-85,1112	El Viejo Fm.	Early late Campanian	M beds of fine conglomerate with clasts of basalts, jasper, green shales, komatiites, with 2 levels of rudist reefs. Black calcareous sandstone	13

39	Cerro Cebollin of Colorado	10,2240	-85,1320	Nispero Fm. (Loma Danta Mb.)	Early Maastrichtian	Dm to m polymictic conglomerates with m clasts of limestone	41
40	Bahia Monte del Barco	10,6015	-85,6482	El Viejo Fm.	Early late Campanian	M beds of fossiliferous conglomerates with rudist patch reefs	27
41	Cobano	9,7217	-85,1534	Piedras Blancas Fm.	Latest middle Campanian	Cm beds of red mudstone	8
42	Rio Morote	10,0738	-85,3121	Loma Chumico Fm.	Early late Albian?	Black fine conglomerate	1
43	Caballito	10,2350	-85,3600	Curu Fm. (San Juan Conglomerates and Calcarenites)	Latest Campanian	Dm-thick beds of calcareous sandstones	11
44	Across Copal's cemetery	10,1547	-85,2727	Curu Fm. (San Juan Conglomerates and Calcarenites)	Early late Campanian	M blocks of polymictic mega conglomerate with bioclasts	10
45	Rio Cañamazo	10,1810	-84,9890	El Viejo Fm.	Early late Campanian	Fossiliferous calcareous sandstone	0
46	Quebrada Chilamate	10,2106	-85,4841	Nambi Fm. (lower)	Early late Campanian	Well compact dark gray fine sandstones interbedded with cm beds, lenses and wedges of brown to red shales of very fine sandstones	0
47	Rio Blanco, Tacanis	10,0476	-85,3157	Nambi Fm. (lower)	Early late Campanian	Well compact dark gray fine sandstones interbedded with cm beds, lenses and wedges of brown to red shales of very fine sandstones	0
48	Rio Blanco Este	10,0091	-85,3265	Nambi Fm. (upper)	Early late Campanian	Well compact dark gray fine sandstones interbedded with cm beds, lenses and wedges of brown to red shales of very fine sandstones	7
49	E of Cerros Cerco de Piedra (3)	10,2039	-85,1178	Nispero Fm. (Loma Danta Mb.)	Early Maastrichtian	Cm-thick beds of bioclastic grainstone interbedded with calcareous shale with mm-thick tuff laminae	20

						and 5 beds of cm-thick Inoceramids	
50	Across Finca La Irma	10,1876	-84,9982	Nispero Fm. (Loma Danta Mb.)	Early Maastrichtian	Dm-thick beds of wackestone with coral patch reefs	2
51	Cerro Copal	10,1740	-85,2615	Nispero Fm.	Early Maastrichtian	Dm-thick beds of wackestone and mudstone	1

APPENDIX 3.

Stratigraphic logs done.

Code	Name	Lat	Long	Localities	Author
C1	Antigua Marmolina	10,9044	-85,6385	26	Pons et al. (2016)
C2	Caballito	10,2353	-85,3583	35, 43	Fieldwork
C3	Castilla de Oro	10,4355	-85,5992	36	Fieldwork
C4	Copal's cemetery-N Copal	10,1547	-85,2727	31, 44, 51	Fieldwork
C5	Cerro Cebollin Colorado	10,2191	-85,1286	39	Fieldwork
C6	Cerro Cebollin	10,3768	-85,4318	20, 21	Fieldwork
C7	Cerro Congo	10,1838	-84,9989	3, 4, 5, 50	Fieldwork, Aguilar and Denyer (2002)
C8	Cerro Coyolar	10,3857	-85,6292	38	Fieldwork
C9	Cerro Sombrero	10,1665	-85,2584	None	Fieldwork, Flores (2003)
C10	Cobano	9,7207	-85,1521	41	Fieldwork
C11	Colorado de Abangares	10,2109	-85,1058	39, 8, 9, 49	Fieldwork, Flores (2003)
C12	Nambi	10,2181	-85,5183	18	Flores (2003)
C13	Fila Machete	10,3704	-85,5685	22	Fieldwork
C14	Jicaral	9,9585	-85,1238	14	Fieldwork
C15	Loma Chumico	10,0620	-85,2640	15, 42	Fieldwork, Flores (2003)
C16	Manzanillo	10,1283	-85,0011	1	Fieldwork
C17	Montezuma	9,6584	-85,0622	11	Fieldwork
C18	Playa Organos	9,8145	-84,8940	13	Fieldwork, Flores (2003)
C19	Playa Panama	10,6005	-85,6494	40, 23	Fieldwork

C20	Puerto Nispero	10,2137	-85,2306	7, 6	Fieldwork
C21	Punta Conejo	10,3673	-85,8666	24	Denyer et al. (2014)
C22	Punta Pochote	9,7416	-84,9854	12	Flores (2003)
C23	Quebrada Cacao	11,1288	-85,6296	30	Arroyo et al. (2016)
C24	Quebrada Chilamate	10,2106	-85,4841	46	Flores (2003)
C25	Quebrada Grande, Tacanis	10,0381	-85,3052	16	Flores (2003)
C26	Quebrada Honda, Nambi	10,2092	-85,5101	19	Flores (2003)
C27	Quebrada Pavas	10,0317	-85,3187	17	Flores (2003)
C28	Rio Blanco Este	10,0091	-85,3265	48	Fieldwork
C29	Rio Blanco, Tacanis	10,0476	-85,3157	47	Flores (2003)
C30	San Buenaventura	10,1940	-85,1516	10	Fieldwork, Flores (2003)

APPENDIX 4.

Paleontological database.

Genus	Species	Locality	Abundance	Age	Stratigraphic unit	Lithology
Gaudryceras	sp. A	1. Manzanillo quarry	4	Latest Campanian	San Buenaventura Fm.	Calcareous siltstone
Glyptoxoceras	sp.	1. Manzanillo quarry	3	Latest Campanian	San Buenaventura Fm.	Calcareous siltstone
Scaphites	sp.	1. Manzanillo quarry	1	Latest Campanian	San Buenaventura Fm.	Calcareous siltstone
Ammonoidea	indet. (jaw)	1. Manzanillo quarry	1	Latest Campanian	San Buenaventura Fm.	Calcareous siltstone
Cataceramus	sp. A	1. Manzanillo quarry	1	Latest Campanian	San Buenaventura Fm.	Calcareous siltstone
Cataceramus	sp. B	1. Manzanillo quarry	2	Latest Campanian	San Buenaventura Fm.	Calcareous siltstone
Inoceramidae	indet.	1. Manzanillo quarry	4	Latest Campanian	San Buenaventura Fm.	Calcareous siltstone
Mytilidae	indet.	1. Manzanillo quarry	1	Latest Campanian	San Buenaventura Fm.	Calcareous siltstone
Plicatula	sp. A	1. Manzanillo quarry	1	Latest Campanian	San Buenaventura Fm.	Calcareous siltstone
Ficus	sp.	1. Manzanillo quarry	1	Latest Campanian	San Buenaventura Fm.	Calcareous siltstone
Cerithium	sp.	1. Manzanillo quarry	1	Latest Campanian	San Buenaventura Fm.	Calcareous siltstone
Neithea	sp. A	3. Cerro Congo's abandoned quarry	3	Early late Campanian	El Viejo Fm.	Calcareous sandstone
Veniella	*jamaicensis*	3. Cerro Congo's abandoned quarry	7	Early late Campanian	El Viejo Fm.	Calcareous sandstone
Notoscabrotrigonia?	sp.	3. Cerro Congo's abandoned quarry	20	Early late Campanian	El Viejo Fm.	Calcareous sandstone
Plicatula	sp. B	3. Cerro Congo's abandoned quarry	7	Early late Campanian	El Viejo Fm.	Calcareous sandstone
Ostrea	sp. B	3. Cerro Congo's abandoned quarry	10	Early late Campanian	El Viejo Fm.	Calcareous sandstone
Inoceramidae	indet.	3. Cerro Congo's abandoned quarry	5	Early late Campanian	El Viejo Fm.	Calcareous sandstone

Brachiodontes?	sp.	3. Cerro Congo's abandoned quarry	1	Early late Campanian	El Viejo Fm.	Calcareous sandstone
Trachycardium	sp. A	3. Cerro Congo's abandoned quarry	2	Early late Campanian	El Viejo Fm.	Calcareous sandstone
Trachycardium	sp. B	3. Cerro Congo's abandoned quarry	2	Early late Campanian	El Viejo Fm.	Calcareous sandstone
Dosinia?	sp.	3. Cerro Congo's abandoned quarry	1	Early late Campanian	El Viejo Fm.	Calcareous sandstone
Turritella	sp.	3. Cerro Congo's abandoned quarry	1	Early late Campanian	El Viejo Fm.	Calcareous sandstone
? Cerithium	sp.	3. Cerro Congo's abandoned quarry	2	Early late Campanian	El Viejo Fm.	Calcareous sandstone
Astraea (Astralium)	sp.	3. Cerro Congo's abandoned quarry	2	Early late Campanian	El Viejo Fm.	Calcareous sandstone
Alvania?	sp.	3. Cerro Congo's abandoned quarry	1	Early late Campanian	El Viejo Fm.	Calcareous sandstone
Terebra	sp.	3. Cerro Congo's abandoned quarry	1	Early late Campanian	El Viejo Fm.	Calcareous sandstone
Fusinus	sp.	3. Cerro Congo's abandoned quarry	1	Early late Campanian	El Viejo Fm.	Calcareous sandstone
Parasimploptyxis	*epelys*	3. Cerro Congo's abandoned quarry	2	Early late Campanian	El Viejo Fm.	Calcareous sandstone
Ostrea	sp. C	4. Unnamed ridge	3	Early late Campanian	El Viejo Fm.	Conglomeratic rudstone
Baculites	sp. front ribs	5. La Irma Quarry	2	Latest Campanian	San Buenaventura Fm.	Calcareous fine sandstone
Baculites	*leopoliensis*	5. La Irma Quarry	1	Latest Campanian	San Buenaventura Fm.	Calcareous fine sandstone
Baculites	sp. smooth 1	5. La Irma Quarry	1	Latest Campanian	San Buenaventura Fm.	Calcareous fine sandstone
Baculites	sp. smooth 2	5. La Irma Quarry	1	Latest Campanian	San Buenaventura Fm.	Calcareous fine sandstone
Baculites	sp. weak ribs 1	5. La Irma Quarry	3	Latest Campanian	San Buenaventura Fm.	Calcareous fine sandstone
Gaudryceras	sp. A	5. La Irma Quarry	1	Latest Campanian	San Buenaventura Fm.	Calcareous fine sandstone
Neophylloceras	*surya*	5. La Irma Quarry	1	Latest Campanian	San Buenaventura Fm.	Calcareous fine sandstone

Pachydiscus	sp. A	5. La Irma Quarry	1	Latest Campanian	San Buenaventura Fm.	Calcareous fine sandstone
Pachydiscus	sp. B	5. La Irma Quarry	1	Latest Campanian	San Buenaventura Fm.	Calcareous fine sandstone
Pseudokossmaticeras	sp. A	5. La Irma Quarry	1	Latest Campanian	San Buenaventura Fm.	Calcareous fine sandstone
Scaphites	sp.	5. La Irma Quarry	2	Latest Campanian	San Buenaventura Fm.	Calcareous fine sandstone
Solenoceras	sp.	5. La Irma Quarry	1	Latest Campanian	San Buenaventura Fm.	Calcareous fine sandstone
Belemnitella	sp.	5. La Irma Quarry	4	Latest Campanian	San Buenaventura Fm.	Calcareous fine sandstone
Acila	sp. A	5. La Irma Quarry	7	Latest Campanian	San Buenaventura Fm.	Calcareous fine sandstone
Acila	sp. B	5. La Irma Quarry	3	Latest Campanian	San Buenaventura Fm.	Calcareous fine sandstone
Macrocallista?	sp.	5. La Irma Quarry	1	Latest Campanian	San Buenaventura Fm.	Calcareous fine sandstone
Mytilus?	sp.	5. La Irma Quarry	1	Latest Campanian	San Buenaventura Fm.	Calcareous fine sandstone
Modiolus?	sp.	5. La Irma Quarry	5	Latest Campanian	San Buenaventura Fm.	Calcareous fine sandstone
Mytilus?	sp.	5. La Irma Quarry	3	Latest Campanian	San Buenaventura Fm.	Calcareous fine sandstone
Neithea	sp. B	5. La Irma Quarry	2	Latest Campanian	San Buenaventura Fm.	Calcareous fine sandstone
Ostrea	sp. D	5. La Irma Quarry	1	Latest Campanian	San Buenaventura Fm.	Calcareous fine sandstone
Ostrea	sp. E	5. La Irma Quarry	1	Latest Campanian	San Buenaventura Fm.	Calcareous fine sandstone
Ostrea	sp. F	5. La Irma Quarry	2	Latest Campanian	San Buenaventura Fm.	Calcareous fine sandstone
Ostrea	sp. G	5. La Irma Quarry	2	Latest Campanian	San Buenaventura Fm.	Calcareous fine sandstone
Peyssonella	sp.	5. La Irma Quarry	1	Latest Campanian	San Buenaventura Fm.	Calcareous fine sandstone
Pinna	sp.	5. La Irma Quarry	3	Latest Campanian	San Buenaventura Fm.	Calcareous fine sandstone

Trachycardium	sp. C	5. La Irma Quarry	3	Latest Campanian	San Buenaventura Fm.	Calcareous fine sandstone
Terebra?	sp.	5. La Irma Quarry	1	Latest Campanian	San Buenaventura Fm.	Calcareous fine sandstone
Fusinus	sp.	5. La Irma Quarry	2	Latest Campanian	San Buenaventura Fm.	Calcareous fine sandstone
Ostrea	sp. H	6. N of Puerto Nispero (middle part)	6	Early Maastrichtian	Nispero Fm.	Algal wackestone
Pteria	sp.	6. N of Puerto Nispero (middle part)	1	Early Maastrichtian	Nispero Fm.	Algal wackestone
Acteonella	*duckettsensis*	6. N of Puerto Nispero (middle part)	2	Early Maastrichtian	Nispero Fm.	Algal wackestone
Natica	sp.	6. N of Puerto Nispero (middle part)	1	Early Maastrichtian	Nispero Fm.	Algal wackestone
Rostellana	sp.	6. N of Puerto Nispero (middle part)	3	Early Maastrichtian	Nispero Fm.	Algal wackestone
Plesioptygmatis?	sp. A	6. N of Puerto Nispero (middle part)	20	Early Maastrichtian	Nispero Fm.	Algal wackestone
Ostrea	sp. H	7. N of Puerto Nispero (lower part)	5	Early Maastrichtian	Nispero Fm.	Poorly sorted grainstone
Plesioptygmatis	sp. B	7. N of Puerto Nispero (lower part)	4	Early Maastrichtian	Nispero Fm.	Poorly sorted grainstone
Gaudryceras	sp. A	9. E of Cerros Cerco de Piedra (2)	1	Latest Campanian	San Buenaventura Fm.	Calcareous fine sandstone
Gaudryceras	sp. B	9. E of Cerros Cerco de Piedra (2)	1	Latest Campanian	San Buenaventura Fm.	Calcareous fine sandstone
Solenoceras	sp.	9. E of Cerros Cerco de Piedra (2)	1	Latest Campanian	San Buenaventura Fm.	Calcareous fine sandstone
Neophylloceras	*surya*	9. E of Cerros Cerco de Piedra (2)	1	Latest Campanian	San Buenaventura Fm.	Calcareous fine sandstone
Belemnitella	sp.	9. E of Cerros Cerco de Piedra (2)	1	Latest Campanian	San Buenaventura Fm.	Calcareous fine sandstone
Glyptoxoceras	*retrorsum*	10. San Buenaventura	2	Latest Campanian	San Buenaventura Fm.	Calcareous fine sandstone
Pseudokossmaticeras	*brandti*	10. San Buenaventura	2	Latest Campanian	San Buenaventura Fm.	Calcareous fine sandstone
Solenoceras	sp.	10. San Buenaventura	1	Latest Campanian	San Buenaventura Fm.	Calcareous fine sandstone

Baculites	sp. weak ribs 2	10. San Buenaventura	1	Latest Campanian	San Buenaventura Fm.	Calcareous fine sandstone
Ammonoidea	indet. (jaw)	10. San Buenaventura	1	Latest Campanian	San Buenaventura Fm.	Calcareous fine sandstone
Ostrea	sp. I	10. San Buenaventura	1	Latest Campanian	San Buenaventura Fm.	Fine conglomerate
Pinna	sp.	10. San Buenaventura	10	Latest Campanian	San Buenaventura Fm.	Calcareous fine sandstone
Archeogastropoda	indet.	10. San Buenaventura	1	Latest Campanian	San Buenaventura Fm.	Calcareous medium sandstone
Cerithium	sp.	10. San Buenaventura	1	Latest Campanian	San Buenaventura Fm.	Calcareous fine sandstone
Inoceramidae	indet.	11. Montezuma	4	Latest middle Campanian	Piedras Blancas Fm.	Mudstone
Acanthoceratidae	indet.	12. Punta Pochote	5	Early late Albian?	Loma Chumico Fm.	Oil shale
Inoceramidae	indet.	13. Playa Organos	6	Latest middle Campanian	Piedras Blancas Fm.	Mudstone
Belemnitella	sp.	14. Jicaral	1	Early Maastrichtian	Curu Fm.	Fine conglomerate
Ammonoidea	indet.	14. Jicaral	4	Early Maastrichtian	Curu Fm.	Fine conglomerate
Ammonoidea	indet.	15. Loma Chumico	4	Early late Albian?	Loma Chumico Fm.	Oil shale
Neokentroceras?	sp.	15. Loma Chumico	5	Early late Albian?	Loma Chumico Fm.	Oil shale
Acanthoceratidae	indet.	15. Loma Chumico	12	Early late Albian?	Loma Chumico Fm.	Oil shale
Gaudryceras?	sp.	15. Loma Chumico	4	Early late Albian?	Loma Chumico Fm.	Oil shale
Cataceramus?	sp.	15. Loma Chumico	1	Early late Albian?	Loma Chumico Fm.	Fine conglomerate
Inoceramidae	indet.	15. Loma Chumico	1	Early late Albian?	Loma Chumico Fm.	Oil shale
Inoceramidae	indet.	16. W of Santa Rita	3	Latest Campanian	Piedras Blancas Fm.	Mudstone
Inoceramidae	indet.	18. Nambi	10	Early late Campanian	Nambi Fm.	Fine sandstones

Parasimploptyxis	*epelys*	20. Top of Cerro Cebollin	5	Early late Campanian	El Viejo Fm.	Rudist and coral framestone
Parasimploptyxis	sp. B	20. Top of Cerro Cebollin	4	Early late Campanian	El Viejo Fm.	Rudist and coral framestone
Plicatula	sp.	21. NE slope of Cerro Cebollin	1	Early late Campanian	El Viejo Fm.	Fine grainstone
Parasimploptyxis	*epelys*	26. Antigua Marmolina (old "marble" quarry)	1	Early late Campanian	El Viejo Fm.	Coarse sandstone
Acteonella	sp. B	28. El Hachal hill	30	Early late Campanian	El Viejo Fm.	Poorly sorted grainstone
Trochacteon	sp.	28. El Hachal hill	1	Early late Campanian	El Viejo Fm.	Poorly sorted grainstone
Calliomphalus?	sp.	28. El Hachal hill	1	Early late Campanian	El Viejo Fm.	Poorly sorted grainstone
Campanile	sp.	28. El Hachal hill	1	Early late Campanian	El Viejo Fm.	Poorly sorted grainstone
Inoceramus	sp.	30. Quebrada Cacao	4	Early Maastrichtian	Rivas Fm.	Calcareous medium sandstone
Glyptoxoceras	*retrorsum*	31. N of Copal	2	Latest Campanian	Curu Fm. (San Juan Conglomerates and Calcarenites)	Coarse sandstone
Inoceramidae	indet.	31. N of Copal	2	Latest Campanian	Curu Fm. (San Juan Conglomerates and Calcarenites)	Coarse sandstone
Ostrea	sp. I	31. N of Copal	4	Latest Campanian	Curu Fm. (San Juan Conglomerates and Calcarenites)	Coarse sandstone
Ostrea	sp. J	31. N of Copal	1	Latest Campanian	Curu Fm. (San Juan Conglomerates and Calcarenites)	Coarse sandstone
Inoceramidae	indet.	32. Cerro Taburete	1	Latest Campanian	Curu Fm. (San Juan Conglomerates and Calcarenites)	Mudstone
Inoceramidae	indet.	35. NW of Cerro Barra Honda	1	Latest Campanian	Curu Fm. (San Juan	Calcareous coarse sandstone

					Conglomerates and Calcarenites)	
Parasimploptyxis	sp.	36. Castilla de Oro	1	Early late Campanian	El Viejo Fm.	Medium basaltic conglomerate
Acteonella	sp. A	36. Castilla de Oro	1	Early late Campanian	El Viejo Fm.	Medium basaltic conglomerate
Parasimploptyxis	sp.	36. Castilla de Oro	1	Early late Campanian	El Viejo Fm.	Medium basaltic conglomerate
Nostoceras	*hyatti*	38. Los Almendros Quarry	6	Early late Campanian	El Viejo Fm.	Medium basaltic conglomerate
Chione	sp.	38. Los Almendros Quarry	1	Early late Campanian	El Viejo Fm.	Medium basaltic conglomerate
Pecten	sp. B	38. Los Almendros Quarry	1	Early late Campanian	El Viejo Fm.	Medium basaltic conglomerate
Dallocardia	sp.	38. Los Almendros Quarry	4	Early late Campanian	El Viejo Fm.	Medium basaltic conglomerate
Trochoceramus?	sp.	38. Los Almendros Quarry	1	Early late Campanian	El Viejo Fm.	Medium basaltic conglomerate
Neithea	sp. C	38. Los Almendros Quarry	1	Early late Campanian	El Viejo Fm.	Medium basaltic conglomerate
Pinna	cf. *laqueata*	38. Los Almendros Quarry	1	Early late Campanian	El Viejo Fm.	Medium basaltic sandstone
Bivalvia	indet.	38. Los Almendros Quarry	1	Early late Campanian	El Viejo Fm.	Medium basaltic conglomerate
Pecten	sp. A	38. Los Almendros Quarry	1	Early late Campanian	El Viejo Fm.	Medium basaltic conglomerate
Modiolus	sp.	38. Los Almendros Quarry	1	Early late Campanian	El Viejo Fm.	Medium basaltic conglomerate
Nucula	cf. *ciboloensis*	38. Los Almendros Quarry	1	Early late Campanian	El Viejo Fm.	Medium basaltic conglomerate
Veniella	*jamaicensis*	38. Los Almendros Quarry	1	Early late Campanian	El Viejo Fm.	Medium basaltic sandstone
Gyrodes	sp.	38. Los Almendros Quarry	3	Early late Campanian	El Viejo Fm.	Medium basaltic conglomerate
Acteonella	sp. C	39. Cerro Cebollin of Colorado	30	Early Maastrichtian	Nispero Fm. (Loma Danta Mb.)	Algal wackestone
Acteonella	sp. D	39. Cerro Cebollin of Colorado	1	Early Maastrichtian	Nispero Fm. (Loma Danta Mb.)	Algal wackestone

Nerineidae	indet.	39. Cerro Cebollin of Colorado	10	Early Maastrichtian	Nispero Fm. (Loma Danta Mb.)	Algal wackestone
Parasimploptyxis	*epelys*	40. Bahia Monte del Barco	18	Early late Campanian	El Viejo	Coarse basaltic conglomerates
Parasimploptyxis	sp. B	40. Bahia Monte del Barco	9	Early late Campanian	El Viejo	Coarse basaltic conglomerates
Inoceramidae	indet.	41. Cobano	4	Latest middle Campanian	Piedras Blancas	Mudstone
Ostrea	sp. J	41. Cobano	4	Latest middle Campanian	Piedras Blancas	Mudstone
Inoceramidae	indet.	43. Caballito	3	Latest Campanian	Curu Fm. (San Juan Conglomerates and Calcarenites)	Fine conglomerate
Ostrea	sp. I	43. Caballito	1	Latest Campanian	Curu Fm. (San Juan Conglomerates and Calcarenites)	Fine conglomerate
Cataceramus?	sp.	43. Caballito	1	Latest Campanian	Curu Fm. (San Juan Conglomerates and Calcarenites)	Fine conglomerate
Inoceramidae	indet.	43. Caballito	5	Latest Campanian	Curu Fm. (San Juan Conglomerates and Calcarenites)	Fine sandstone
Cataceramus	*goldfussianus?*	43. Caballito	1	Latest Campanian	Curu Fm. (San Juan Conglomerates and Calcarenites)	Fine sandstone
Inoceramidae	indet.	44. Across Copal's cemetery	1	Early late Campanian	Curu Fm. (San Juan Conglomerates and Calcarenites)	Coarse sandstone
Trochoceramus?	sp.	44. Across Copal's cemetery	1	Early late Campanian	Curu Fm. (San Juan Conglomerates and Calcarenites)	Coarse sandstone
Pecten	sp.	44. Across Copal's cemetery	1	Early late Campanian	Curu Fm. (San Juan Conglomerates and Calcarenites)	Coarse sandstone

Trochacteon	sp.	44. Across Copal's cemetery	6	Early late Campanian	Curu Fm. (San Juan Conglomerates and Calcarenites)	Coarse sandstone
Parasimploptyxis	sp.	44. Across Copal's cemetery	1	Early late Campanian	Curu Fm. (San Juan Conglomerates and Calcarenites)	Coarse sandstone
Ammonoidea	indet.	48. Rio Blanco Este	4	Early late Campanian	Nambi Fm.	Coarse basaltic sandstone
Terebra	sp.	48. Rio Blanco Este	4	Early late Campanian	Nambi Fm.	Coarse basaltic sandstone
Inoceramidae	indet.	49. E of Cerros Cerco de Piedra (3)	20	Early Maastrichtian	Nispero Fm. (Loma Danta Mb.)	Grainstone
Turritellidae	indet.	50. Across Finca La Irma	1	Early Maastrichtian	Nispero Fm. (Loma Danta Mb.)	Algal wackestone
Plesioptygmatis?	sp. B	50. Across Finca La Irma	1	Early Maastrichtian	Nispero Fm. (Loma Danta Mb.)	Algal wackestone
Plesioptygmatis?	sp. B	51. Cerro Copal	1	Early Maastrichtian	Nispero Fm.	Algal wackestone